



**A Study of the Optimized Conditions for a Closed-loop HHO
Production System Using A/C Power Supply**

Nuttaporn Choodum

**A Thesis Submitted in Partial Fulfillment of the Requirements for the
Degree of Doctor of Philosophy in Chemical Engineering
Prince of Songkla University**

2017

Copyright of Prince of Songkla University



**A Study of the Optimized Conditions for a Closed-loop HHO
Production System Using A/C Power Supply**

Nuttaporn Choodum

**A Thesis Submitted in Partial Fulfillment of the Requirements for the
Degree of Doctor of Philosophy in Chemical Engineering
Prince of Songkla University**

2017

Copyright of Prince of Songkla University

Thesis Title A Study of the Optimized Conditions for a Closed-loop HHO
Production System Using A/C Power Supply

Author Mr. Nuttaporn Choodum

Major Program Chemical Engineering

Major Advisor**Examining Committee :**

.....Chairperson
(Assoc.Prof.Dr. Ram Yamsaengsung) (Asst.Prof.Dr. Sompong Putivisutisak)

Co-advisor

.....Committee
(Assoc.Prof.Dr. Ram Yamsaengsung)

.....Committee
(Assoc.Prof.Dr. Chayanoot Sangwichien)

.....Committee
(Assoc.Prof.Dr. Lupong Kaewsichan)

.....Committee
(Assoc.Prof.Dr. Taweesak Reungpeerakul)

The Graduate School, Prince of Songkla University, has approved this thesis as partial fulfillment of the requirements for the Doctor of Philosophy Degree in Chemical Engineering.

.....
(Assoc.Prof.Dr. Teerapol Srichana)

Dean of Graduate School

This is to certify that the work here submitted is the result of the candidate's own investigations. Due acknowledgement has been made of any assistance received.

.....Signature
(Assoc. Prof. Dr. Ram Yamsaengsung)
Major Advisor

.....Signature
(Assoc. Prof. Dr. Chayanoot Sangwichien)
Co-advisor

.....Signature
(Mr. Nuttaporn Choodum)
Candidate

I hereby certify that this work has not been accepted in substance for any degree, and is not being currently submitted in candidature for any degree.

.....Signature
(Mr. Nuttaporn Choodum)

ชื่อวิทยานิพนธ์	การศึกษาสภาวะที่เหมาะสมของกระบวนการผลิตก๊าซเชื้อเพลิงไฮดรอกซี (HHO) โดยใช้ไฟฟ้ากระแสสลับ
ชื่อผู้เขียน	นายณัฐพร ชูคำ
สาขาวิชา	วิศวกรรมเคมี
ปีการศึกษา	2559

บทคัดย่อ

งานศึกษาวิจัยนี้มุ่งศึกษาค้นคว้าหาสภาวะที่เหมาะสมของกระบวนการผลิตก๊าซเชื้อเพลิงไฮดรอกซี (HHO) ซึ่งใช้สารละลายโพแทสเซียมไฮดรอกไซด์ (KOH) เป็นสารละลายอิเล็กโทรไลต์ โดยดำเนินการผ่านระบบการผลิตแบบไหลวนในกระแสปัด ซึ่งประกอบด้วยอุปกรณ์ดำเนินการหลักได้แก่ เครื่องกำเนิดก๊าซเชื้อเพลิงไฮดรอกซี (HHO), เครื่องแยกของผสมระหว่างก๊าซและของเหลวออกจากกันและระบบหล่อเย็นต่างๆ ในการทดลองได้ใช้สารละลายโพแทสเซียมไฮดรอกไซด์ ที่ความเข้มข้น 0.50, 0.75, 1.00, 1.25 และ 1.50 เปอร์เซ็นต์โดยน้ำหนักเป็นสารละลายอิเล็กโทรไลต์, ใช้ขั้วเซลล์ไฟฟ้าเป็นแบบแผ่นโลหะสแตนเลสขนาด 20x30 มิลลิเมตร, โดยช่องว่างระหว่างขั้วแผ่นโลหะถูกปรับตั้งค่าอยู่ที่ 1, 3, 5, 7 และ 9 มิลลิเมตร ตามลำดับ ในกระบวนการทดลองนี้อุณหภูมิสารละลายอิเล็กโทรไลต์ถูกควบคุมให้คงตัว ที่อุณหภูมิ 40, 45, 50, 55, 60, 65, 70, 75, 80, 85, 90 และ 95 เซลเซียส เป็นเวลา 10 นาที จากการทดลองพบว่า การเพิ่มขึ้นของความเข้มข้นสารละลายอิเล็กโทรไลต์จาก 0.50 เป็น 1.50 เปอร์เซ็นต์โดยน้ำหนัก ส่งผลให้อัตราการผลิตก๊าซเชื้อเพลิงไฮดรอกซีเพิ่มขึ้นมากกว่า 50 เปอร์เซ็นต์, และเพิ่มขึ้นมากกว่า 60 เปอร์เซ็นต์จากการเพิ่มอุณหภูมิดำเนินการ ยิ่งไปกว่านั้นพบว่า ที่ปริมาณอุณหภูมิดำเนินการสูง ณ ตอนท้ายของการทดลอง อัตราการผลิตการผลิตก๊าซเชื้อเพลิงไฮดรอกซี ของระยะขั้วเซลล์ไฟฟ้า 1 และ 3 มิลลิเมตร มีปริมาณน้อยกว่า ระยะขั้วเซลล์ไฟฟ้าที่มากกว่า สภาวะที่เหมาะสมต่อการผลิตก๊าซเชื้อเพลิงไฮดรอกซีในการทดลองนี้อยู่ที่ระยะขั้วเซลล์ไฟฟ้า 7 มิลลิเมตร ที่สารละลายโพแทสเซียมไฮดรอกซี

อกไซด์เข้มข้น 1.50 เปอร์เซ็นต์โดยน้ำหนัก และอุณหภูมิดำเนินการผลิตอยู่ที่ 90.0 ± 1.0 องศาเซลเซียส ด้วยระบบการผลิตก๊าซเชื้อเพลิงไฮดรอกซีแบบไหลวนในกระแสนี้ ความดันดำเนินการที่เหมาะสมในการผลิตก๊าซเชื้อเพลิงดังกล่าวได้ถูกดำเนินการศึกษาค้นคว้าด้วยเช่นกัน โดยอุปกรณ์ดำเนินการทดลองต่างๆยังคงประกอบด้วย เครื่องกำเนิดก๊าซเชื้อเพลิงไฮดรอกซี (HHO), เครื่องแยกของผสมระหว่างก๊าซและของเหลวออกจากกัน และระบบหล่อเย็นต่างๆ โดยความดันดำเนินการถูกปรับตั้งค่าที่ 60.8, 70.9, 81.0, 91.2 หรือ 101.3 กิโลปาสกาลสัมบูรณ์ โดยอาศัยการปรับค่าการเปิดของวาล์วปรับความดันสูญญากาศที่ต้นทางขาเข้าของปั๊มสูญญากาศชนิดวงแหวนน้ำ จากการทดลองพบว่า ความดันดำเนินการผลิตก๊าซเชื้อเพลิงไฮดรอกซีที่เหมาะสม มีความเข้ากันได้สอดคล้องกับความดันอากาศขาเข้าใช้งานปกติของเครื่องยนต์สันดาปภายใน โดยค่าความดันดำเนินการดังกล่าวมีค่าอยู่ระหว่าง 81.0 ถึง 91.2 กิโลปาสกาลสัมบูรณ์ และพบว่าอัตราการผลิตก๊าซเชื้อเพลิงไฮดรอกซีสูงสุดเกิดขึ้นที่ค่าความดันดำเนินการ 81.0 กิโลปาสกาลสัมบูรณ์ และจะมีปริมาณเป็นสองเท่าเมื่อเทียบค่าเดียวกันที่ความดันดำเนินการ 101.3 กิโลปาสกาลสัมบูรณ์ อย่างไรก็ตามที่ค่าความดันดำเนินการ 70.9 และ 60.8 กิโลปาสกาลสัมบูรณ์ อัตราการผลิตก๊าซเชื้อเพลิงไฮดรอกซีจะลดลงมากกว่า 50 และ 80 เปอร์เซ็นต์ตามลำดับ ยิ่งไปกว่านั้นค่าความดันดำเนินการ 81.0 กิโลปาสกาลสัมบูรณ์ดังกล่าวข้างต้น เป็นค่าที่สอดคล้องกับความดันดำเนินการที่ช่องทางเข้าอากาศของเครื่องยนต์สันดาปภายในซึ่งมีค่าปกติใช้งานอยู่ที่ระหว่าง 72.0 ถึง 87.0 กิโลปาสกาลสัมบูรณ์

Thesis Title	A Study of the Optimized Conditions for a Closed-loop HHO Production System Using A/C Power Supply
Author	Mr. Nuttaporn Choodum
Major Program	Chemical Engineering
Academic Year	2016

ABSTRACT

This study focused on finding appropriate conditions for HHO production by electrolysis using alkaline KOH electrolyte solution. The closed-loop HHO production unit designed consisted of a HHO generator, a liquid-gas separator and a cooling system. The experiments used electrolyte concentrations of 0.50, 0.75, 1.00, 1.25 and 1.50% w/w KOH (aq.), and 316L stainless steel 20x30 mm electrode plates. The gap between the plates was adjusted to 1, 3, 5, 7 and 9 mm, and experiments were conducted at the steady state temperatures 40, 45, 50, 55, 60, 65, 70, 75, 80, 85, 90 and 95°C for 10 minutes. It was found that as the electrolyte concentration increased from 0.50% to 1.50% w/w KOH, the HHO production rate increased by more than 50%, and also by more than 60% with increased operating temperature. Furthermore, at the high end of our operating temperatures, the small 1 and 3 mm cell gaps produced less HHO than the larger cell gaps. The optimized production conditions in this study had 7 mm cell gap and 1.50% w/w KOH at $90.0 \pm 1.0^\circ\text{C}$ operating temperature.

The appropriate operating pressure was also investigated for this closed-loop system to produce HHO by electrolysis of alkaline KOH electrolyte solution. The HHO production system still consisted of an HHO-generator, a liquid-gas separator and a cooling system. The operating pressure was set to 60.8, 70.9, 81.0, 91.2 or 101.3 kPa abs. The vacuum level was adjusted by varying the opening of the breathing valve at the suction line of the water-ring vacuum pump. It was found that the appropriate operating pressures matching an internal combustion engine (ICE) ranged from 81.0 to 91.2 kPa abs. The highest HHO production throughput occurred

at 81.0 kPa abs, and was over twofold that at 101.3 kPa abs. However, at the lower pressures 70.9 and 60.8 kPa abs, the HHO throughput decreased by more than 50% and 80%, respectively. Furthermore, the 81.0 kPa abs operating pressure matches the intake manifold pressure of a running ICE, which generally ranges from 72.0 to 87.0 kPa abs.

ACKNOWLEDGEMENTS

I would like to thank the Prince of Songkla University (PSU) Graduate School Research Fund, the PSU research and development office (RDO) and the PSU Faculty of Engineering Lecturer Development Scholarship. Sincere appreciations are extended to the Department of Chemical Engineering, Faculty of Engineering, PSU, in facilitating equipment and laboratory support.

I am deeply impressed and would like to thank my advisor: Asst. Prof. Dr. Ram Yamsaengsung and coordinate advisor: Assoc. Prof. Dr. Chayanoot Sangwichien in many supporting and the valued suggestions.

And special thanks go to who cannot live without a senior lecturer Mr. Wiwat Sutiwipakorn and Assoc. Prof. Dr. Seppo Karrila for polishing the English of this research papers. And also Ms. Anatta Patcharawijit for kindly introduced in the appropriate scientific analytical method of this research.

Finally, I would like to especially thank my parent, older brothers, staff of PSU chemical engineering and friends for the best of spirit and supporting while I was studying.

Nuttaporn Choodum

TABLE OF CONTENT

	Page
ACKNOWLEDGEMENTS	ix
TABLE OF CONTENT	x
LIST OF TABLES	xiii
LIST OF FIGURES	xx
CHAPTER 1	1
Introduction	1
1.1 Rationale/Problem statement	1
1.2 Theoretical Background	4
1.2.1 History of Browns Gas (HHO)	4
1.2.2 Characteristics of HHO	14
1.2.3 HHO Properties	19
1.2.4 Comparative of Hydrogen and Fossil Fuel Cost	22
1.2.5 General Applications and Others	26
1.3 Review of Literatures	35
1.3.1 Phase I: Investigation of a Closed-loop HHO Production System using AC supply	35
1.3.2 Phase II: Optimization of the Operating Pressure of a Closed-loop HHO production system for operation with an Internal Combustion Engine (ICE)	38
1.4 Objectives	42

TABLE OF CONTENT (Continued)

	Page
CHAPTER 2	43
Research Methodology	43
2.1 Experiment phase I: Investigation of a Closed-loop HHO Production System using AC supply.	43
2.2 Experiment phase II: Optimization of the Operating Pressure of a Closed-loop HHO production system for operation with an Internal Combustion Engine (ICE).	46
CHAPTER 3	48
Result and Discussions	48
3.1 Phase I: Investigation of a Closed-loop HHO Production System using AC supply.	48
3.1.1 The relation between HHO Temperature (°C) and Electrolyte Temperature (°C)	48
3.1.2 The relation between electric current consumption (A) and electrolyte temperature (°C)	56
3.2 Phase II: Optimization of the Operating Pressure of a Closed-loop HHO production system for operation with an Internal Combustion Engine (ICE)	66
3.3 The relation between HHO production rate (L/h) and electrolyte temperature (°C)	67

TABLE OF CONTENT (Continued)

	Page
CHAPTER 4	80
Conclusions and Suggestions	80
4.1 Conclusions	80
4.1.1 Conclusion (phase I)	80
4.1.2 Conclusion (phase II)	80
4.2 Suggestions	81
References	83
Appendices	88
Appendix A Experiment data	89
Appendix B Equipments	140
VITAE	147

LIST OF TABLES

	Page
Table 1. Vehicle with average fuel consumption	12
Table 2 Density of Comparative Fuels	20
Table 3 Heating Values of Comparative Fuels	20
Table 4 Energy Densities of Comparative Fuels	21
Table 5 Comparative of energy content of hydrogen and fossil fuel	21
Table 6 Comparative of cost of hydrogen and gasoline	23
Table 7 Results of HHO production rate (L/h) at 5 mm cell gap with electrolyte temperature from 40°C to 65°C (Figure 51(a))	70
Table 8 Results of HHO production rate (L/h) at 5 mm cell gap with electrolyte temperature from 70°C to 95°C. (Figure 51(a))	71
Table 9 Results of HHO production rate (L/h) at 7 mm cell gap with electrolyte temperature from 40°C to 65°C (Figure 51(b))	72
Table 10 Results of HHO production rate (L/h) at 7 mm cell gap with electrolyte temperature from 70°C to 95°C ((Figure 51(b))	73
Table 11 Optimized conditions of HHO production throughput	78
Table 12 Relation between electrolyte temperature (°C) and HHO product temperature (°C) of electrolyte concentration from 0.50 to 1.50% w/w KOH, 1 mm cell gap, 20 x 30 mm ² , 52.9 volt and 1 atm	89
Table 13 Relation between electrolyte temperature (°C) and HHO product temperature (°C) of electrolyte concentration from 0.50 to 1.50% w/w KOH, 3 mm cell gap, 20 x 30 mm ² , 52.9 volt and 1 atm	90
Table 14 Relation between electrolyte temperature (°C) and HHO product temperature (°C) of electrolyte concentration from 0.50 to 1.50% w/w KOH, 5 mm cell gap, 20 x 30 mm ² , 52.9 volt and 1 atm	91
Table 15 Relation between electrolyte temperature (°C) and HHO product temperature (°C) of electrolyte concentration from 0.50 to 1.50% w/w KOH, 7 mm cell gap 20 x 30 mm ² 52.9 volt and 1 atm	92

LIST OF TABLES (Continued)

	Page
Table 16 Relation between electrolyte temperature ($^{\circ}\text{C}$) and HHO product temperature ($^{\circ}\text{C}$) of electrolyte concentration from 0.50 to 1.50% w/w KOH, 9 mm cell gap, 20 x 30 mm ² , 52.9 volt and 1 atm	93
Table 17 Relation between electrolyte temperature ($^{\circ}\text{C}$) and HHO product temperature ($^{\circ}\text{C}$) of cell gap set up from 1 to 9 mm, 0.50% w/w KOH, 20 x 30 mm ² , 52.9 volt and 1 atm	94
Table 18 Relation between electrolyte temperature ($^{\circ}\text{C}$) and HHO product temperature ($^{\circ}\text{C}$) of cell gap set up from 1 to 9 mm, 0.75% w/w KOH, 20 x 30 mm ² , 52.9 volt and 1 atm	95
Table 19 Relation between electrolyte temperature ($^{\circ}\text{C}$) and HHO product temperature ($^{\circ}\text{C}$) of cell gap set up from 1 to 9 mm, 1.00% w/w KOH 20 x 30 mm ² , 52.9 volt and 1 atm	96
Table 20 Relation between electrolyte temperature ($^{\circ}\text{C}$) and HHO product temperature ($^{\circ}\text{C}$) of cell gap set up from 1 to 9 mm, 1.25% w/w KOH 20 x 30 mm ² , 52.9 volt and 1 atm	97
Table 21 Relation between electrolyte temperature ($^{\circ}\text{C}$) and HHO product temperature ($^{\circ}\text{C}$) of cell gap set up from 1 to 9 mm, of 1.50% w/w KOH, 20 x 30 mm ² , 52.9 volt and 1 atm	98
Table 22 Relation between electrolyte temperature ($^{\circ}\text{C}$) and HHO product temperature ($^{\circ}\text{C}$) of electrical voltage from 47.5 to 52.9 volt of 1.25% w/w KOH, 20 x 30 mm ² , 5 mm cell gap, 47.5 to 52.9 volt and 1 atm	99
Table 23 Relation between electrolyte temperature ($^{\circ}\text{C}$) and HHO product temperature ($^{\circ}\text{C}$) of operating pressure from 60.8 to 101.3 kPa of 1.25% w/w KOH, 20 x 30 mm ² , 5 mm cell gap, 52.9 volt and 1 atm	100
Table 24 Relation between electrolyte temperature ($^{\circ}\text{C}$) and HHO product temperature ($^{\circ}\text{C}$) of anode-cathode area from 300 to 1500 mm ² of 1.25% w/w KOH, 20 x 30 mm ² , 5 mm cell gap, 52.9 volt and 1 atm	101

LIST OF TABLES (Continued)

	Page
Table 25 Relation between electrolyte temperature ($^{\circ}\text{C}$) and electrical current consumption (A) of electrolyte concentration from 0.50 to 1.50% w/w KOH, of 1 mm cell gap, $20 \times 30 \text{ mm}^2$, 52.9 volt and 1 atm	102
Table 26 Relation between electrolyte temperature ($^{\circ}\text{C}$) and electrical current consumption (A) of electrolyte concentration from 0.50 to 1.50% w/w KOH, of 3 mm cell gap, $20 \times 30 \text{ mm}^2$, 52.9 volt and 1 atm	103
Table 27 Relation between electrolyte temperature ($^{\circ}\text{C}$) and electrical current consumption (A) of electrolyte concentration from 0.50 to 1.50% w/w KOH, of 5 mm cell gap, $20 \times 30 \text{ mm}^2$, 52.9 volt and 1 atm	104
Table 28 Relation between electrolyte temperature ($^{\circ}\text{C}$) and electrical current consumption (A) of electrolyte concentration from 0.50 to 1.50% w/w KOH, of 7 mm cell gap, $20 \times 30 \text{ mm}^2$, 52.9 volt and 1 atm	105
Table 29 Relation between electrolyte temperature ($^{\circ}\text{C}$) and electrical current consumption (A) of electrolyte concentration from 0.50 to 1.50% w/w KOH, of 9 mm cell gap, $20 \times 30 \text{ mm}^2$, 52.9 volt and 1 atm	106
Table 30 Relation between electrolyte temperature ($^{\circ}\text{C}$) and electrical current consumption (A) of cell gap set up from 1 to 9 mm, of 0.50% w/w KOH, $20 \times 30 \text{ mm}^2$, 52.9 volt and 1 atm	107
Table 31 Relation between electrolyte temperature ($^{\circ}\text{C}$) and electrical current consumption (A) of cell gap set up from 1 to 9 mm, of 0.75% w/w KOH, $20 \times 30 \text{ mm}^2$, 52.9 volt and 1 atm	108

LIST OF TABLES (Continued)

	Page
Table 32 Relation between electrolyte temperature ($^{\circ}\text{C}$) and electrical current consumption (A) of cell gap set up from 1 to 9 mm, of 1.00% w/w KOH, $20 \times 30 \text{ mm}^2$, 52.9 volt and 1 atm	109
Table 33 Relation between electrolyte temperature ($^{\circ}\text{C}$) and electrical current consumption (A) of cell gap set up from 1 to 9 mm, of 1.25% w/w KOH, $20 \times 30 \text{ mm}^2$, 52.9 volt and 1 atm	110
Table 34 Relation between electrolyte temperature ($^{\circ}\text{C}$) and electrical current consumption (A) of cell gap set up from 1 to 9 mm, of 1.50% w/w KOH, $20 \times 30 \text{ mm}^2$, 52.9 volt and 1 atm	111
Table 35 Relation between electrolyte temperature ($^{\circ}\text{C}$) and electrical current consumption (A) of electrical voltage from 47.5 to 52.9 volt of 1.25% w/w KOH, $20 \times 30 \text{ mm}^2$, 5 mm cell gap, 47.5 to 52.9 volt and 1 atm	112
Table 36 Relation between electrolyte temperature ($^{\circ}\text{C}$) and electrical current consumption (A) of operating pressure from 60.8 to 101.3 kPa of 1.25% w/w KOH, $20 \times 30 \text{ mm}^2$, 5 mm cell gap, 52.9 volt and 1 atm	113
Table 37 Relation between electrolyte temperature ($^{\circ}\text{C}$) and electrical current consumption (A) of anode-cathode area from 300 to 1500 mm^2 of 1.25% w/w KOH, $20 \times 30 \text{ mm}^2$, 5 mm cell gap, 52.9 volt and 1 atm	114
Table 38 Relation between electrolyte temperature ($^{\circ}\text{C}$) and HHO production rate (L/h) of anode-cathode area 600 mm^2 , 0.50% w/w KOH, 1 mm cell gap, 52.9 volt and 1 atm	115
Table 39 Relation between electrolyte temperature ($^{\circ}\text{C}$) and HHO production rate (L/h) of anode-cathode area 600 mm^2 , 0.75% w/w KOH, 1 mm cell gap, 52.9 volt and 1 atm	116

LIST OF TABLES (Continued)

	Page
Table 40 Relation between electrolyte temperature ($^{\circ}\text{C}$) and HHO production rate (L/h) of anode-cathode area 600 mm^2 , 1.00% w/w KOH, 1 mm cell gap, 52.9 volt and 1 atm	117
Table 41 Relation between electrolyte temperature ($^{\circ}\text{C}$) and HHO production rate (L/h) of anode-cathode area 600 mm^2 , 1.25% w/w KOH, 1 mm cell gap, 52.9 volt and 1 atm	118
Table 42 Relation between electrolyte temperature ($^{\circ}\text{C}$) and HHO production rate (L/h) of anode-cathode area 600 mm^2 , 1.50% w/w KOH, 1 mm cell gap, 52.9 volt and 1 atm	119
Table 43 Relation between electrolyte temperature ($^{\circ}\text{C}$) and HHO production rate (L/h) of anode-cathode area 600 mm^2 , 0.50% w/w KOH, 3 mm cell gap, 52.9 volt and 1 atm	120
Table 44 Relation between electrolyte temperature ($^{\circ}\text{C}$) and HHO production rate (L/h) of anode-cathode area 600 mm^2 , 0.75% w/w KOH, 3 mm cell gap, 52.9 volt and 1 atm	121
Table 45 Relation between electrolyte temperature ($^{\circ}\text{C}$) and HHO production rate (L/h) of anode-cathode area 600 mm^2 , 1.00% w/w KOH, 3 mm cell gap, 52.9 volt and 1 atm	122
Table 46 Relation between electrolyte temperature ($^{\circ}\text{C}$) and HHO production rate (L/h) of anode-cathode area 600 mm^2 , 1.25% w/w KOH, 3 mm cell gap, 52.9 volt and 1 atm	123
Table 47 Relation between electrolyte temperature ($^{\circ}\text{C}$) and HHO production rate (L/h) of anode-cathode area 600 mm^2 , 1.50% w/w KOH, 3 mm cell gap, 52.9 volt and 1 atm	124
Table 48 Relation between electrolyte temperature ($^{\circ}\text{C}$) and HHO production rate (L/h) of anode-cathode area 600 mm^2 , 0.50% w/w KOH, 5 mm cell gap, 52.9 volt and 1 atm	125

LIST OF TABLES (Continued)

	Page
Table 49 Relation between electrolyte temperature ($^{\circ}\text{C}$) and HHO production rate (L/h) of anode-cathode area 600 mm^2 , 0.75% w/w KOH, 5 mm cell gap, 52.9 volt and 1 atm	126
Table 50 Relation between electrolyte temperature ($^{\circ}\text{C}$) and HHO production rate (L/h) of anode-cathode area 600 mm^2 , 1.00% w/w KOH, 5 mm cell gap, 52.9 volt and 1 atm	127
Table 51 Relation between electrolyte temperature ($^{\circ}\text{C}$) and HHO production rate (L/h) of anode-cathode area 600 mm^2 , 1.25% w/w KOH, 5 mm cell gap, 52.9 volt and 1 atm	128
Table 52 Relation between electrolyte temperature ($^{\circ}\text{C}$) and HHO production rate (L/h) of anode-cathode area 600 mm^2 , 1.50% w/w KOH, 5 mm cell gap, 52.9 volt and 1 atm	129
Table 53 Relation between electrolyte temperature ($^{\circ}\text{C}$) and HHO production rate (L/h) of anode-cathode area 600 mm^2 , 0.50% w/w KOH, 7 mm cell gap, 52.9 volt and 1 atm	130
Table 54 Relation between electrolyte temperature ($^{\circ}\text{C}$) and HHO production rate (L/h) of anode-cathode area 600 mm^2 , 0.75% w/w KOH, 7 mm cell gap, 52.9 volt and 1 atm	131
Table 55 Relation between electrolyte temperature ($^{\circ}\text{C}$) and HHO production rate (L/h) of anode-cathode area 600 mm^2 , 1.00% w/w KOH, 7 mm cell gap, 52.9 volt and 1 atm	132
Table 56 Relation between electrolyte temperature ($^{\circ}\text{C}$) and HHO production rate (L/h) of anode-cathode area 600 mm^2 , 1.25% w/w KOH, 7 mm cell gap, 52.9 volt and 1 atm	133
Table 57 Relation between electrolyte temperature ($^{\circ}\text{C}$) and HHO production rate (L/h) of anode-cathode area 600 mm^2 , 1.50% w/w KOH, 7 mm cell gap, 52.9 volt and 1 atm	134

LIST OF TABLES (Continued)

	Page
Table 58 Relation between electrolyte temperature ($^{\circ}\text{C}$) and HHO production rate (L/h) of anode-cathode area 600 mm^2 , 0.50% w/w KOH, 9 mm cell gap, 52.9 volt and 1 atm	135
Table 59 Relation between electrolyte temperature ($^{\circ}\text{C}$) and HHO production rate (L/h) of anode-cathode area 600 mm^2 , 0.75% w/w KOH, 9 mm cell gap, 52.9 volt and 1 atm	136
Table 60 Relation between electrolyte temperature ($^{\circ}\text{C}$) and HHO production rate (L/h) of anode-cathode area 600 mm^2 , 1.00% w/w KOH, 9 mm cell gap, 52.9 volt and 1 atm	137
Table 61 Relation between electrolyte temperature ($^{\circ}\text{C}$) and HHO production rate (L/h) of anode-cathode area 600 mm^2 , 1.25% w/w KOH, 9 mm cell gap, 52.9 volt and 1 atm	138
Table 62 Relation between electrolyte temperature ($^{\circ}\text{C}$) and HHO production rate (L/h) of anode-cathode area 600 mm^2 , 1.50% w/w KOH, 9 mm cell gap, 52.9 volt and 1 atm	139

LIST OF FIGURES

	Page
Figure 1 Well known HHO inventor: Yull Brown	5
Figure 2 William A. Rhodes	6
Figure 3 Standard electrolysis	7
Figure 4 Name plate of Yull Brown's multiple HHO generator	13
Figure 5 Multi-HHO generator unit (Left) and system controller (Right)	13
Figure 6 The conceptual rendering of an atomic hydrogen (H)	15
Figure 7 The conceptual rendering of the valence bond of two H atomics	16
Figure 8 The conceptual rendering of H, H ₂ and H ₃ in HHO gas	16
Figure 9 The conceptual rendering of the H- bond in the HHO: H (top), HxH (middle), HxHxH (left), (H-H)xH (right)	17
Figure 10 The conceptual rendering of water: H ₂ O	17
Figure 11 The H-O-H molecule in which all electric polarizations have been removed	18
Figure 12 Magnetic polarities of the two H-atoms, as well as the unstable character of the configuration	18
Figure 13 Twin HHO generator	29
Figure 14 HHO Generator	30
Figure 15 Drawing of HHO generator	30
Figure 16 Electrical pole and level of electrolyte solution	31
Figure 17 Brown gas generator	32
Figure 18 Diagram of power supply system of gas generator	32
Figure 19 Block diagram of HHO dry cell	34
Figure 20 Schematic of water fueled engine	39
Figure 21 HHO generator with variable anode-cathode distance (cell gap)	44
Figure 22 Process flow diagram of the closed-loop HHO production system (Phase I)	45
Figure 23 Process flow diagram of the closed-loop HHO production system (Phase II)	47

LIST OF FIGURES (Continued)

	Page
Figure 24 HHO temperatures (°C) and electrolyte temperatures (°C) by varying electrolyte concentrations from 0.50 to 1.50% w/w KOH of 1 mm cell gap	49
Figure 25 HHO temperatures (°C) and electrolyte temperatures (°C) by varying electrolyte concentrations from 0.50 to 1.50% w/w KOH of 3 mm cell gap	50
Figure 26 HHO temperatures (°C) and electrolyte temperatures (°C) by varying electrolyte concentrations from 0.50 to 1.50% w/w KOH of 5 mm cell gap	50
Figure 27 HHO temperatures (°C) and electrolyte temperatures (°C) by varying electrolyte concentrations from 0.50 to 1.50% w/w KOH of 7 mm cell gap	51
Figure 28 HHO temperatures (°C) and electrolyte temperatures (°C) by varying electrolyte concentrations from 0.50 to 1.50% w/w KOH of 9 mm cell gap	51
Figure 29 HHO temperatures (°C) and electrolyte temperatures (°C) by varying cell gaps from 1 to 9 mm. of 0.50% w/w KOH	52
Figure 30 HHO temperatures (°C) and electrolyte temperatures (°C) by varying cell gaps from 1 to 9 mm. of 0.75% w/w KOH	52
Figure 31 HHO temperatures (°C) and electrolyte temperatures (°C) by varying cell gaps from 1 to 9 mm. of 1.00% w/w KOH	53
Figure 32 HHO temperatures (°C) and electrolyte temperatures (°C) by varying cell gaps from 1 to 9 mm. of 1.25% w/w KOH	53
Figure 33 HHO temperatures (°C) and electrolyte temperatures (°C) by varying cell gaps from 1 to 9 mm. of 1.50% w/w KOH	54
Figure 34 HHO temperatures (°C) and electrolyte temperatures (°C) by varying cell voltages from 47.5 to 52.9 volt of 5 mm cell gap and 1.25% w/w KOH	54

LIST OF FIGURES (Continued)

	Page
Figure 35 HHO temperatures (°C) and electrolyte temperatures (°C) by varying operating pressures from 60.8 kPa to 101.3 kPa of 5 mm cell gap and 1.25% w/w KOH	55
Figure 36 HHO temperatures (°C) and electrolyte temperatures (°C) by varying electrical poles areas from 300 mm ² to 1500 mm ² of 5 mm cell gap and 1.25% w/w KOH	55
Figure 37 Electric current consumption (A) and electrolyte temperatures (°C) by varying electrolyte concentrations from 0.50 to 1.50% w/w KOH of 1 mm cell gap	56
Figure 38 Electric current consumption (A) and electrolyte temperatures (°C) by varying electrolyte concentrations from 0.50 to 1.50% w/w KOH of 3 mm cell gap	57
Figure 39 Electric current consumption and electrolyte temperatures (°C) by varying electrolyte concentrations from 0.50 to 1.50% w/w KOH of 5 mm cell gap	58
Figure 40 Electric current consumption (A) and electrolyte temperatures (°C) by varying electrolyte concentrations from 0.50 to 1.50% w/w KOH of 7 mm cell gap	58
Figure 41 Electric current consumptions (A) and electrolyte temperatures (°C) by varying electrolyte concentrations from 0.50 to 1.50% w/w KOH of 9 mm cell gap	59
Figure 42 Electric current consumptions (A) and electrolyte temperatures (°C) by varying cell gaps from 0.50 to 1.50% w/w KOH of 0.50% w/w KOH	60
Figure 43 Electric current consumptions (A) and electrolyte temperatures (°C) by varying cell gaps from 0.50 to 1.50% w/w KOH of 0.75% w/w KOH	60

LIST OF FIGURES (Continued)

	Page
Figure 44 Electric current consumptions (A) and electrolyte temperatures ($^{\circ}\text{C}$) by varying cell gaps from 0.50 to 1.50% w/w KOH of 1.00% w/w KOH	61
Figure 45 Electric current consumptions (A) and electrolyte temperatures ($^{\circ}\text{C}$) by varying cell gaps from 0.50 to 1.50% w/w KOH of 1.25% w/w KOH	61
Figure 46 Electric current consumptions (A) and electrolyte temperatures ($^{\circ}\text{C}$) by varying cell gaps from 0.50 to 1.50% w/w KOH of 1.50% w/w KOH	62
Figure 47 Electric current consumptions (A) and electrolyte temperatures ($^{\circ}\text{C}$) by varying cell voltages from 47.5 to 52.9 volt of 5 mm cell gap and 1.25% w/w KOH	63
Figure 48 Electric current consumptions (A) and electrolyte temperatures ($^{\circ}\text{C}$) by varying operating pressures from 60.8 to 101.3 kPa abs of 5 mm cell gap and 1.25% w/w KOH	64
Figure 49 Electric current consumptions (A) and electrolyte temperatures ($^{\circ}\text{C}$) by varying electrical poles areas from 300 mm ² to 1500 mm ² of 5 mm cell gap and 1.25% w/w KOH	65
Figure 50 HHO production throughput at cell gap of: (a) 1-mm. (b) 3-mm.	67
Figure 51 HHO production throughput at cell gap of: (a) 5-mm. (b) 7-mm (c) 9-mm.	68
Figure 52 Cooling water (28 $^{\circ}\text{C}$) consumption	69
Figure 53 HHO production throughput of KOH electrolyte concentration at 0.50% w/w	75
Figure 54 HHO production throughput of KOH electrolyte concentration at 0.75% w/w	76

LIST OF FIGURES (Continued)

	Page
Figure 55 HHO production throughput of KOH electrolyte concentration at 1.00% w/w	76
Figure 56 HHO production throughput of KOH electrolyte concentration at 1.25% w/w	77
Figure 57 HHO production throughput of KOH electrolyte concentration at 1.50% w/w	77
Figure 58 Maximum HHO production throughput (L/h) versus electrolyte concentration, anode-cathode area: 600 mm ² , AC voltage: 52.9 V, operating temperature: 40 to 95°C	79
Figure 59 Simple diagram of HHO production system (color)	140
Figure 60 Weigh distilled water on weight scale	141
Figure 61 Weigh electrolyte KOH(s) on scale weight	141
Figure 62 Anode-cathode poles: stainless steel plate	142
Figure 63 Set up cell gap with digital Vernier Caliper	142
Figure 64 Liquid-gas separator with temperature sensor	143
Figure 65 Shell and SS. ring coil exchanger	143
Figure 66 Centrifugal circulation pump and cooling fan	144
Figure 67 Temperature control panel	144
Figure 68 Glass type HHO generator	145
Figure 69 HHO gas condenser	145
Figure 70 Breathing valve with positive & negative pressure indicator	146
Figure 71 Water bath for checking HHO bubble	146

CHAPTER 1

Introduction

1.1 Rationale/Problem statement

HHO (hydroxy gas or Brown's Gas) fuel gas is a clean and renewable energy due to the absence of hydrocarbon compounds, carbon dioxide and other hazardous gases that are released during combustion. HHO, which is produced by splitting water into hydrogen and oxygen molecules through electrolysis, releases vapor as its combustion gas. Momirlan and Veziroglu (2005) described that electrical current can be used to separate water into its components of oxygen and hydrogen [1]. Santilli (2006) also introduced the working hypothesis of the existence of HHO fuel gas as a new cluster called "magnecules" using numerous experimental measurements [2]. The researcher found that HHO gas is composed of H and O atoms, dimers H-O, molecules of H₂, O₂ and H₂O.

Furthermore, Santilli (2001) also indicated that one of the most important features of magnecules is their anomalous release of energy in thermochemical reactors which in turn, could serve as a possible source of new, clean fuel [3]. Dülger and Özçelik (2000) presented the production of HHO using water electrolysis that can be installed on different vehicles of various engine types and sizes. The system is based on the electrolysis of water in closed cell electrodes, and the feeding of the HHO gas directly into the intake manifold of the engine. The researchers concluded that emissions were reduced by up to 40-50% depending on the type of the engine without any reduction in engine performance. Moreover, they found that the system led to 35-40% fuel savings [4]. Likewise, Yilmaz *et al.*, (2010) studied the usage of HHO produced by electrolysis as a supplementary fuel in a four-cylinder, four-stroke, compression ignition (CI) engine without any modification and without the need for storage tanks. The HHO modified system resulted in increasing

engine torque output by an average of 19.1% and the reduction of CO emissions by an average of 13.5%, HC emissions by an average of 5% and SFC by an average of 14% [5]. Ammar and Al-Rousan (2010) proposed an HHO generator installed in a Honda G 200, 197cc, single cylinder engine and found that by feeding HHO mixed with gasoline, the fuel consumption was reduced by 20-30% with lower exhaust temperature [6].

Moreover, after running the experiment with the same gasoline engine, Musmar and Al-Rousan (2011) found that NO, NO_x and CO emissions were reduced by approximately 50%, 50% and 20%, respectively [7]. Durairaj *et al.*, (2012) investigated the production and characterization of bio-diesel by adding HHO fuel gas and found that the use of HHO with bio-diesel produced lower unburned HC, CO and particulates while enhancing the engine power and reducing the engine vibration [8].

In addition, Masjuki *et al.* (2016) tested a mixture of biodiesel fuel with HHO fuel gas using 1% w/w KOH electrolyte concentration. Their results showed that the engine power increased by about 2%, biodiesel fuel consumption decreased by about 5%, and CO and HC reduced by 20% and 10%, respectively [9]. Arat *et al.* (2016) studied by feeding 25% HHO with 75% CNG (Compressed Natural Gas) into a non-modified diesel engine and found this mixture increased engine performance and reduced exhaust emission compared to ordinary diesel operations [10]. Baltacioglu *et al.* (2016) tested a pilot - four cylinders - injection diesel engine with alternative fuels; pure hydrogen, HHO, and biodiesel. All fuels were fed into the engine running at 1200 and 2600 rpm. The results indicated that engine performance using HHO fed with the intake air was higher than using pure hydrogen and biodiesel fuel at standard operation. Nonetheless, they found that the exhaust emissions for pure hydrogen were better than for HHO [11].

EL-Kassaby *et al.* (2016) fabricated an electrolysis generator and fed the HHO fuel into a Skoda Felicia 1.3 GLXi gasoline engine. The researcher found that the engine thermal efficiency increased by 10%, while the fuel consumption, CO, HC and NO_x emissions were reduced by 34%, 18%, 14% and 15%, respectively [12]. Dahake *et al.*, (2016) also found that HHO enrichment resulted in better combustion and reduced emission outputs in compression ignition engines. The researcher discovered that the thermal efficiency for compression ratio 18 was increased by

9.25% compared to baseline diesel combustion, while the specific fuel consumption was reduced by 15% at full load condition. Moreover, the HC emission was reduced at an average of 33% and CO emission at an average of 23% [13]. Putha and Babu (2015) found that if 100% HHO were to be fed into an internal combustion engine, pollution after combustion would be cut down to almost zero, while the inside surface of the engine was found to be cleaner than engines using purely fossil fuel [14].

In addition, Bharathi *et al.* (2015) found that HHO helped improve efficiency of an engine and its life span [15]. Furthermore, a number of researchers including Desai *et al.* (2014), Chaudhari *et al.* (2015) and Vino *et al.* (2012) have found that by varying the ratio of fossil fuel to HHO gas, there is a high potential for improving engine efficiency and reducing the emission of air pollutants such as HC, CO₂, CO and NO_x [16-18].

For HHO production, Dweepson (2014) found aqueous potassium hydroxide (KOH) to be the most suitable and low cost electrolyte for enhancing conductivity of the electrolysis solution [19], while Göllei (2014) concluded that 20-30% w/w KOH produced the optimal conductivity for this process [20]. Aqueous KOH, typically, is highly soluble in either hot or cold water and will decompose at temperature up to 1334°C. KOH has a melting point of 380°C and a pH of 13 at 1% w/w concentration. Göllei (2014) also indicated that the higher the temperature of the solution (through electrical current being fed into the system) the more HHO gas could be produced, the closer the anode and the cathode plates are the better the efficiency [20]. Joshi and Naik (2015) reported that ideal operating temperatures and pressures for HHO production should be from 70-100°C and 1-30 bars, respectively [21]. Thus, the key parameters affecting the rate of HHO production include the concentration of electrolytes, solution temperature, and the anode-cathode distance.

In this research, the experiment was designed to comply with real operations whereby the main necessary equipment components should be operated in conjunction with future-appended auxiliary systems. This conceptuality is useful for scaling up the unit from a pilot-scaled prototype. A closed-loop circulation system deemed more flexible was designed to investigate appropriate conditions for HHO production. The parameters evaluated were: system temperature, electrolyte concentration, and operating pressure, inclusive of vacuum pressure. A/C current

supply was utilized so that the positive and negative cycles provide forward-reverse directions that bring about two wires of alternate polarity.

Global warming is one of greatest threat to humanity according to scientists from around the world and the usage of fossil fuel for internal combustion engines (ICEs) is one the major causes of CO₂ released into the atmosphere. With that in mind, hydrogen and fuel cells have been largely considered as one of the cleanest and most efficient energy source for the future world. Momirlan and Veziroglu (2005) reiterated that hydrogen and hydrogen fuel cells can be used to fuel vehicles and aircraft and provide power for our homes and offices.

Hydrogen can be fed into internal combustion engines as pure hydrogen or blended with natural gas, and are three times more efficient than a gasoline-powered engine. On the other hand, HHO is a relatively new alternative source of clean energy that can produce up to 3 times the energy of combustion for hydrogen [1]. Its combustion releases H₂O vapor as the exhaust from the internal combustion engine (ICE) and can be fed back into the combustion chamber and reused to produce HHO once more (see Figure 1). Santilli (2006) described the interior oxygen in HHO gas as sufficient for combustion, while the other fuels have to combust with the outside atmospheric oxygen, thus causing a serious pollution problem [2] due to nitrogen in the air which came together with oxygen would converted be toxic gases (NO_x) and also remained unburned HC in the ICE cylinder.

1.2 Theoretical Background

1.2.1 History of Browns Gas (HHO)

Yull Brown is an engineer inventor who designed a real running pilot scale HHO generator using 100% water to fuel an internal combustion engine (ICE). He was a well-known inventor and a creative Bulgarian engineer. He was born in Bulgaria in 1922 and died in 1998. Yull Brown has a difficult life in the time of the Second World War. He interested in the clean and low cost alternative energy. He tried to find a new lower price fuel for general people and investigated a new energy

fuel which was more affordable than the present fossil fuel (crude oil). He found HHO would be an appropriate new fuel in the future with many advantages such as it will provide more energy release by three times compare with the present fossil fuel. Moreover, Yull Brown also found that there is no toxic pollution after test run HHO with an internal combustion engine (ICE). His patent: U.S. # 4,014,777 was issued on 29 March 1977.

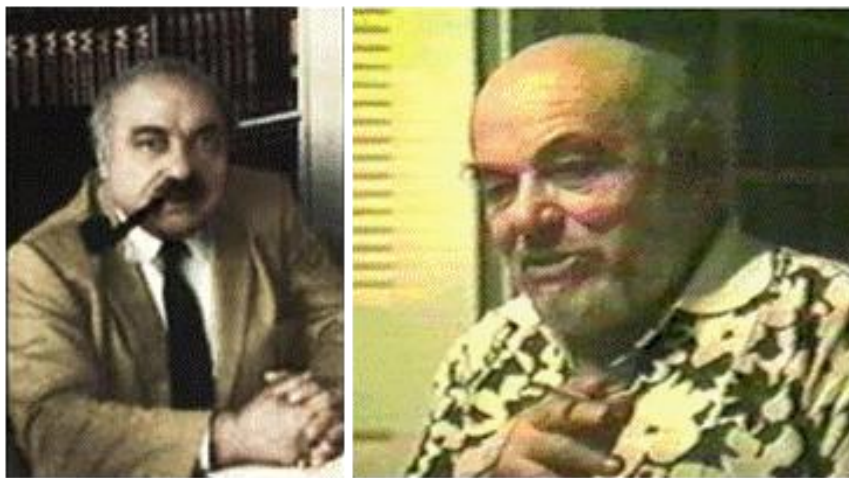


Figure 1 Well known HHO inventor: Yull Brown [22, 23].

HHO gas was called “Brows gas” because it was first tested with ICE by Yull Brown. He developed a water fueled engine which made many people be stunned and think it unbelievable to run engine with water.

However, the first person who discovered HHO fuel gas is William A. Rhodes. He produced a mixed gas which that time many scientists assumed: it was a mixing of hydrogen and oxygen in a chemical structure of diatomic elements, this HHO produced by the multi-cell oxy-hydrogen generator, and his patent: # 3,262,872 was issued in 26 July 1966.

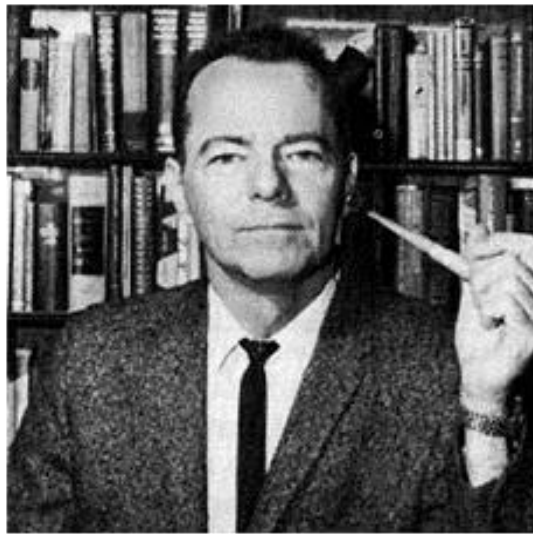
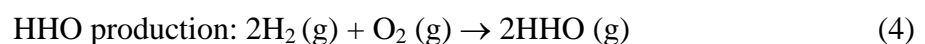
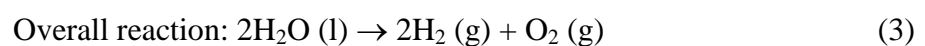
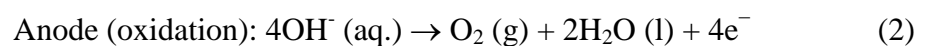
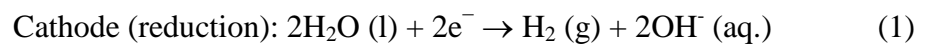


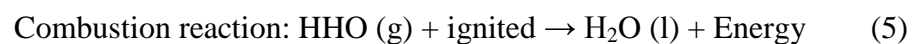
Figure 2 William A. Rhodes [24].

HHO is produced by splitting water molecules (H_2O) be two components as hydrogen and oxygen (see figure 3.).

The basic reactions of the HHO production are



The chemical reaction by combusting HHO show as below



From a reaction (1), the hydrogen gas will be generated at cathode electrical pole (-) and at anode electrical pole (+) is oxygen gas as a reaction (2).

There are many researchers and inventors doubted in the real existence in HHO fuel gas, they would like to know: how much the input energy require for HHO production and how much energy will be released by combustion.

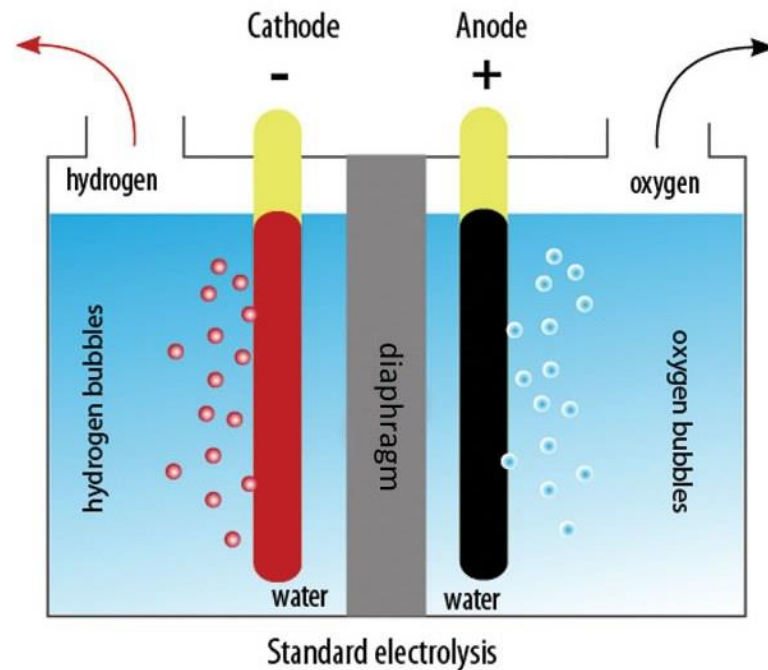


Figure 3 Standard electrolysis [50].

Puharich (1970) studied in the energy requirement for splitting water molecules be the gases of hydrogen and oxygen. He found the molecules require ΔG 249.68 Btu for production and the energy will release with ΔH equal 302.375 Btu by combustion reaction where hydrogen and oxygen are ignited [25].

There are many ideas for the characteristic of Brown's gas. Investigators assume: there are both diatomic and monatomic have performed in its molecules. In general, by comparing between the physical property of hydrogen and HHO gas, hydrogen has a standard bond strength estimate 23 kJ/mol but HHO have a lower than this value. To study in the existence of HHO, electromagnetic field change which occure in the stept of transform diatomic to monatomic is focused.

Yull brown discovered the excellent methode to produce HHO gas in a partly of electrical current signal form which feed into the electrolysis process. By using a small careful electrical current or pulse signal, the HHO production throughput will increase more than thousands times with the high current consumption. He tried to contribute new sheaper clean fuel that provide higher thermal efficiency.

Better MPG indicated the monatomic that call “ free radicals” have energy more than the common diatomic about three times. This point made many inventors interested to investigate in the best effective method to producing lot of free radicals.

Some inventors fed a pulse-electrical current signal to the electrical cells that submerged in the electrolyte solution. The different shape of pulse signal such as square-wave pulse was studied, pulse width were controlled at the appropriate frequencies tuned that matched with the space-apart between positive and negative charge.

In 2008, Steve Windish reported; for a perfect mixture of 66.67% of hydrogen with oxygen, there will be an implosion reaction instead explosion that maybe the result of water product-forming [26]. This result is useful to explain in the “over unity” phenomenon. Some reachers suggested the over unity where the HHO combustion energy release more than input energy to produce HHO maybe comes from the state of monatomic hydrogen. There is a lot of assumption in this concern, if this excess energy in not come from monatomic hydrogen, it should have a some source of power that provide high energy field.

Moray King (2001) described; the excess combustion energy of HHO is not caused by simply diatomic hydrogen molecules it could be other elements that he call “charged water gas clusters” where exist of a type of plasmoid or plasma vortex ring. Those reasons maybe the cause of implosive reaction type of HHO gas [27].

Viktor Schauberger (1885-1958) who is scientist and engineer studied about vortexes of energy and is the first person who has observed the phenomenon of the stoichiometric mixture of HHO gas. He described the vortices inside HHO molecule behave like the surface of lakes that made an appearance of energy occurred by unknown energy source. He also created an “implosion generator” whice work by rotate one cone-shaped spiral inside with the condition of vacuum pressure and exactly 4°C operating temperature, and provide for the implosive phenomenon inside [28].

Trombly offered very interesting result, he found the volumetric unit of water is 1,867 volumetric unit and after implosion of HHO gas, most if not all of

1,867 unit of the gas will become one unit of vapor in very short time less than 0.001 second. We can conclude it is a nearly 100% backward water forming reaction and it is an endothermic not exothermic reaction. He also studied the Schauberger's generator, and assumed the substance which Schauberger has found is HHO gas that was occurred via the electromagnetic potentiation in the vortices of fluidic electrodynamics and is the result of explosion or implosion [29].

Trombly is also studied in the Brown's experiment that provide 15-mm wall thickness of steel cylinder. In the beginning of Brown's experiment, he has full filled the cylinder with water and then blew the positive-pressure-HHO gas replaced. At the top of cylinder the Tesla-type spark plug was installed. When the spark plug was ignited the water that before was replaced by gas was sucked into the cylinder due to the effect of implosion processes [29].

He conducted his experiment same as Yull Brown and he invited the president of a major oil company came to relize the new effective fueled energy, HHO. He proposed to develop the engine with higher efficiency and created zero pollution. That president relized that HHO could be replaced fossil fuel in the future.

1.2.1.1 HHO Applications

With the specific of HHO properties, HHO applied to many applications such as production of electricity, atmospheric motors, welding and brazing, hydrogen production, pure water production, air conditioning and cooling, destruction of toxic wastes, underwater welding, nuclear waste decontamination, glazing and Kiln operation, production of hard materials, drying of fruit and legumes, coal to oil conversion, oxygen production, deep-sea life support, silica conversion, curing, cleansing of smokestack, graphite production, mineral separation, water pumps, fuel Cell, heating, space life support, vacuum systems, ore separation. All in application, the item: atmospheric motors is one of the most topic that many people interested in because there are many advantages points by consume HHO instead oil such as the lower cost with no pollution.

Yull Brown also studied in application of welding by HHO gas, he found HHO can generate a very cool flame that can touch in a short time by not

burning the skin, it able to use for weld metal or destroy a brick. When the frame is placed on a ceramic, the surface temperature will increase to over 2,500°C. In the open air, the frame temperature is 135°C. With the same flame apply to aluminium metal, the temperature is 702°C and for the brick is 1,704°C.

George Wiseman informed; for him HHO is not completely consist of the hydrogen gas but it is the electrically expanded water that called “ExW”. Inventor, Stanley Meyer conducted a car running by water, his work could explain about the “ExW” very well. He designed an special injectors for replace the car’s spark plugs. This injectors were an electrified to generate an special resonant frequency where operate with the on-board hydrogen fuel cell. Hydrogen and Oxygen gas (contain of monatomic and diatomic) from electrolyte process were injected into engine through the air intake manifold. He applied this knowledge with his car; Volkswagen did buggy and run engine with 100% HHO.

In Japan, HHO also was studied but they called it “Ohmasa gas”, Ryushin Omasa, president of Japan technology company in Tokyo described about HHO improvement in his country, Ohmasa gas likely consist of diatomic and monoatomic of hydrogen and oxygen, support to Wiseman with ExW concept. The HHO production method at Japan is they produced it by use 100 Hz wave that may be like RF frequency by Meyer. Omasa informed they can store HHO gas in a long time and also demonstrate the real appication by real running with both motorcycle and car. He affirmed vehicle can run with 100% HHO gas. [30]. John Kanzius (1944-2009) found the method to burn water while studying to cure for a cancer by dose radio frequencies (RF) like Meyer and Omasa even he maybe used the different range of wave frequencies [31].

There are some inventor tend to studied a HHO as a booster, they used very small amount of HHO dosed into engine by mixing with the intake air and fed into cylinder. The ratio of HHO and fossil fuels were varied in many ranges and each range will run in many conditions. HHO application in this part was generated by a small kit of HHO generator which consumed the DC electrical current from compact battery which installed by original manufacturer. In this case, if require the higher HHO production rate, the experimenter can get by add a new battery with same voltage series with the first one. There are reports about using 12 volt DC battery; the

current consumption with electrolyser consume current at estimate 20 amps and if double that battery be 24 volt, it will be perform with higher current consumption of 40-50 amps.

The empire hydrogen fuel enhancement system (EHFES) is the system that used an electronic device (ECU) to optimize the HHO production throughput while running the engine. This system will calculate when the HHO could feed into engine and how much current is required. A small HHO throughput will act like a catalyst to improve the combustion by mainly use fossil fuel. The main objective of this application is for improve the combustion efficiency. However, there still have a problem while running EHFES with newer cars where was designed with the new technology of controller. These cars were installed an oxygen sensor at the exhaust gas to value the oxygen still maintains after combusted inside cylinder. If still running a car with the original default parameter, while HHO was feeding into the engine, ECU will detect the high amount of oxygen by sensor then analyze and have a command to increase a dosing of gasoline or diesel that mean we will lose some fuel by adding HHO. So, to achieve higher engine efficiency by adding HHO, car owner should change a air-fuel ratio parameter at ECU from 14.7:1 be 20:1.

Inventor, Chistoph Beiser initiated an idea to keep homes warm by using HHO. He indicated the multiple safety features are workable to protect accident by explosion, safety bubbler can protect a spark by flash back in to the HHO generator. He studied in HHO production by different designation of HHO generator, he built the classic square-shaped dry cell and found only one hole that for release HHO gas and refill electrolyte solution provide a HHO production throughput better than two hole. 220-volt was fed into dry cell and produced 1 litre of HHO in one hour use an electrical power estimate 1.9-2.5 watts [29].

The main operating cost of electrolysis process is cost by electrical consumption. So, some inventors solve this concern by using the electricity from sola-cell electrical generator. That's mean we will get a better benefit by lower cost of HHO fuel. However, for internal combustion engine (ICE), it can product the electricity by itself because normally, the manufacturer would install a compact electrical generator (DC, dynamo) with all vehicle.

Table 1. Vehicle with average fuel consumption [29].

Vehicle	Average Fuel Consumption		Improvement
	Baseline (mpg)	With EHFES	
2003 KW cummins 15-Litre ISX	4.10	5.10	24.39%
1997 KW 3406E Caterpillar 14.6 Litre	4.01	4.82	20.20%
1997 KW Detroit 12.6 Litre	4.50	5.37	19.33%
2012 KW Cummins 15-Litre SX	5.29	6.11	15.50%
2011 Freightliner Detroit 15 Litre	4.50	5.50	22.22%
2004 Mazda RX8 (Rotary)	15.12	18.48	22.17%
2008 Ford F350 6.4-Litre Turbo Diesel	15.03	18.09	20.34%
2007 Dodge 5.9-Litre Cummins Turbo Diesel	16.00	19.85	24.10%
2000 Lincoln Navigator/ 5.4-Litre Gas	15.60	19.25	22.53%
2007 GMC W5500 5.4-Litre Diesel	11.44	13.29	16.19%

HHO also using for reducing a radioactive from an atomic power generator [32]. An initial amount of radioactive was reduced from 1/3 to 1/120 by burning inside a brown's incinerator.

Dr. Andrew Michrowski informed by took an experiment at Australia and USA; HHO can reduce radioactive particles about 50 percent. Michrowski and Poringa (2000) informed the real experiment at China's Baotou's Nuclear Fuel Component Plant (No.202), they used HHO treat a cobalt-60 radiation source. They found the radioactive decreased approx. 50 percent. Include with other experiments at a present, HHO able to reduce a radioactive more than 50-95 percent.

In Japan, Omasa offered to the Japan official to help people by reduce the radiation at Fukushima Daiichi Nuclear Power Plant. He suggested to using a nano-bubbles agitate with the thing which is a cause of nuclear transmutation. He informed this method could reduce the radio-active be zero contamination [29].

There is no other method capable of producing such a gas. Browns Gas is a new product and there is no literature describing its properties which are sufficiently different from a combined molecular hydrogen and oxygen gas mixture, in 2:1 proportion, to be significant in industrial and commercial applications. Brown, 1979



Figure 4 Name plate of Yull Brown's multiple HHO generator [33].



Figure 5 Multi-HHO generator unit (Left) and system controller (Right) [33].

The HHO behaviors and characteristics

1. By using with an internal combustion engine, the product by reaction inside engine cylinder is vapor.
2. No smoke after used with heater in the house completely affirms: HHO is safe for living thing.
3. HHO does not burn skin in a short time touching because cool flame is occurred while having the combustion.
4. The combustion reaction of HHO is implosion type due to the recombination of H and O be water, and the volume after took a combustion is lower than the initial gas volume; 1:1860
5. Heat steel with a flame of HHO, the grain structure inside it will be changed and provide better property in the partly of rust protection.
6. HHO can use to produce a composite material such as fuse plastic to Titanium
7. Effective radioactive treatment by use HHO flame direct contact to Cobalt-60 and Americium, the radioactive were reduced 70 and 96%, respectively.

1.2.2 Characteristics of HHO

General theory of HHO, described HHO gas is a fuel gas that splitting from water that consisted of hydrogen gas (H_2) and oxygen gas (O_2). The electrochemical reaction process of HHO production is an electrolysis where electrical current was fed across to the electrodes: cathode and anode in which were submerged in the alkaline electrolyte solution. There are many electrolyte solutions workable for this production such as NaOH and KOH.

A mixing ratio of Hydrogen and oxygen 2:1 is enough to perform the maximum thermal efficiency in application of applying with internal combustion engine. However, there are many scientists, engineers and inventors doubt in the actual existence of the combination of HHO molecule because they found; the amount of energy released after combustion is higher than pure hydrogen diatomic molecule.

Ruggero Maria Santilli who works at the Institute for Basic Research Palm Harbor, FL, U.S.A. investigated in the structural of HHO mixture in 2006. His

literature was published in titled “A new gaseous and combustible form of water” with the international of hydrogen energy that published by Elsevier publisher, he investigated the combination of HHO by using many measurement methods. Unclear outstanding was solved and found; there were composed of H and O atoms, the molecules of H_2 , O_2 and none separated H_2O molecules exist in the HHO molecule, he called this combination substances is “Magnecules” [2].

As below figures, the figures from number 6 to 12 illustrate the result of HHO characteristics investigation and for the number of 25 to 31 is the model of HHO by Santilli.

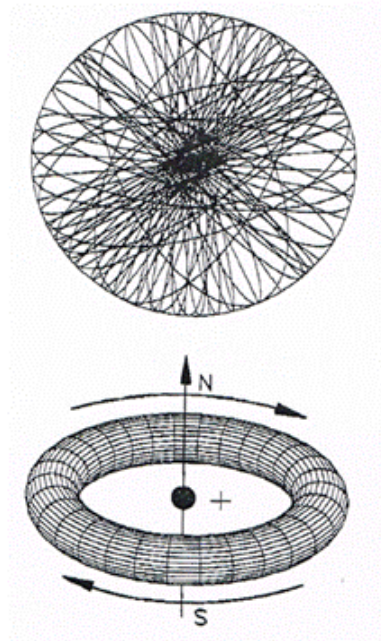


Figure 6 The conceptual rendering of an atomic hydrogen (H) [2].

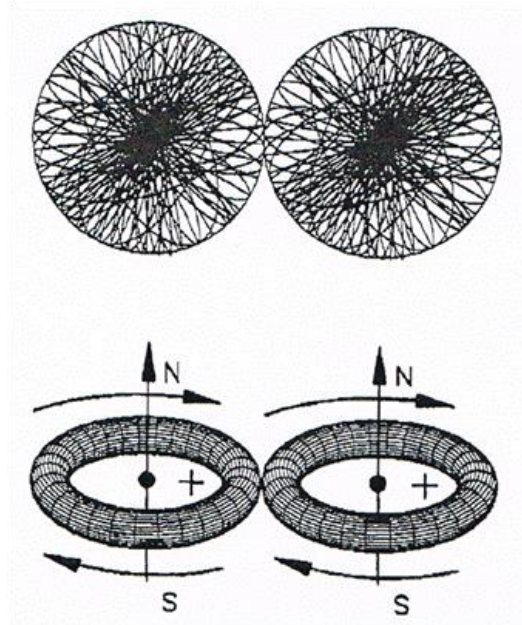


Figure 7 The conceptual rendering of the valence bond of two H atoms [2].

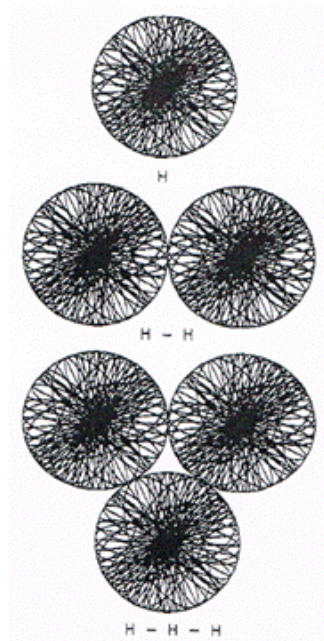


Figure 8 The conceptual rendering of H, H₂ and H₃ in HHO gas [2].

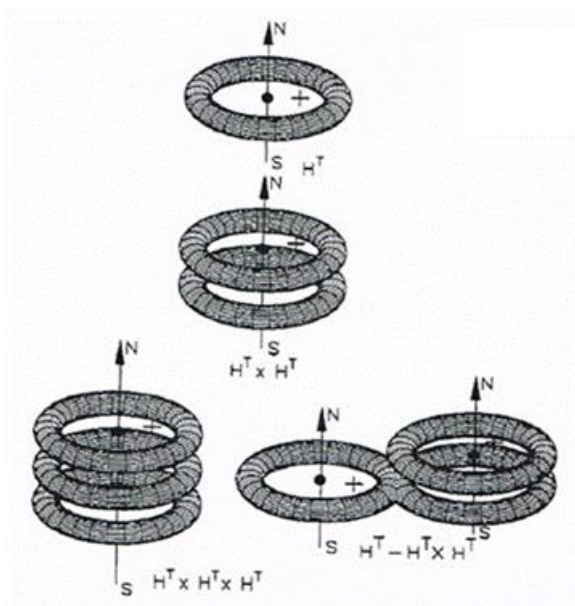


Figure 9 The conceptual rendering of the H- bond in the HHO: H (top), HxH (middle), HxHxH (left), (H-H)xH (right) [2].

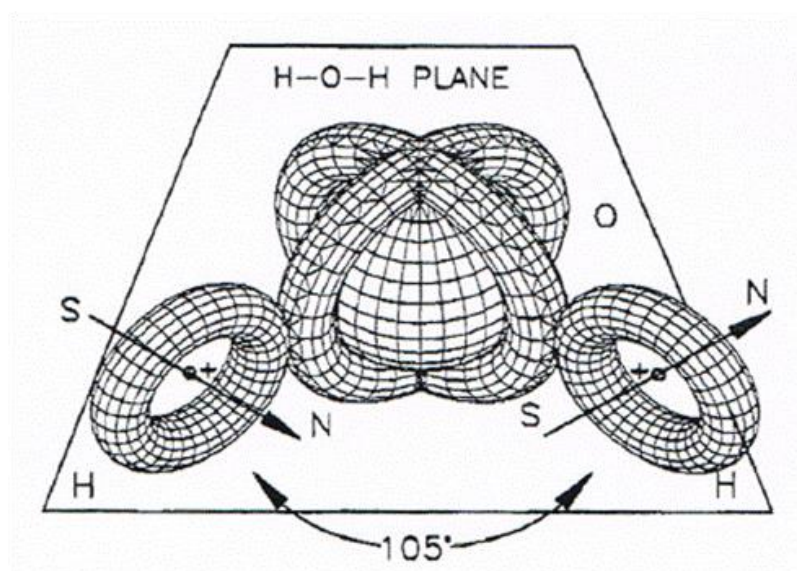


Figure 10 The conceptual rendering of water: H₂O [2].

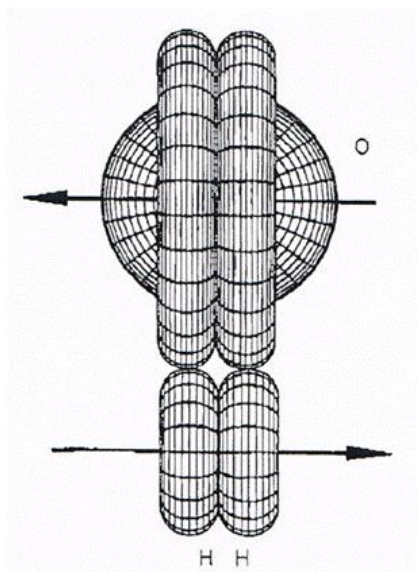


Figure 11 The H-O-H molecule in which all electric polarizations have been removed [2].

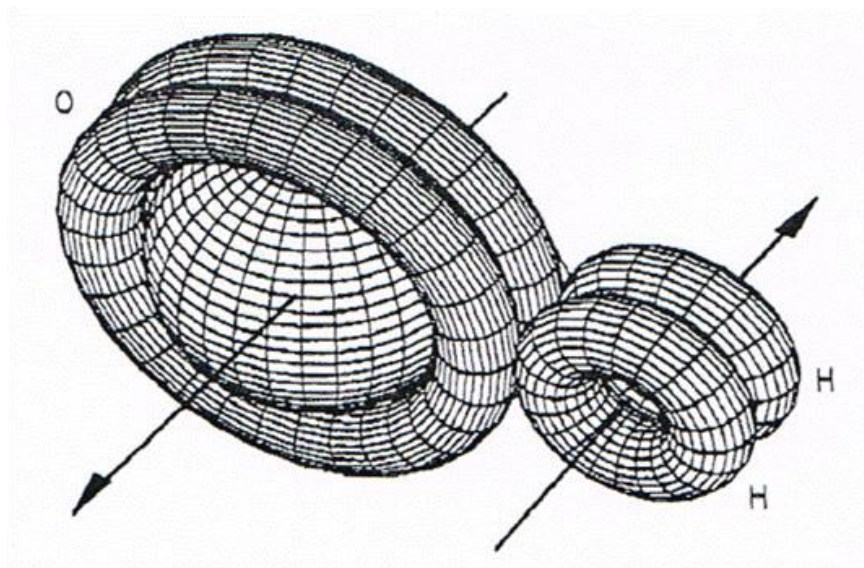


Figure 12 Magnetic polarities of the two H-atoms, as well as the unstable character of the configuration [2].

Wall (2010) studied in HHO application with internal combustion (I.C.) engine. He found a compressed hydrogen which feed into the intake of I.C. engine would improve the engine efficiency, using electrical power that was produced by engine does not increase an overall system efficiency, using HHO from a common-ducted electrolysis unit improve the engine efficiency 20% [34].

Wall also found the mixture (HHO) was not consisted of only hydrogen (H_2) and oxygen (O_2) gas. By mass spectrum analysis measurement, he found there were consist of diatomic and mono-atomic type of hydrogen and oxygen included with plasma water exist in this mixture. A flame color of HHO was one characteristic that many researchers and inventers interested in because it provided a specific temperature and heat flux while combusting in the air and spotting on the various material.

Yull Brown was the first inventor who studied in characteristics of HHO flame. He used HHO for welding and heat material. He found HHO able to create a very cool flame that could be touched in a short time. The temperature of flame is 135°C . If used HHO flame spotted at metal, ceramic or glass surface, the surface temperature will increase over 2500°C . For aluminium and brick, it can heat up to 702 and $1,704^\circ\text{C}$, respectively.

Prisecaru (2008) studied the validation of HHO gas cutting flame CFD model. Hydrogen and oxygen gas were mixed in a quasi-stoichiometric proportion. The experiment set up at gas flow rate $750 \text{ Nm}^3/\text{h}$, gas pressure 0.2 MPa , gas temperature $20\text{-}47^\circ\text{C}$ [35]. Prisecaru found a flame of HHO gas (H_2 mixed with O_2) had a specific characteristic cause by a huge oxidation rate, the temperature at the primary zone of flame point display about 3036°C . At the secondary combustion zone which defined by considering between the length of flame and nozzle diameter 10 to 15 times, the temperature of flame was about 645°C .

1.2.3 HHO Properties

At atmospheric pressure, HHO has an auto-ignition at estimate 570°C (1065°F) and the minimum energy require for ignition estimate 20 micro-joules at STP condition. At the percentage of hydrogen of 4.0 and 95.0%, HHO can burn when

it ignited. The product after combust HHO is only partly of water and conduct heat of reaction 241.8 kJ per every mole of H₂ burned. The maximum HHO flame temperature is 2800°C.

At a present, there are no much more properties data of HHO fuel gas have generally presented in social network and text book, and due to hydrogen is the main component that contain in HHO molecule. So, many scientists, engineers and inventers use the properties data of the hydrogen table instead.

Table 2 Density of Comparative Fuels [36].

Substance	Vapor Density (at 68 °F; 20 °C, 1 atm)	Liquid Density (at normal boiling point, 1 atm)
Hydroxy (HHO)	0.033399 lb/ft ³ (0.535 kg/m ³)	- -
Hydrogen	0.005229 lb/ft ³ (0.08376 kg/m ³)	4.432 lb/ft ³ (70.8 kg/m ³)
Methane	0.0406 lb/ft ³ (0.65 kg/m ³)	26.4 lb/ft ³ (422.8 kg/m ³)
Gasoline	0.275 lb/ft ³ (4.4 kg/m ³)	43.7 lb/ft ³ (700 kg/m ³)

Table 3 Heating Values of Comparative Fuels [36].

Fuel	Higher Heating Value (at 25 °C and 1 atm)	Lower Heating Value (at 25 °C and 1 atm)
Hydroxy (HHO)	-	51,966 Btu/lb (120.90 kJ/g-H ₂)
Hydrogen	61,000 Btu/lb (141.86 kJ/g)	51,500 Btu/lb (119.93 kJ/g)
Methane	24,000 Btu/lb (55.53 kJ/g)	21,500 Btu/lb (50.02 kJ/g)
Propane	21,650 Btu/lb (50.36 kJ/g)	19,600 Btu/lb (45.6 kJ/g)
Gasoline	20,360 Btu/lb (47.5 kJ/g)	19,000 Btu/lb (44.5 kJ/g)
Diesel	19,240 Btu/lb (44.8 kJ/g)	18,250 Btu/lb (42.5 kJ/g)
Methanol	8,580 Btu/lb (19.96 kJ/g)	7,760 Btu/lb (18.05 kJ/g)

Table 4 Energy Densities of Comparative Fuels [36].

Fuel	Energy Density (LHV)
Hydroxy (HHO) Hydrogen	1,737 Btu/ft ³ (64,682 kJ/m ³); gas at 1 atm and 77°F (25°C) 270 Btu/ft ³ (10,050 kJ/m ³); gas at 1 atm and 60°F (15°C) 48,900 Btu/ft ³ (1,825,000 kJ/m ³); gas at 3,000 psig (200 barg) and 60°F (15°C) 121,000 Btu/ft ³ (4,500,000 kJ/m ³); gas at 10,000 psig (690 barg) and 60°F (15°C) 227,850 Btu/ft ³ (8,491,000 kJ/m ³); liquid
Methane	875 Btu/ft ³ (32,560 kJ/m ³); gas at 1 atm and 60°F (15°C) 184,100 Btu/ft ³ (6,860,300 kJ/m ³); gas at 3,000 psig (200 barg) and 60°F (15°C) 561,500 Btu/ft ³ (20,920,400 kJ/m ³); liquid
Propane	2,325 Btu/ft ³ (86,670 kJ/m ³); gas at 1 atm and 60°F (15°C) 630,400 Btu/ft ³ (23,488,800 kJ/m ³); liquid
Gasoline	836,000 Btu/ft ³ (31,150,000 kJ/m ³); liquid
Diesel	843,700 Btu/ft ³ (31,435,800 kJ/m ³) minimum; liquid
Methanol	424,100 Btu/ft ³ (15,800,100 kJ/m ³); liquid

Table 5 Comparative of energy content of hydrogen and fossil fuel. [37]

	Density at STP (kg/m ³)	Ratio of HHV to LHV energy content	Net Calorific Value / LHV (MJ/L) (MJ/kg)		Gross Calorific Value / HHV (MJ/L) (MJ/kg)		Carbon Intensity (g CO ₂ -eq / MJ LHV)	
Crude Oil	856 ± 24	1.052 ± 0.001	36.84 ± 1.05	43.05 ± 1.40	38.76 ± 1.10	45.30 ± 1.47	73.5 ± 2.6	
Petrol / Gasoline	741 ± 4	1.063 ± 0.015	32.70 ± 0.44	44.15 ± 0.74	34.77 ± 0.47	46.94 ± 0.70	70.8 ± 4.4	
Diesel	837 ± 8	1.063 ± 0.011	35.94 ± 0.45	42.91 ± 0.46	38.19 ± 0.47	45.60 ± 0.49	74.3 ± 2.3	
Fuel Oil	959 ± 17	1.058 ± 0.008	39.21 ± 1.09	40.87 ± 0.94	41.50 ± 1.15	43.26 ± 1.00	77.8 ± 2.1	
LPG	533 ± 18	1.077 ± 0.008	24.67 ± 0.80	46.28 ± 0.74	26.57 ± 0.86	49.84 ± 0.80	63.9 ± 2.1	
Kerosene	807 ± 6	1.053 ± 0.001	35.24 ± 0.41	43.69 ± 0.51	37.10 ± 0.43	45.99 ± 0.54	72.0 ± 1.8	
Hydrogen	(35 MPa)	23.65 ± 0.09	2.837 ± 0.003		3.355 ± 0.004		0	
	(70 MPa)	39.69 ± 0.16	1.183 ± 0.001	4.761 ± 0.005	119.95 ± 0.13	5.631 ± 0.006		141.88 ± 0.16
	(liquid)	72.41 ± 0.72		8.685 ± 0.010		10.273 ± 0.011		
	(kg/m ³)	(HHV / LHV)	(MJ/kg)	(MJ/kg)	(MJ/kg)	(MJ/kg)	(g/MJ LHV)	
Coal		1.050 ± 0.004	-	25.75 ± 2.64	-	27.05 ± 2.77	95.7 ± 7.0	
	(kg/m ³)	(HHV / LHV)	(MJ/m ³)	(MJ/kg)	(MJ/m ³)	(MJ/kg)	(g/MJ LHV)	
Natural Gas	0.768 ± 0.039	1.109 ± 0.003	35.22 ± 2.22	45.86 ± 3.95	39.05 ± 2.47	50.84 ± 4.38	56.9 ± 3.4	
Hydrogen (1 atm.)	0.0838 ± 0.0008	1.183 ± 0.001	10.05 ± 0.01	119.95 ± 0.13	11.88 ± 0.01	141.88 ± 0.16	0	

Advantage points of hydrogen energy, about energy content, hydrogen has energy content more than gasoline or LPG or diesel more than three times, and also has higher auto-ignition temperature which contribute more safety factor for real application with IC-engine or other combustion devices such as burner and cooking stove. However, as we know, more powerful energy should be operated with more safety management. Operator should use a safety device which suitable for each applications.

1.2.3.1 Economic and energy balance

In 2011, the efficiency of electrolysis of water to produce HHO gas is at 57%. The electrical supply is lost as heat.

- By using potassium hydroxide as electrolyte solution, the efficiency of electrolyte reach between 70 to 80% at high operating electrolyte temperature (800 to 1000 °C) on solid electrolytes. The hydrogen production throughput 1 m³ require 4.3 to 4.9 kWh electrical energy.
- The current efficiency of HHO production by electrolysis process is about 70%.
- Running HHO production by using DC pulse-signal increase the production efficiency better than normal DC more than 100%.
- To apply HHO with the internal combustion engine (ICE), the combustion process is unnecessary to supply access air from outside because the molecule of HHO consists of appropriate H:O ratio that release energy after combustion enough for driving vehicle with good performance and only one product; vapor can use to re-process again and again by no toxic pollution.

1.2.4 Comparative of Hydrogen and Fossil Fuel Cost

American water work association, reported the hydrogen fuel and gasoline cost illustrates as table below

Table 6 Comparative of cost of hydrogen and gasoline. (American Water Work Association, United States Department of Energy information Administration (EIA)).

Description	Hydrogen	Gasoline
Source	Water	Crude oil
Supply	Infinite	Finite
Renewable	Yes	No.
Carbon Footprint	No.	Yes
Cost per gallon	\$ 1.00-1.80 kg (gge)	\$ 2.32 ¹
Source cost	\$ 1.50 per 1000/gal.	\$ 101.14/ Barrel ²
Refinery costs	\$ 700-\$ 3,500/bpd	\$ 1,000-\$ 5,000/bpd
Miles per kg of Hydrogen	81	18-31
Additional Environmental Impact cost	No	Yes

Sources: American Water Work Association, United States Department of Energy information Administration (EIA). Washington DC, National Hydrogen Association, U.S. Environmental Protection Agency (U.S.EPA) [38].

In 2004 and 2016, the information about hydrogen manufacturer was surveyed and studied in the partly of hydrogen production, they found 96% of hydrogen was produced from fossil fuels and 4% from water electrolysis process. In the part of production from fossil fuels; there are 48% from natural gas, 30% from oil and 18% from coal.

At the present in the part of petrochemical industry, there are two major primary uses for hydrogen. Half of hydrogen quantity was used in the Haber process, in the partly of Ammonia production process which use as a fertilizer for various plans. Other half of hydrogen is used for produce the lighter fossil fuel which

produced by supplying hydrogen gas to the process of catalytic cracking of heavy petroleum.

In 2004, by consider cost of refining, extraction, transportation and product cost. Hydrogen product by steam reformation and electrolysis process is more expensive than product from natural gas approx. 3 to 6 times. To produce high purity hydrogen, one kilogram of hydrogen requires more than 35 kWh of electricity. The cost of hydrogen which produced by steam reformation process is higher than by natural gas approx. three times. And higher than six times by electrolysis process. The relation between hydrogen cost and electricity is a linear function.

ITM Power proposed advances of the electrolyzer and fuel cell technology and described for hydrogen that made from water and using with vehicles, the electricity cost would reduce if made hydrogen from an individual renewable power source of solar cell. Due to hydrogen had a bulk density lower than natural gas estimate three times and when it blow in pipe, it would accelerate the cracking of pipeline. These reasons were cause of high maintenance and material cost and also high risk of leaking and huge explosion.

Pacific Northwest National Laboratory for the US Department of Energy in December 2006 found investment cost of hydrogen plant and gas distribution by pipeline network connection was very high. In the opposite way, the electrical car was more interesting to improve and expand in real situation because it no needed to expand the existing infrastructure for electrical distribution. Every home usually have a prompt electricity connector. The lower peak of electricity consumption that performed at night was available for recharging electric vehicles.

In United States 2004, hydrogen production increased around ten percent per year. Fifty-seven million metric tons were produced. And for 2005, hydrogen in the partly of economic sector is about \$135 billion per year. Increasing of world population and intensive agriculture contributed the high hydrogen consumption, hydrogen was used in many applications. Mostly of hydrogen was used in the Haber process to produce fertilizer (ammonia: NH_3) and converted the heavy petroleum to the lighter molecule structure in the hydro-cracking process to produce vehicle fuel.

The U.S.A. used hydrogen in the process of hydro-cracking approx. 4 Mt/year, 37.7 Mt/year of hydrogen was used to convert the domestic coal to liquid fuels. The factor of hydrogen 5 to 10 was used by hydrocarbon synthetic fuel production. The sources of global hydrogen production, 30% of hydrogen was produced from oil, 48% from natural gas, 18% from coal and 4% from water. The place of hydrogen production is significantly to hydrogen price, in which hydrogen produced on site, the price was approx. \$0.70/kg and \$2.20/kg to \$3.08/kg if not on site.

1.2.4.1 Environmental concerns

There are many topics concern about the effect of using or producing hydrogen gas to global environmental. For the hydrogen which produced by electrolysis process, we found this process is quite appropriate for hydrogen production because it does not produce toxic produce while running the production system, in contrast, the other one product from this process is oxygen gas that necessary for living thing. But for fossil fuel reforming where produce hydrogen from fossil fuels. It leads to a high emissions of carbon dioxide that a cause of global warming situation as we confront in daily living today. So electrolysis process is preferable for hydrogen production due to it provide oxygen gas and none toxic release. For the production cost by electrolysis today, researchers have found the method which increase the production efficiency by using a pulse electrical wave of DC current fed into the hydrogen generator where submerged anode-cathode cell inside.

Even through the production cost of hydrogen is higher than electricity but the advance of hydrogen is producing water after combustion and no limited running time cause by deterioration of energy buffer such as electrical battery. Moreover, the hydrogen production technology has developed by producing the mixing hydrogen gas with oxygen gas that called Brow's gas, hydroxyl gas, oxy-hydrogen or HHO gas matching with internal combustion engine instead pure hydrogen supply. A self- electrical generator which compact with all vehicle's engine

will provide a sufficient electrical DC current enough for HHO self- production for individual running engine.

If hydrogen leak to atmospheric it will occur some problem in the stratosphere cause by ultraviolet radiation. The free radicals of hydrogen will act like as catalysts and destroy ozone in the depletion process.

1.2.4.2 Hydrogen safety

Hydrogen is odorless and cannot detect by smell. It leads to explosion when it was ignited by touching with a spark point or flame. Hydrogen with a condition: high velocity flow in pipe line or vessel able to erode the steel wall that cause of leaking to outside. If it was leaked in enclosed areas it will be cause of huge explosion. To protect the huge explosion, hydrogen vessel or pipe line should fabricate in the open areas and have to design the conveying system with high safe priority such as combined with the isolation system, have high-low pressure indicator and alarm and hydrogen detector above vessel or pipeline at the weak point.

Generally, there are the standard codes of hydrogen that implemented by the National Fire Protection Association. This codes was defined by considering in engineering knowledge in the partly of material handling and storage. The Canadian Hydrogen Safety Program reported hydrogen fuel is safer than a compressed natural gas. The European Commission informed general public can use hydrogen in daily living like today's fossil fuels.

1.2.5 General Applications and Others

HHO can use instead fossil fuel because it has a thermal efficiency enough for internal combustion. By considering in an energy balance of thermodynamic process, the energy of combustion of HHO is higher than fossil fuel and no pollution in the exhaust gas, the combustion product is only water in a vapor form cause by heat inside cylinder. For pure hydrogen energy balance in 2004, in partly of hydrogen production, transportation and delivery, all processes require total energy approx. 50 MJ, a thermal energy efficiency approx. 60%. But for gasoline it

requires less energy consumption at the refinery power plant and also for transportation and storage. From power plant to storage tank, the efficiency of gasoline is approx. 80% [39].

There are two parts of energy losses by converting fossil fuel to hydrogen gas: electricity lost 10 percent efficient during transmission along power lines, and 33 percent for primary produce electricity from fossil fuel for electrolysis process. The efficiency loss of hydrogen production is the reason why hydrogen vehicle was not developed and distributed worldwide in applications. That's why electric vehicles are developed by using light-weight vehicle's frame structure and long operating time of light weight battery.

Norwegian energy system studied the efficiency of hydrogen vehicles compared to other vehicles and found hydrogen fuel cell vehicles have higher efficiency more than electric vehicle (EVs) estimate three times and barely six times for internal combustion engines (ICE). 25% of hydrogen produced from natural gas was consumed by EVs, 13% for a H₂ ICE, 14 % for a gasoline ICE, 27% for a diesel ICE.

By considering with the former technology of hydrogen production, hydrogen was called the least efficient and the most expensive to instead gasoline in the partly of reducing CO₂ that cause of global warming situation. The other technologies are easier to implement with less expensive operation and investment cost due to there are disadvantage in the vision of hydrogen economy.

Because of expensive of hydrogen in economy, Ford Motor Company and French Renault-Nissan have cancelled their research to running vehicle with hydrogen in 2008 and 2009. They designed to contribute the research with other the manufacture and Now GMBH in September 2009. UK Department of energy and Climate Change reported; hydrogen fuel has the high potential to operating with UK transport with no toxic gas release.

Even through, hydrogen can apply with internal combustion engines, turbines and also convert chemical energy to electrical energy for fuel cell and conduct advantage procedure to eliminate green house gas that bring about global warming situation. The researchers found fuel cells are more expensive to produce than existing internal combustion engine. Inventors and engineer have improved fuel

cell which can run parallel with internal combustion engine. This technology reduces the investment cost by using an individual fuel cell for each vehicle. They suggested that should be used this technology at large gas-fired power plants.

One reason that could be the importance reason why fuel cell is not suitable for application is fuel cell requires very high purity hydrogen feed into its cell. The impurity-hydrogen will make fuel cell stack dirty and degrade the lifetime because of sulfur contamination in the steam reformation of natural gas process. Current hydrogen fuel cells contain low power with much of weight if researcher can develop and produce the high efficiency fuel cell. It would possible to use fuel cell parallel running with internal combustion engine and also can be economically viable to power hybrid fuel cell or battery vehicles.

Using the mixing between hydrogen gas and oxygen gas is one idea that suitable to solve concern high NO_x release after taking combustion. At a present we have a membrane technology to filter air and separate air to the pure component of oxygen, nitrogen and others. This technology is useful to install at the intake manifold of internal combustion engine to split N₂ out and supply only oxygen mix with hydrogen fuel in combustion cylinder. The mixing of hydrogen and oxygen is Brown's Gas or HHO.

Yull Brown is well-known in the circle of renewable energy application. The famous success by Yull Brown is real running HHO generator with internal combustion engine. He found the higher combustion efficiency and no pollution with low cost by using HHO fuel gas. His HHO production system is the electrolysis process with alkaline electrolyte solution. Yull Brown has a very brave heart to announce his success to the public while many refinery plant are producing energy by fossil, his work initiate the inspiration of many researchers, inventors and engineers to drive engine with water-fueled (HHO) that he called "Brow's Gas".

1.2.5.1 HHO General Improvement

KEMA GmbH is the public organization which interested in Germany technology. They studied in the HHO generator which running with high current and high voltage consumption. The system was separate be two part individually. The

high voltage and high current generator were installed in a series and both are workable to operating with solar energy and wind energy. The electricity was store in 12 volt DC battery like a buffer of operating current for start-up HHO production at the first time.



Figure 13 Twin HHO generator [40].

Dry cell hydrogen generator is well-known in the society of engineering in the partly of hydrogen energy today. This cell has advantage in many concerns such as it is flexible for running it with high operating pressure and high operating temperature, require low installation area, easy to clean and maintain, occur very low corrosion at the wall of electrical poles, no hydrogen accumulate between cell gap, flexible to up-scale be a pilot scale [25].

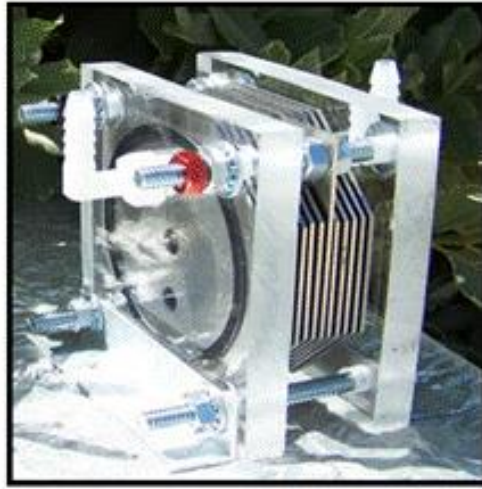


Figure 14 HHO Generator [41].

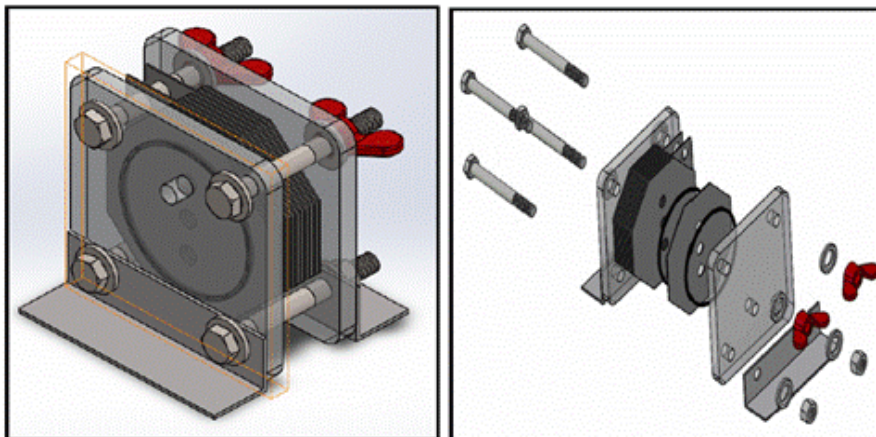


Figure 15 Drawing of HHO generator [41].

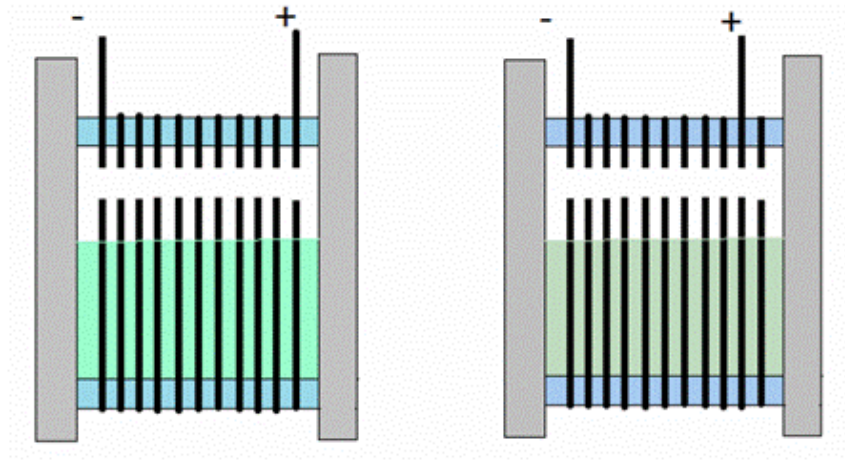


Figure 16 Electrical pole and level of electrolyte solution [41].

Chraplewska *et al.*, (2011) found the electricity power that was generated by itself electrical generator which compact with the internal combustion engine is access and enough for using with HHO generator that running by electrolysis process. They found the engine run with higher efficiency and the vapor product at the exhaust pipe would absorb energy and condense by water. Using pure hydrogen with oxygen provided in better properties of the combusted fuel mixing between gasoline or diesel with hydrogen [42].

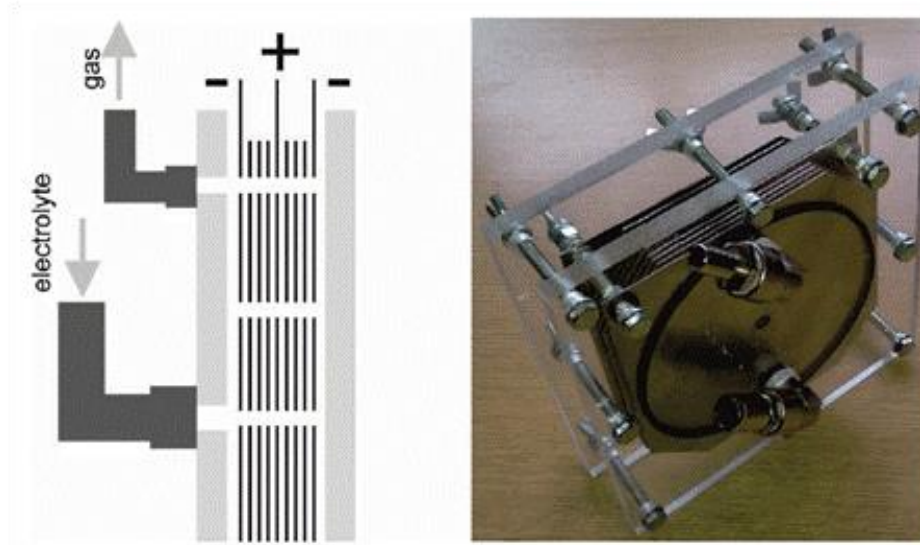


Figure 17 Brown gas generator [42].



Figure 18 Diagram of power supply system of gas generator [42].

Yadav *et al.* (2011) studied in a HHO production by electrolysis process. They informed electrolysis of water could provide hydrogen gas in form of hydroxyl (HHO) which had an ability to use as an alternative fuel for internal combustion engine (ICE). Their research discussed on the various methods for HHO production designation. They blended HHO gas with gasoline or diesel to study the influence of HHO on the running performance of ICE. For electrolyte solution, the alkaline electrolyte solution of KOH was used with HHO generator. They found by running engine with HHO blended with fossil fuels, a brake specific fuel consumption

was decreased, brake thermal efficiency was increased. The engine performance was improved by blend HHO with petrol fuel [43].

Silva *et al.* (2015) designed HHO generator which was used to improve the fuel efficiency of internal combustion engine (ICE). Currently three types of engines such as Spark ignition engine, Compressed fuel engine (Diesel engine) and Turbine engine were operated with uncompleted combustion condition and often have remain unburned fuel after the burning process. The remains of unburned fuels are the cause of pollution. By using HHO with internal combustion engine (ICE), the HHO generator system able to improve the power of ICE and reduce the air pollution [41].

Khulbe *et al.* (2014) applied the HHO gas that was extracted from distilled water by electrolysis process with four stroke SI engine of a motorbike by no modify at the original engine designation. The additional HHO fuel led to providing more power efficiency, the petro fuel consumption reduced approx. 25% depending on blending ratio between HHO and gasoline. Amount of HC and NO_x were reduced 38% and 50%, respectively [44].

Vino and Ap (2012) described HHO fuel gas able to improve the low-grade fuel like a high-octane gasoline because of blending HHO with any fuel will increase the octane rating which protect the before ignition phenomenon that cause of “knocking”, noise and less power. The LPG-HHO engine, by blending HHO with LPG enhance combustion efficiency, the LPG consumption was reduced 20%. The emission of harmful pollutions such as CO and unburned HC were reduced, the engine performance increased approx. 5.7% [45].

Naresh *et al.*, (2014) studied the water hybrid vehicle that using HHO that produced by electrolysis process, the stainless steel plates were used as anode-cathode poles inside electrolysis generator. The internal combustion engine (ICE) would provide the electrical current stored in battery which supply current across submerged electrical cell. This hybrid system provided low emission and higher engine performance [46].

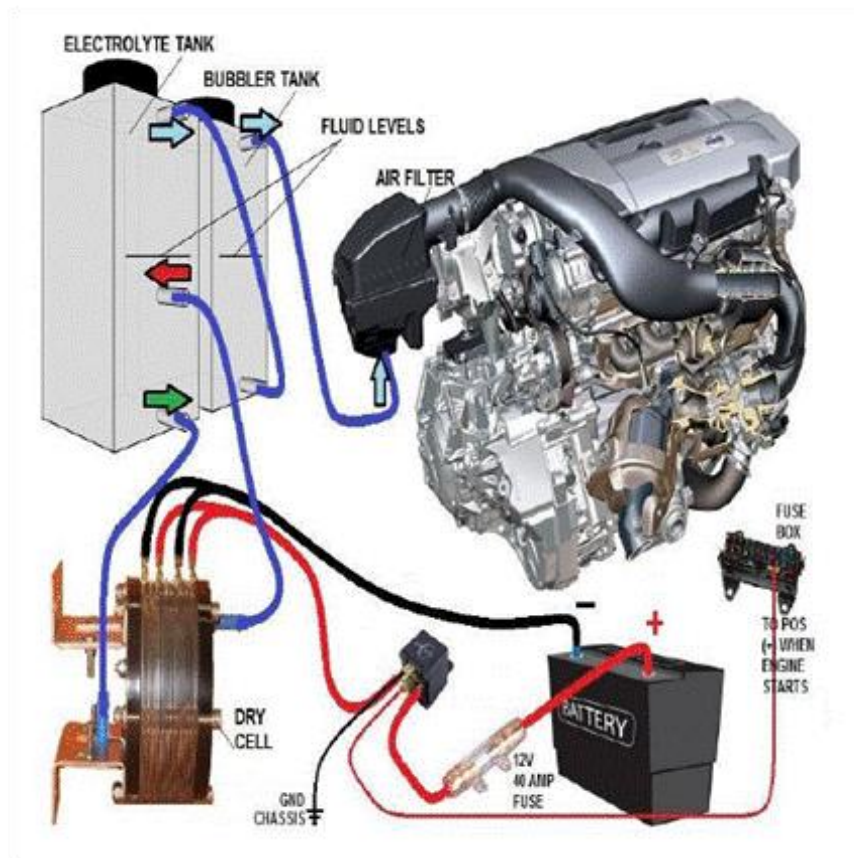


Figure 19 Block diagram of HHO dry cell.

Putha and Babu (2015) investigated in the performance and emission characteristics by feeding HHO into a four stroke single cylinder S.I. engine with original designed and without buffer tanks. Comparing to pure gasoline operation, HC was reduced 6.7%, pollution of the vehicle was reduced almost zero part per million (PPM). The vehicle consumed HHO fuel using based fuel less than before but without pollution. The fuel mileage by using HHO would increase as much as 60% by no need modification of standard engine [14].

Lodhi *et al.* (2015) studied in the overview of HHO fuel gas production, they found it possible to use HHO generator produce fuel vapors of HHO with KOH electrolyte solution. They found the engine efficiency increased 25 to 28%, with thermodynamics advantages using 1.3 to 1.7 volt at current density 0.4 Amp per square centimeter would increase the total efficiency to 40-50% [47].

Rajasekaran *et al* (2015) investigated in the alternative fuels which produce low emission. They found the mixture fuel between HHO and gasoline and liquefied petroleum gas (LPG) could be conducted on a 150cc single cylinder petrol engine at various speeds (rpm). The test indicated both mixtures lead to a reduction of fuel consumption and emission. By using HHO with fossil fuels able to reduce the exhaust gas that cause of global warming situation [48].

1.3 Review of Literatures

1.3.1 Phase I: Investigation of a Closed-loop HHO Production System using AC supply

HHO (hydroxy gas or Brown's Gas) fuel gas is a clean and renewable energy due to the absence of hydrocarbon compounds, carbon dioxide and other hazardous gases that are released during combustion. HHO, which is produced by splitting water into hydrogen and oxygen molecules through electrolysis, releases vapor as its combustion gas.

Momirlan and Veziroglu (2005) described that electrical current can be used to separate water into its components of oxygen and hydrogen [1]. Santilli (2006) also introduced the working hypothesis of the existence of HHO fuel gas as a new cluster called "magnecules" using numerous experimental measurements [2]. The researcher found that HHO gas is composed of H and O atoms, dimers H-O, molecules of H₂, O₂ and H₂O. Furthermore, Santilli (2001) also indicated that one of the most important features of magnecules is their anomalous release of energy in thermochemical reactors which in turn, could serve as a possible source of new, clean fuel [3].

Dülger and Özçelik (2000) presented the production of HHO using water electrolysis that can be installed on different vehicles of various engine types and sizes. The system is based on the electrolysis of water in closed cell electrodes, and the feeding of the HHO gas directly into the intake manifold of the engine. The

researchers concluded that emissions were reduced by up to 40-50% depending on the type of the engine without any reduction in engine performance. Moreover, they found that the system led to 35-40% fuel savings [4].

Likewise, Yilmaz *et al.*, (2010) studied the usage of HHO produced by electrolysis as a supplementary fuel in a four-cylinder, four-stroke, compression ignition (CI) engine without any modification and without the need for storage tanks. The HHO modified system resulted in increasing engine torque output by an average of 19.1% and the reduction of CO emissions by an average of 13.5%, HC emissions by an average of 5% and SFC by an average of 14% [5].

Ammar and Al-Rousan (2010) proposed an HHO generator installed in a Honda G 200, 197 cc, single cylinder engine and found that by feeding HHO mixed with gasoline, the fuel consumption was reduced by 20-30% with lower exhaust temperature [6]. Moreover, after running the experiment with the same gasoline engine,

Musmar and Al-Rousan (2011) found that NO, NO_x and CO emissions were reduced by approximately 50%, 50% and 20%, respectively [7]. Durairaj, *et al.*, (2012) investigated the production and characterization of bio-diesel by adding HHO fuel gas and found that the use of HHO with bio-diesel produced lower unburned HC, CO and particulates while enhancing the engine power and reducing the engine vibration [8].

In addition, Masjuki *et al.* (2016) tested a mixture of biodiesel fuel with HHO fuel gas using 1% w/w KOH electrolyte concentration. Their results showed that the engine power increased by about 2%, biodiesel fuel consumption decreased by about 5%, and CO and HC reduced by 20% and 10%, respectively [9]. Arat *et al.* studied by feeding 25% HHO with 75% CNG (Compressed Natural Gas) into a non-modified diesel engine and found this mixture increased engine performance and reduced exhaust emission compared to ordinary diesel operations [10].

Baltacioglu *et al.* (2016) tested a pilot - four cylinders - injection diesel engine with alternative fuels; pure hydrogen, HHO, and biodiesel. All fuels were fed into the engine running at 1200 and 2600 rpm. The results indicated that engine performance using HHO fed with the intake air was higher than using pure hydrogen

and biodiesel fuel at standard operation. Nonetheless, they found that the exhaust emissions for pure hydrogen were better than for HHO [11].

EL-Kassaby *et al.* (2016) fabricated an electrolysis generator and fed the HHO fuel into a Skoda Felicia 1.3 GLXi gasoline engine. The researcher found that the engine thermal efficiency increased by 10%, while the fuel consumption, CO, HC and NO_x emissions were reduced by 34%, 18%, 14% and 15%, respectively [12].

Dahake, *et al.*, (2016) also found that HHO enrichment resulted in better combustion and reduced emission outputs in compression ignition engines. The researcher discovered that the thermal efficiency for compression ratio 18 was increased by 9.25% compared to baseline diesel combustion, while the specific fuel consumption was reduced by 15% at full load condition. Moreover, the HC emission was reduced at an average of 33% and CO emission at an average of 23% [13].

Putha and Babu (2015) found that if 100% HHO were to be fed into an internal combustion engine, pollution after combustion would be cut down to almost zero, while the inside surface of the engine was found to be cleaner than engines using purely fossil fuel [14]. In addition, Bharathi *et al.* (2015) found that HHO helped improve efficiency of an engine and its life span [15]. Furthermore, a number of researchers including Desai *et al.* (2014), Chaudhari *et al.* (2015) and Vino *et al.* (2012) have found that by varying the ratio of fossil fuel to HHO gas, there is a high potential for improving engine efficiency and reducing the emission of air pollutants such as HC, CO₂, CO and NO_x [16-18].

For HHO production, Dweepson (2014) found aqueous potassium hydroxide (KOH) to be the most suitable and low cost electrolyte for enhancing conductivity of the electrolysis solution [19], while Göllei (2014) concluded that 20-30% w/w KOH produced the optimal conductivity for this process [20]. Aqueous KOH, typically, is highly soluble in either hot or cold water and will decompose at temperature up to 1334°C. KOH has a melting point of 380°C and a pH of 13 at 1% w/w concentration.

Göllei (2014) also indicated that the higher the temperature of the solution (through electrical current being fed into the system) the more HHO gas could be produced, the closer the anode and the cathode plates are the better the efficiency [20]. Joshi and Naik (2015) reported that ideal operating temperatures and

pressures for HHO production should be from 70-100°C and 1-30 bars, respectively [21]. Thus, the key parameters affecting the rate of HHO production include the concentration of electrolytes, solution temperature, and the anode-cathode distance.

In this research, the experiment was designed to comply with real operations whereby the main necessary equipment components should be operated in conjunction with future-appended auxiliary systems. This conceptuality is useful for scaling up the unit from a pilot-scaled prototype. A closed-loop circulation system deemed more flexible was designed to investigate appropriate conditions for HHO production. The parameters evaluated were: system temperature, electrolyte concentration, and operating pressure, inclusive of vacuum pressure. A/C current supply was utilized so that the positive and negative cycles provide forward-reverse directions that bring about two wires of alternate polarity.

1.3.2 Phase II: Optimization of the Operating Pressure of a Closed-loop HHO production system for operation with an Internal Combustion Engine (ICE)

Global warming is one of greatest threat to humanity according to scientists from around the world and the usage of fossil fuel for internal combustion engines (ICEs) is one the major causes of CO₂ released into the atmosphere. With that in mind, hydrogen and fuel cells have been largely considered as one of the cleanest and most efficient energy source for the future world.

Momirlan and Veziroglu (2005) reiterated that hydrogen and hydrogen fuel cells can be used to fuel vehicles and aircraft and provide power for our homes and offices. Hydrogen can be fed into internal combustion engines as pure hydrogen or blended with natural gas, and are three times more efficient than a gasoline-powered engine. On the other hand, HHO is a relatively new alternative source of clean energy that can produce up to 3 times the energy of combustion for hydrogen [1]. Its combustion releases H₂O vapor as the exhaust from the internal combustion engine (ICE) and can be fed back into the combustion chamber and reused to produce HHO once more (see Figure 1).

Santilly (2006) described the interior oxygen in HHO gas as sufficient for combustion, while the other fuels have to combust with the outside atmospheric oxygen, thus causing a serious pollution problem [2] due to nitrogen in the air which came together with oxygen would converted be toxic gases (NO_x) and also remained unburned HC in the ICE cylinder.

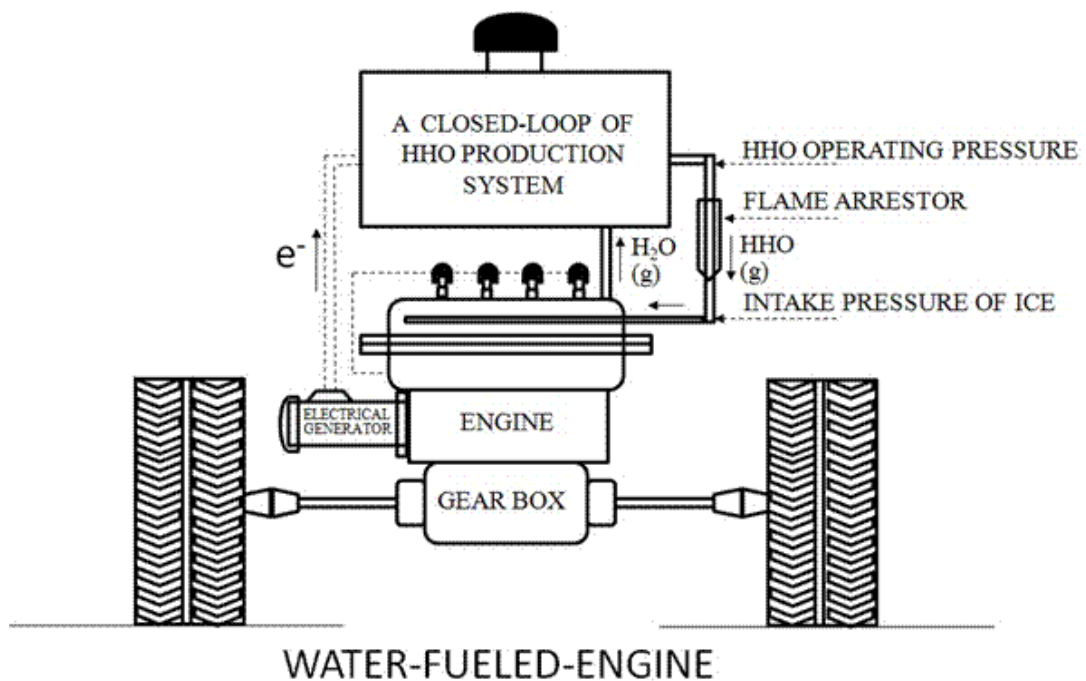


Figure 20 Schematic of water fueled engine.

Andersson (2001) reported that at 80% of the volumetric efficiency of a turbocharged engine with a waste gate and air mass flow rate approx. 0.035 kg/s, the intake manifold pressure and the exhaust pressure varied from 72.0 to 87.0 kPa abs and 110 to 130 kPa abs, respectively [49]. Moreover, Andersson (2002) also found that on a turbocharged spark-ignited (SI) engines with a waste gate and engine speed between 500 and 4500 rpm, the intake manifold pressure varied from as low as 20 kPa abs to 160 kPa abs [50].

In another previous study, Yilmaz, *et al.*, (2010) operated an HHO system without any modification to the engine and found that the torque output

increased by 19.1%. At the same time, CO and HC emissions were reduced by 13.5% and 5%, respectively, while the specific fuel consumption decreased by 14%. Vino (2012), Desai (2014), and Chaudhari (2015) also concluded that using a mixture of HHO gas and fossil fuel improved the ICE efficiency and reduce gas pollutants, including HC, CO₂, CO and NO_x [4-6].

Musmar and Al-Rousan (2011) built and integrated HHO generator with Honda G 200 197 cc single cylinder and found that a mixture of HHO, air, and gasoline produced lower concentration of toxic emission gas [7]. Durairaj *et al.*, (2012) reported that a pre-heating of HHO and air mixed with biodiesel in conventional engines improved the thermal efficiency and reduced the emission of unburned HC, CO and particulates [8]. Ammar and Al-Rousan (2010) found that running a 197 cc (Honda G 200) single-cylinder with HHO gas reduced fuel consumption by 20-30% and yielded lower exhaust temperature and pollution [9].

Moreover, Arat *et al.* (2016) used HHO mixed with CNG (Compressed Natural Gas) and fed them into a non-modified, 3.6 L, four cylinders, four stroke diesel engine. The results showed that this mixture improved engine performance and pollution compared to original diesel engine [10]. Baltacioglu *et al.* (2016) tested HHO and pure hydrogen with a 3.6 L, four cylinders and four stroke diesel engines and found that the engine performance values using HHO were higher than pure hydrogen and standard diesel fuel [11].

Likewise, Masjuki *et al.* (2016) concluded that using HHO mixed with ordinary diesel (OD) and HHO mixed with 20% (v/v) palm biodiesel blended with OD (PB20) with the standard single cylinder ICE contributed to a power increase by more than 2%, reduced fuel consumption by 5%, and decreased in CO and HC emission 20 and 10%, respectively [9]. More recently, El-Kassaby *et al.* (2016) ran a Skoda Felicia GLXi gasoline engine with HHO. The results showed that the engine thermal efficiency increased by 10%, while fuel consumption, CO, HC and NO_x decreased by 34%, 18%, 14% and 15%, respectively [12]. Putha and Babu (2015) reported that using 100% HHO cut down the toxic gas release down to almost zero, while keeping the inside of the engine cleaner than using fossil fuel [14]. Furthermore, Bharathi *et al.* (2015) found that by using HHO gas, not only increased the efficiency of the ICE, but also improved its life span [15].

For a closed-loop alkaline electrolysis process, Dweepson *et al.* (2014) found aqueous potassium hydroxide (KOH) as the most suitable and low cost electrolyte for running HHO process [19], while Göllei (2014) concluded that 20-30% w/w KOH is appropriate for this process [20]. Göllei (2014) also found that using higher operating pressure produced more HHO gas, while closer cell gaps (anode-cathode distance) provided better production efficiency.

Joshi and Niak (2015) recommended that the suitable temperatures and operating pressures for HHO production should be between 70-100°C and 1-30, respectively [21], while Zoulias *et al.*(2004) suggested a range of 70-90°C [51]. However, the vacuum condition at the intake manifold of ICE directly affects the operating pressure the closed-loop HHO production system. The yield of HHO gas produced may be incorrectly predicted due to the fluctuation of the operating pressure. In order to determine the appropriate operating conditions for possible installation to the intake manifold of the ICE as shown in Figure 20, the effects of varying operating pressure on the production of HHO gas in a closed-loop system was investigated.

1.4 Objectives

The objective of this research is the optimization of the HHO production with the closed-loop production system which flexible for running with internal combustion engine (ICE). The research was separated be two phases that are the investigation of a closed-loop HHO production system using AC supply and optimization of the operating pressure of a closed-loop HHO production system for operation with an internal combustion engine (ICE). The objectives of phase one experiment are investigation of the appropriate production conditions for the high HHO production throughput of this production system that are

- The production temperatures. (electrolyte temperatures, operating temperature)
- The electrolyte concentrations.
- The cell gaps set up. (anode-cathode distance)
- The electrode area (cell area, anode-cathode area)
- Electrical voltages supply.
- Electrical currents supply.

Due to inside the intake manifold of ICE is a vacuum pressure. So, the objectives of phase II experiment are the investigation of the effect of operating pressures: atmospheric and vacuum pressure to the HHO production throughput. All experiment results of this research were prepared for the next development of new vehicle generation that will be run with water fuel future.

CHAPTER 2

Research Methodology

2.1 Experiment phase I: Investigation of a Closed-loop HHO Production System using AC supply.

A closed-loop HHO production unit was assembled (Figure 21 and Figure 22) using an HHO generator, a liquid-gas separator, a heat exchanger, a circulation pump (Encapsulated Magnet pump, EYEL4 HS-1, EMP 50/7, S/N Y07163), a condenser, a water trap, an electrical supply (Arc Welder, BX6-160 A.C., JB3643-2000) and flow meter (Rota-meter, AALBORG Orangeburg). A 700-ml glass container housed the HHO generator.

From Figure 21, the HHO generator consisted of a coupled-pair of stainless steel plates serving as the anode and cathode electrical poles. Both electrical poles were adjusted to different gap spacing and can be replaced with smaller or larger plates of different sizes for varying surface area reactions. From preliminary tests, it was observed that HHO throughput generally increased with voltage. For the research, the electrical voltage fed to the anode-cathode poles was set to 52.9 V and the current was varied from 20 to 70 A.

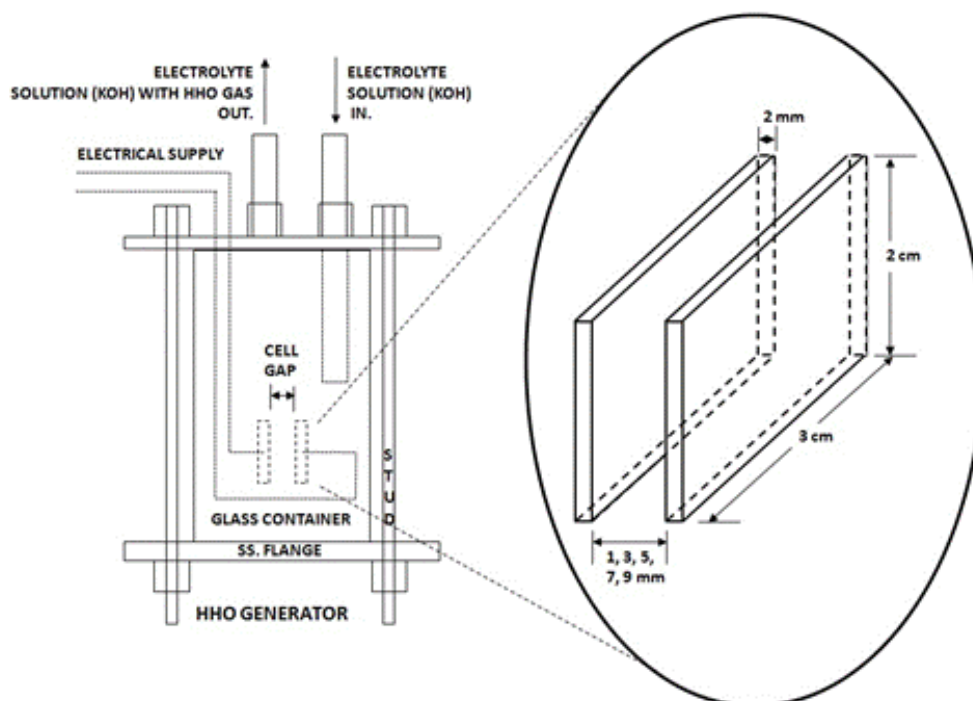


Figure 21 HHO generator with variable anode-cathode distance (cell gap).

A liquid-gas separator was designed using a 6-liter stainless steel tank, and was made to receive the mixed solution of KOH and HHO gas. From the liquid-gas separator, the liquid phase of the KOH electrolyte solution was passed through the ring coil of the heat exchanger and transferred back into the HHO generator using a circulating pump.

Figure 22 illustrates the process flow diagram of the closed-loop HHO production system. The operation begins by turning on the circulating pump. After switching on the AC power supply, electrolysis reaction takes place and HHO gas is produced. The HHO gas then flows into a condenser where water vapor is condensed and collected in a trap. The dry HHO gas leaves the condenser and passes through a Rota-meter where its production throughput (L/h) is measured.

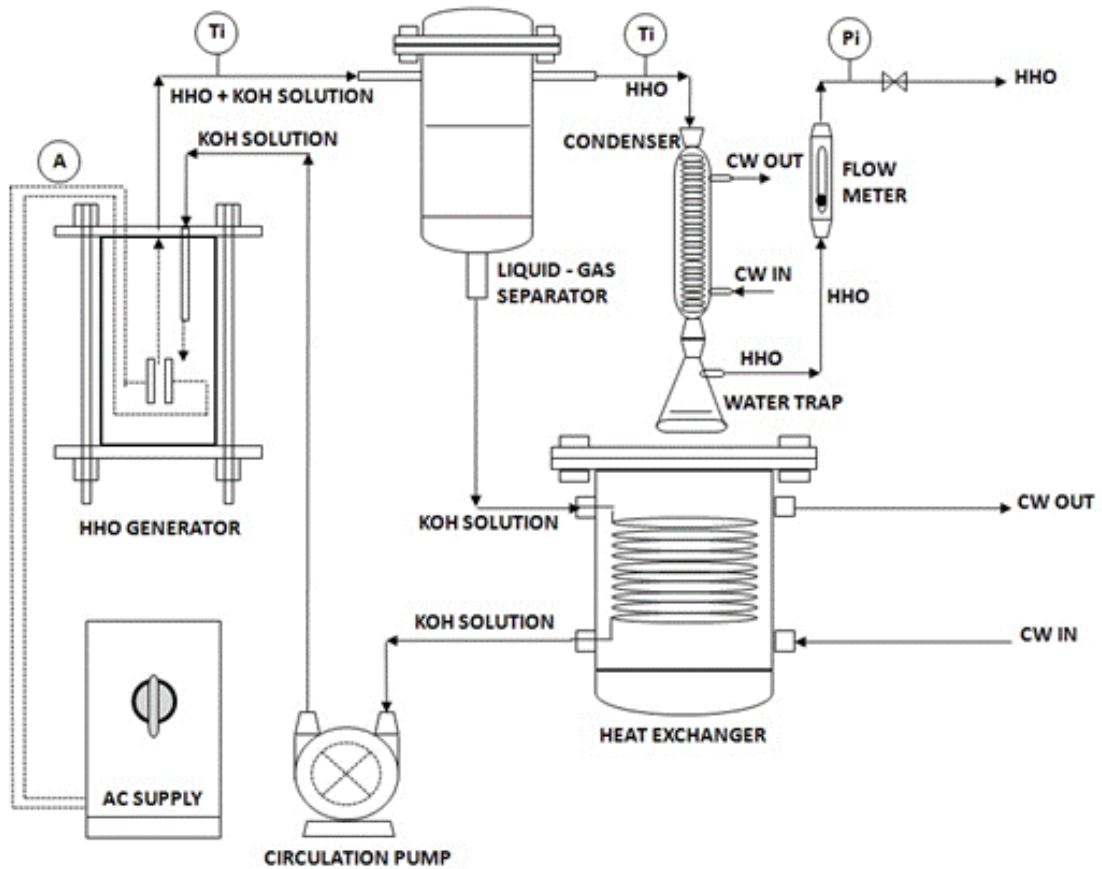


Figure 22 Process flow diagram of the closed-loop HHO production system (Phase I).

Note: CW = Cooling Water

In order to control the electrolyte temperature in the reactor, a heat exchanger with circulating cooling water is used. Once the steady-state condition is reached, the operation was allowed to run for 10 minutes. For this research, the area of the square stainless steel anode-cathode plate type 316L was fixed at 600 mm^2 . The electrical voltage was set at 52.9 V to provide the highest available HHO production through put using an AC power supply. All experiments were operated at electrolyte temperatures of 40, 45, 50, 55, 60, 65, 70, 75, 80, 85, 90 and 95°C , The electrolyte concentrations were used at 0.50, 0.75, 1.00, 1.25 and 1.50% w/w KOH and anode-cathode distance (cell gaps) was set at 1, 3, 5, 7 and 9 mm.

2.2 Experiment phase II: Optimization of the Operating Pressure of a Closed-loop HHO production system for operation with an Internal Combustion Engine (ICE).

A closed-loop HHO production unit (see Figure 23) features of a 700-ml glass HHO generator, a 6-liter stainless steel liquid-gas separator, a shell and ring coil heat exchanger, an electrolyte circulation pump (Encapsulated Magnetic Pump, EYEL4 HS-1, Japan), a glass condenser assembled with a water trap, an electrical supply (Arc Welder, BX6-160 A.C., JB3643-2000, Thailand), a flow meter (Rota-meter, AALBORG, Orangeburg, US), and a water ring vacuum pump (Hi-vac, Model: VDV 20, South Africa).

For a 700-ml glass HHO generator, there is a coupled 20 x 30 mm stainless steel anode-cathode cell inside. A 6-liter stainless steel liquid-gas separator is used to separate HHO gas from the continuous circulation of KOH solution. The floated HHO has H₂O vapor will flow through the glass condenser where mostly H₂O vapor will be converted back into liquid water and drip into the water trap container.

A process flow diagram (Figure 23) illustrates the overall concept of the closed-loop HHO production system. The production process would be started by turning on the circulation pump then switching on the AC power supply to begin the electrolysis reaction and, thus, the production of HHO gas. The wet HHO gas from the liquid-gas separator will flow into glass condenser where the contaminated vapor is condensed and collected in a water trap container. The dry HHO gas from glass condenser will flow through a Rota-meter to measure the production throughput (L/h). For the negative operating pressures, all conditions were created using the water ring vacuum pump that able to be adjusted to pressures of 60.8, 70.9, 81.0, 91.2 and 101.3 kPa abs by varying the percent opening of a breathing valve at the suction line.

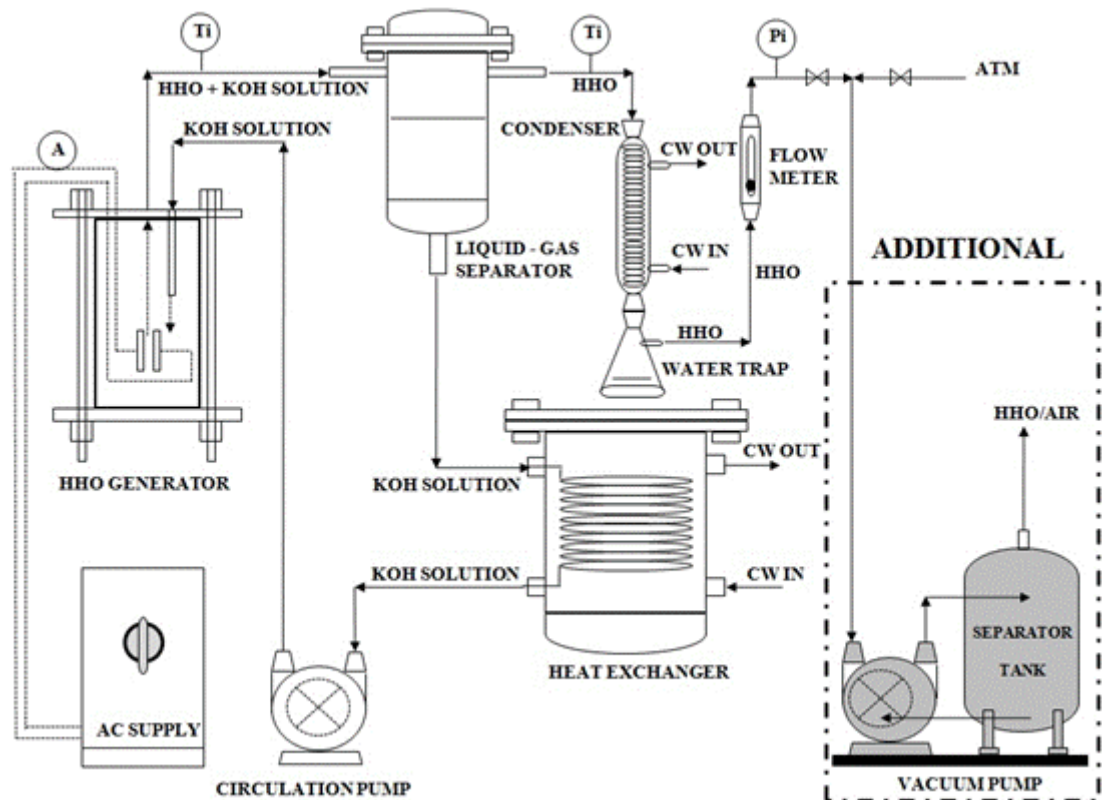


Figure 23 Process flow diagram of the closed-loop HHO production system (Phase II)

Note: CW = Cooling Water

For the operating temperatures control, the feeding of cooling water supply (CW-IN) of the heat exchanger were controlled by adjusting the percent opening of an outlet manual control valve (HV) at the discharge line (CW-OUT). The operating temperatures were set up at 40, 45, 50, 55, 60, 65, 70, 75, 80, 85, 90 and 95°C for all running conditions. Also for the others controlled parameter, the rectangular area of a couple 316L stainless steel anode-cathode plate was fixed at 600-mm². The aqueous KOH electrolyte concentration was fixed at 1.25% w/w and anode-cathode distance (cell gap) was set up at 5 mm. Once the steady-state condition is reached, the operation was allowed to run for 10 minutes.

CHAPTER 3

Result and Discussions

3.1 Phase I: Investigation of a Closed-loop HHO Production System using AC supply.

The results of this experiment were indicated in three topics as bellow.

1. The relation between HHO temperature ($^{\circ}\text{C}$) and electrolyte temperature ($^{\circ}\text{C}$).
2. The relation between electric current consumption (A) and electrolyte temperature ($^{\circ}\text{C}$).
3. The relation between HHO production rate (L/h) and electrolyte temperature ($^{\circ}\text{C}$).

3.1.1 The relation between HHO Temperature ($^{\circ}\text{C}$) and Electrolyte Temperature ($^{\circ}\text{C}$)

In this study, the heat of HHO production system was occurred by the electric current that directly supply into the electrodes (anode-cathode) which submerged in the KOH electrolyte solutions which were increased the conductivity by adding the alkaline substance. The study conditions of this part were the varying of electrolyte concentrations from 0.50 to 1.50%, the varying of cell gaps set up from 1, 3, 5 to 9 mm, the varying of cell voltages from 47.5 to 52.9 volt, the varying of operating pressures from 60.8 kPa abs to 101.3 kPa abs and the varying of anode-cathode areas from 300 to 1500 mm². The experimenters found when the electrolyte solution temperature increase, the HHO product temperature increase. The parameter that obvious effect to the HHO product temperature was the operating pressure

showed as Figure 24. For all conditions, the HHO product temperature will continuously increase to boiling points of electrolyte solution which depend on the electrolyte concentrations. This experiment found at 1 atm. the B.P. of electrolyte concentrations from 0.5 to 1.5% w/w KOH are ranging between 100 to 101°C. The increasing paths of HHO product temperature for all conditions behave like a half of parabola showed as Figure 24 to Figure 36.

In the industrial society, the different PV of the HHO product temperature and the electrolyte solution very useful for controlling the HHO production. In this system, the different between HHO product temperature and electrolyte was 0 to 20°C. The trends of all relations between electrolyte temperature and HHO product temperature from Figure 24 to Figure 36 are workable for controlling the closed loop production system as designed.

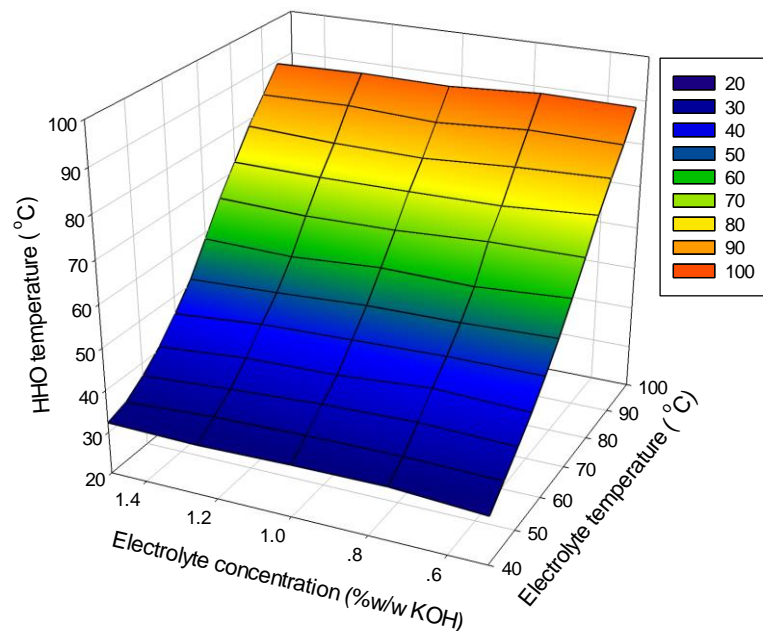


Figure 24 HHO temperatures (°C) and electrolyte temperatures (°C) by varying electrolyte concentrations from 0.50 to 1.50% w/w KOH of 1 mm cell gap.

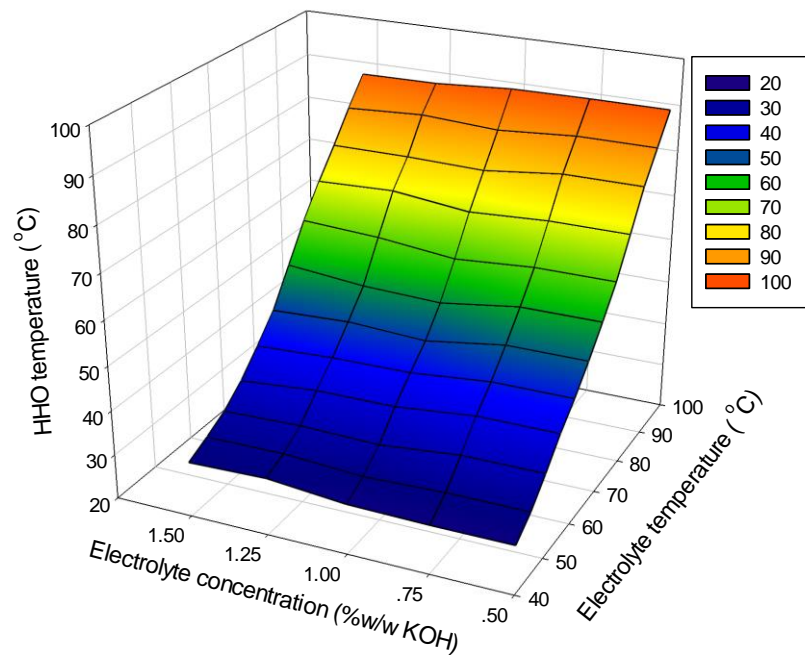


Figure 25 HHO temperatures (°C) and electrolyte temperatures (°C) by varying electrolyte concentrations from 0.50 to 1.50% w/w KOH of 3 mm cell gap.

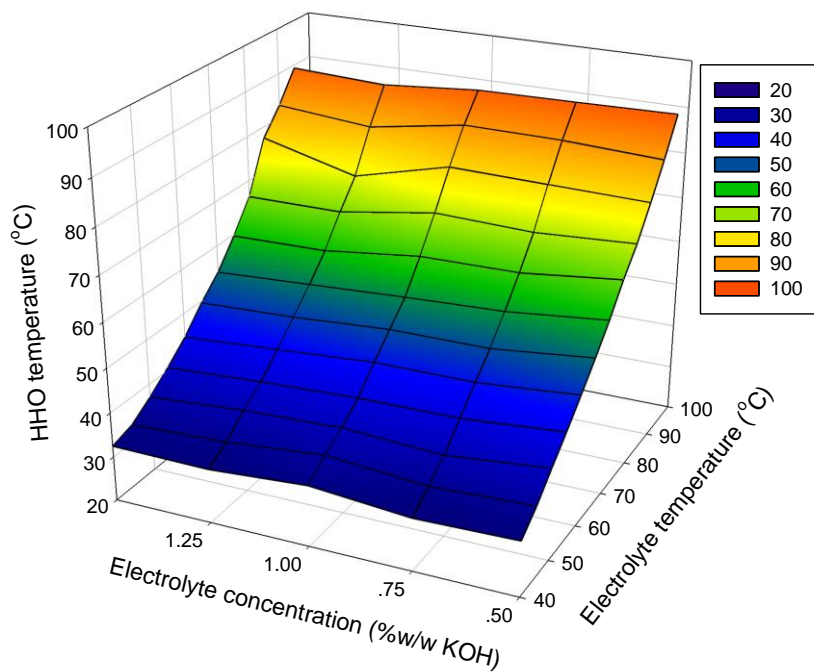


Figure 26 HHO temperatures (°C) and electrolyte temperatures (°C) by varying electrolyte concentrations from 0.50 to 1.50% w/w KOH of 5 mm cell gap.

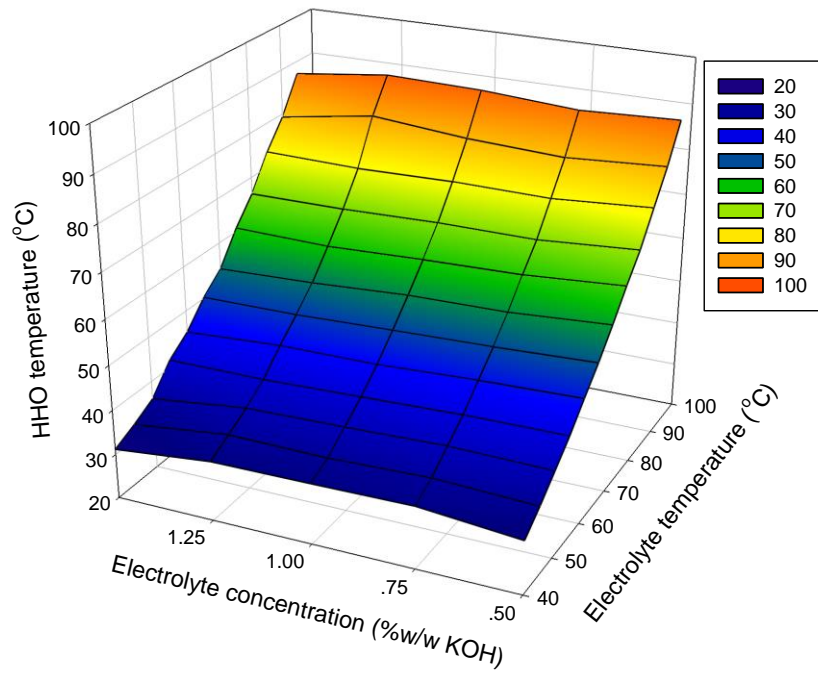


Figure 27 HHO temperatures (°C) and electrolyte temperatures (°C) by varying electrolyte concentrations from 0.50 to 1.50% w/w KOH of 7 mm cell gap.

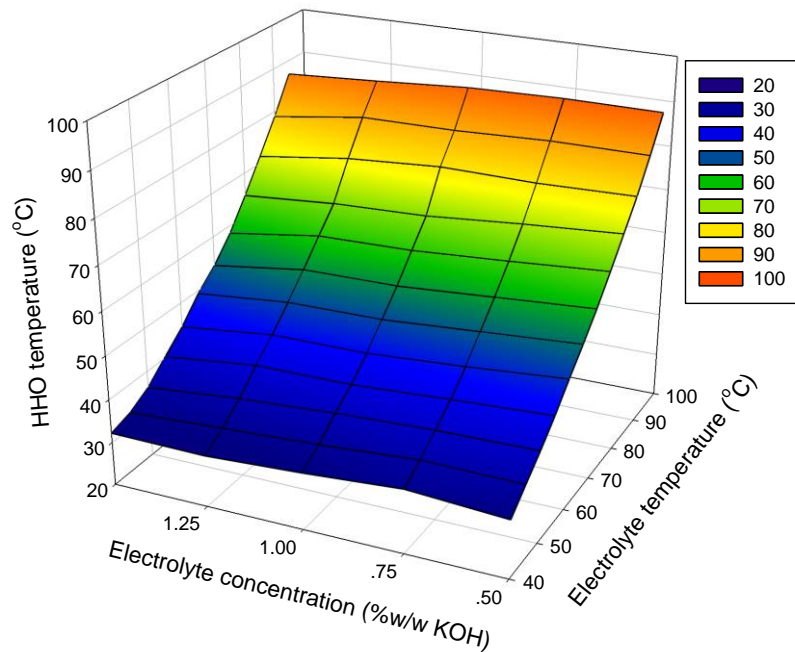


Figure 28 HHO temperatures (°C) and electrolyte temperatures (°C) by varying electrolyte concentrations from 0.50 to 1.50% w/w KOH of 9 mm cell gap.

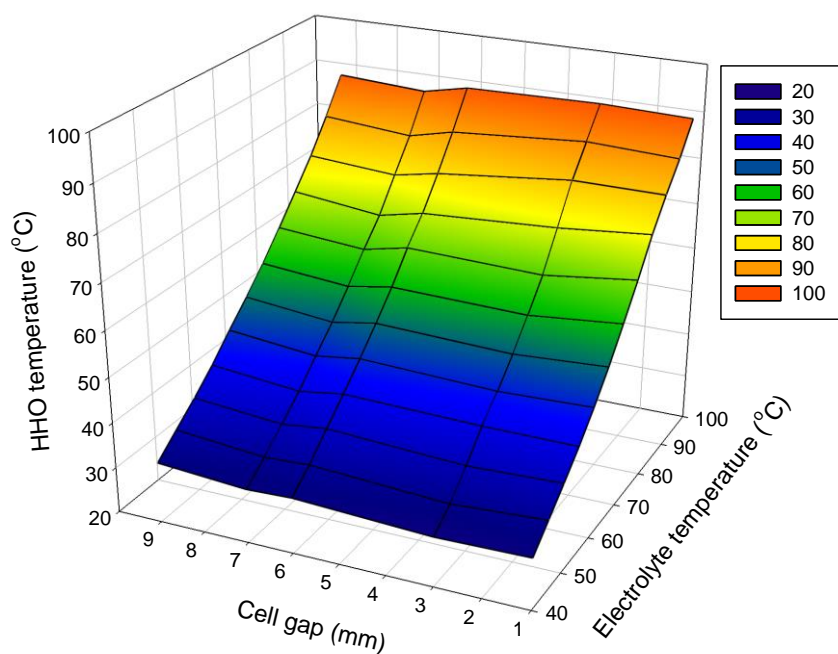


Figure 29 HHO temperatures (°C) and electrolyte temperatures (°C) by varying cell gaps from 1 to 9 mm. of 0.50% w/w KOH.

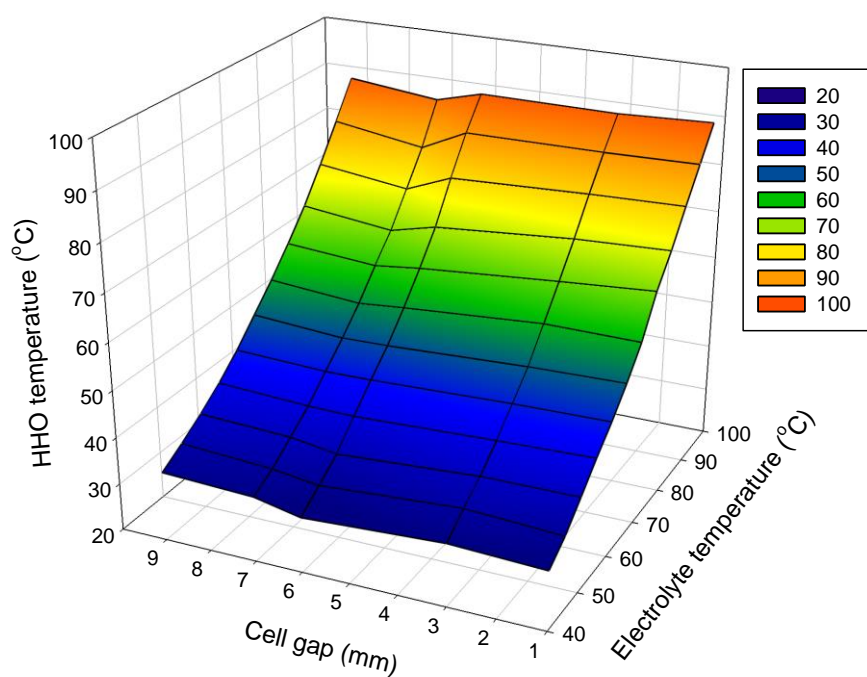


Figure 30 HHO temperatures (°C) and electrolyte temperatures (°C) by varying cell gaps from 1 to 9 mm. of 0.75% w/w KOH.

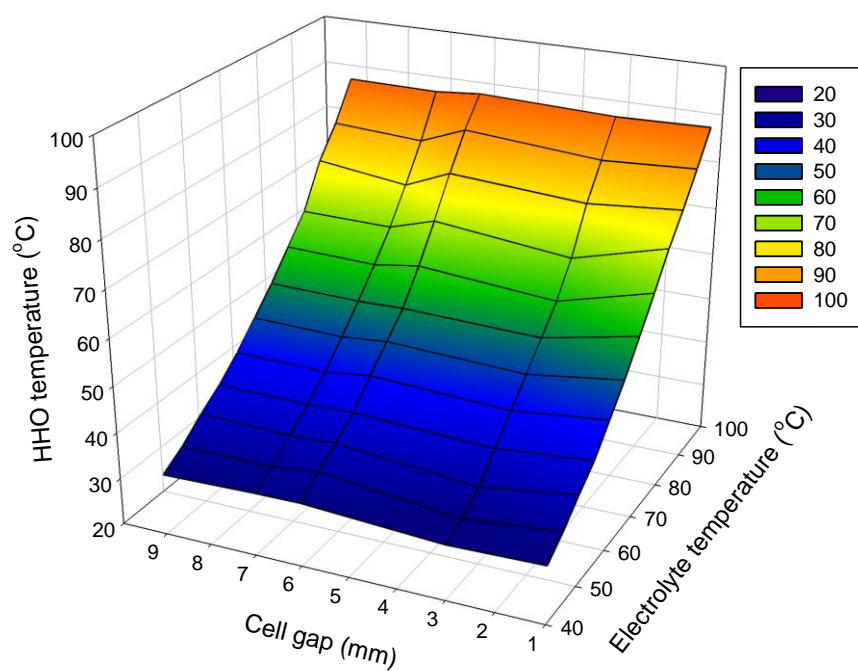


Figure 31 HHO temperatures (°C) and electrolyte temperatures (°C) by varying cell gaps from 1 to 9 mm. of 1.00% w/w KOH.

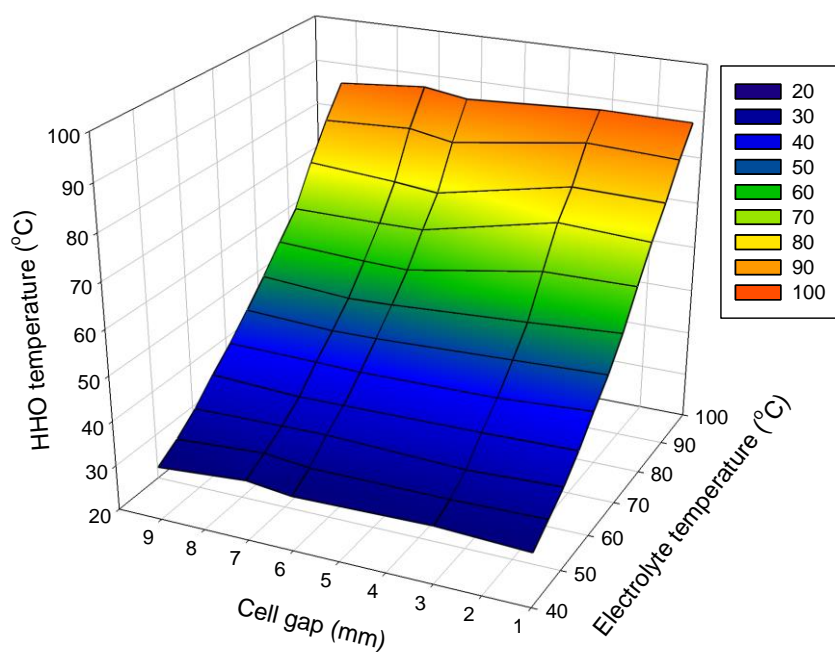


Figure 32 HHO temperatures (°C) and electrolyte temperatures (°C) by varying cell gaps from 1 to 9 mm. of 1.25% w/w KOH.

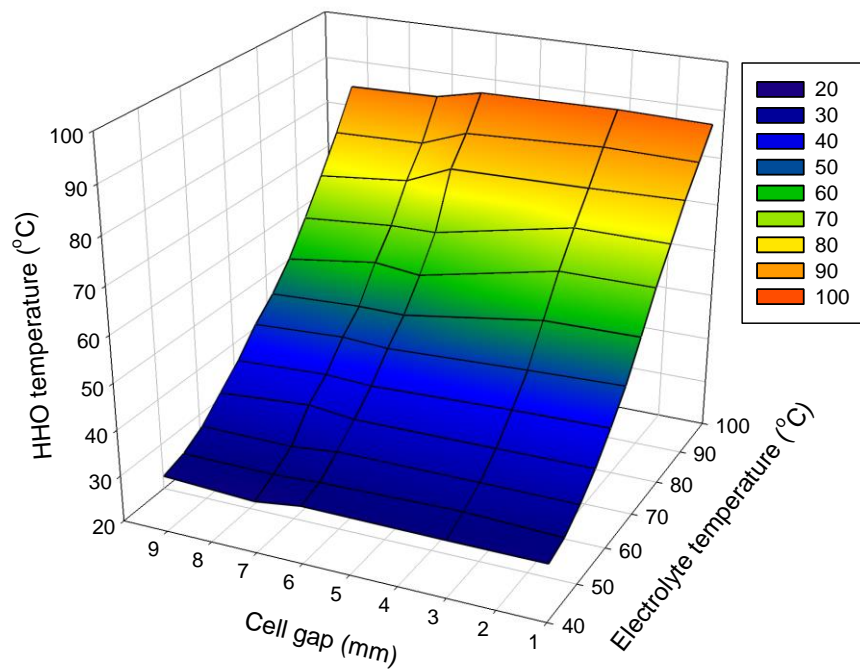


Figure 33 HHO temperatures (°C) and electrolyte temperatures (°C) by varying cell gaps from 1 to 9 mm. of 1.50% w/w KOH.

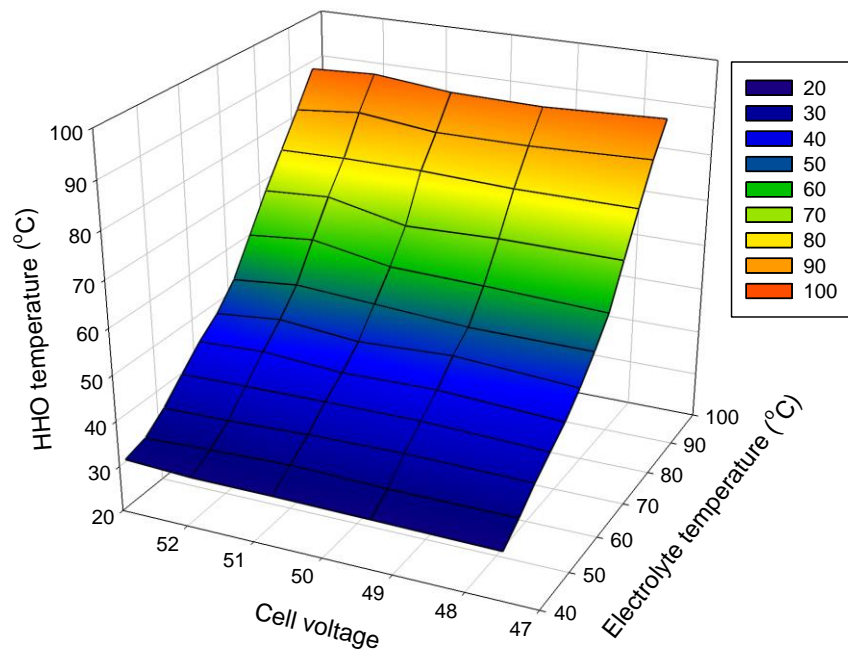


Figure 34 HHO temperatures (°C) and electrolyte temperatures (°C) by varying cell voltages from 47.5 to 52.9 volt of 5 mm cell gap and 1.25% w/w KOH.

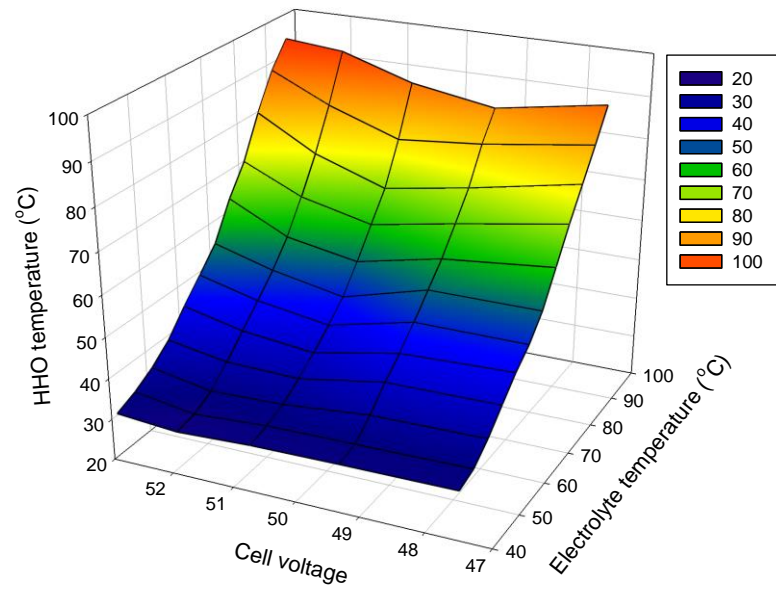


Figure 35 HHO temperatures (°C) and electrolyte temperatures (°C) by varying operating pressures from 60.8 kPa to 101.3 kPa of 5 mm cell gap and 1.25% w/w KOH.

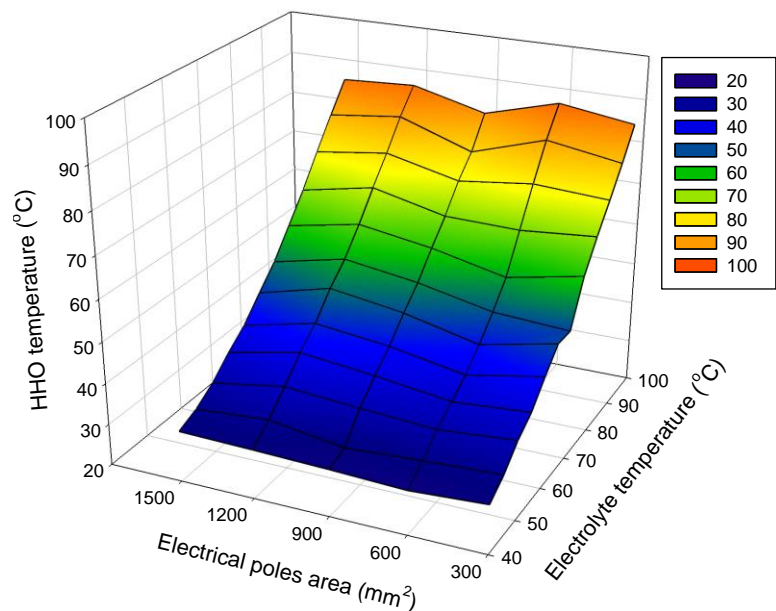


Figure 36 HHO temperatures (°C) and electrolyte temperatures (°C) by varying electrical poles areas from 300 mm² to 1500 mm² of 5 mm cell gap and 1.25% w/w KOH.

3.1.2 The relation between electric current consumption (A) and electrolyte temperature (°C)

The electric current consumption is the key parameter for observation of the behavior of production system because the electric current will immediately response and display in the online monitoring production trend. There are many the effective parameters to the electric current signal such as the difference of electrolyte concentrations, the electrolyte temperatures, the cell gaps distance, the electric voltage supply, the operating pressure, and the size of anode-cathode cell.

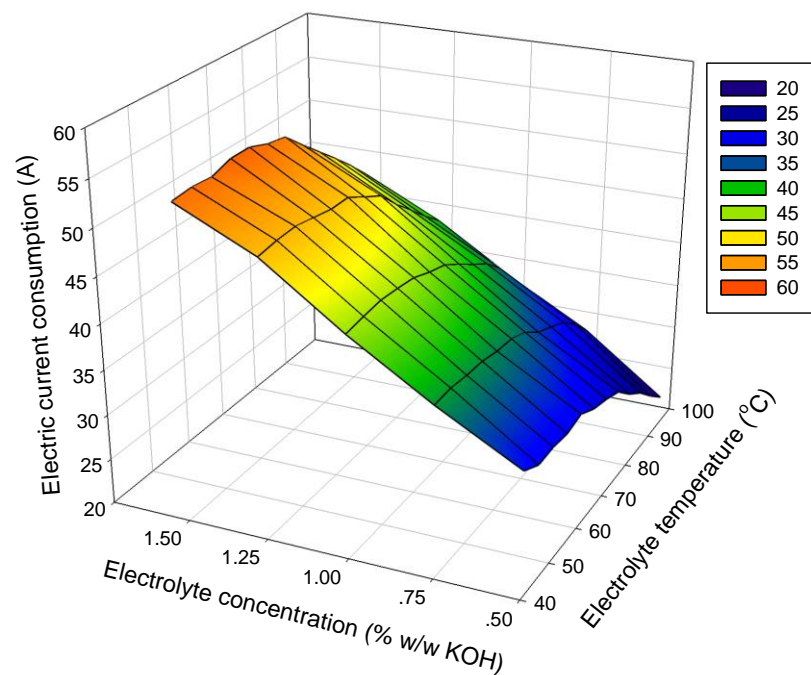


Figure 37 Electric current consumption (A) and electrolyte temperatures (°C) by varying electrolyte concentrations from 0.50 to 1.50% w/w KOH of 1 mm cell gap.

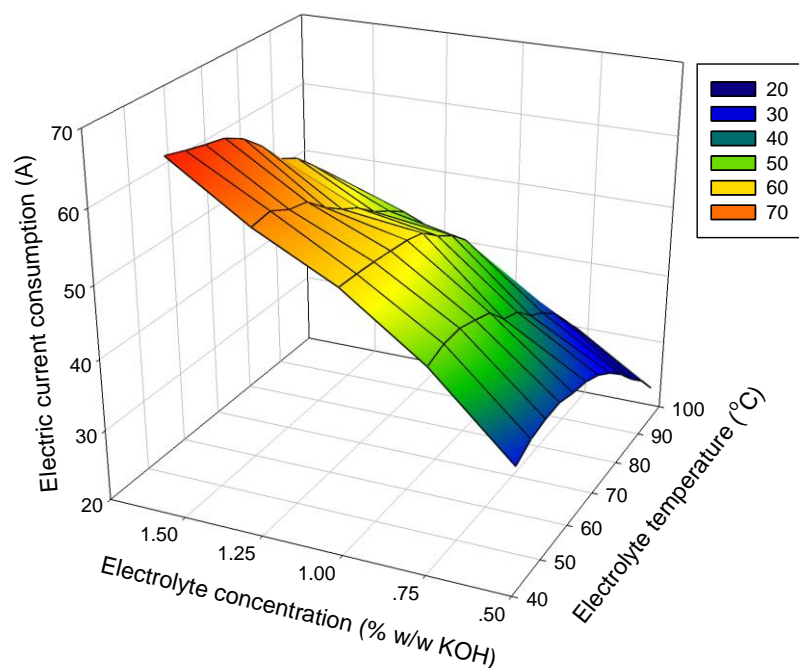


Figure 38 Electric current consumption (A) and electrolyte temperatures ($^{\circ}\text{C}$) by varying electrolyte concentrations from 0.50 to 1.50% w/w KOH of 3 mm cell gap.

Figure 37 and Figure 38 illustrate the current behaviors of 1 mm and 3 mm cell gap. This condition the electrolyte concentrations were varied from 0.50 to 1.50% w/w KOH. The interesting of this point is the current consumption does not increase by increase electrolyte temperature, this phenomenon was described by the effect of too small cell gap set up. In this even, the HHO product bubbles that occurred between anode-cathode poles would expand the size by heat and obstruct the active site of reaction area.

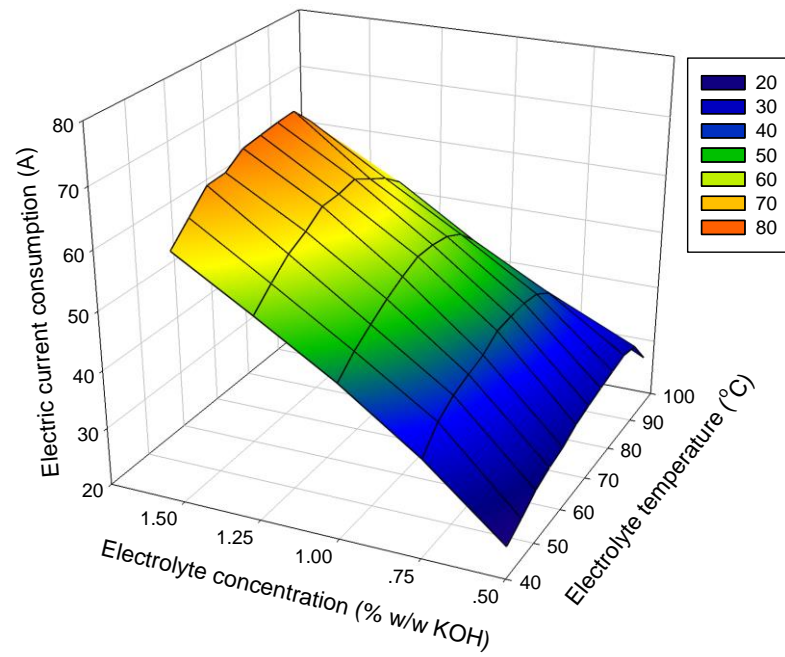


Figure 39 Electric current consumption and electrolyte temperatures ($^{\circ}\text{C}$) by varying electrolyte concentrations from 0.50 to 1.50% w/w KOH of 5 mm cell gap.

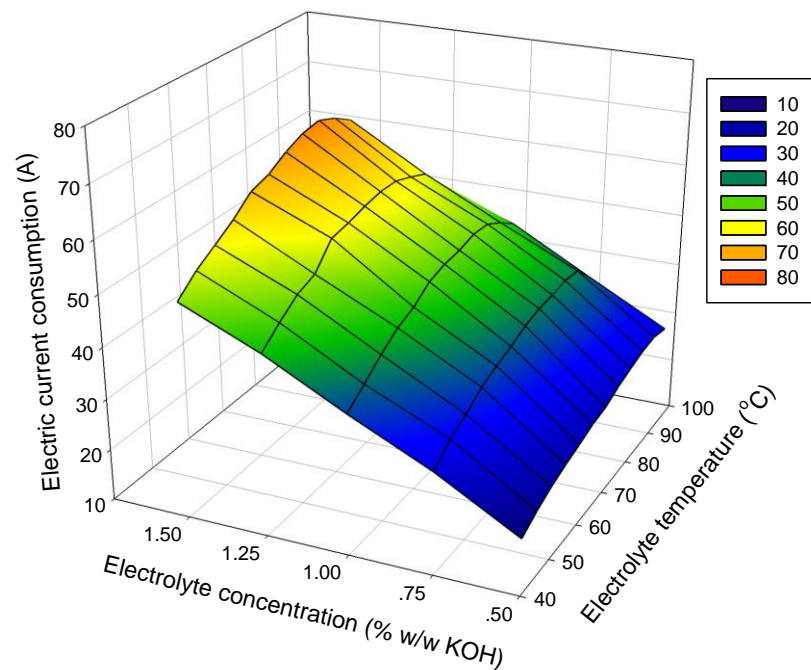


Figure 40 Electric current consumption (A) and electrolyte temperatures ($^{\circ}\text{C}$) by varying electrolyte concentrations from 0.50 to 1.50% w/w KOH of 7 mm cell gap.

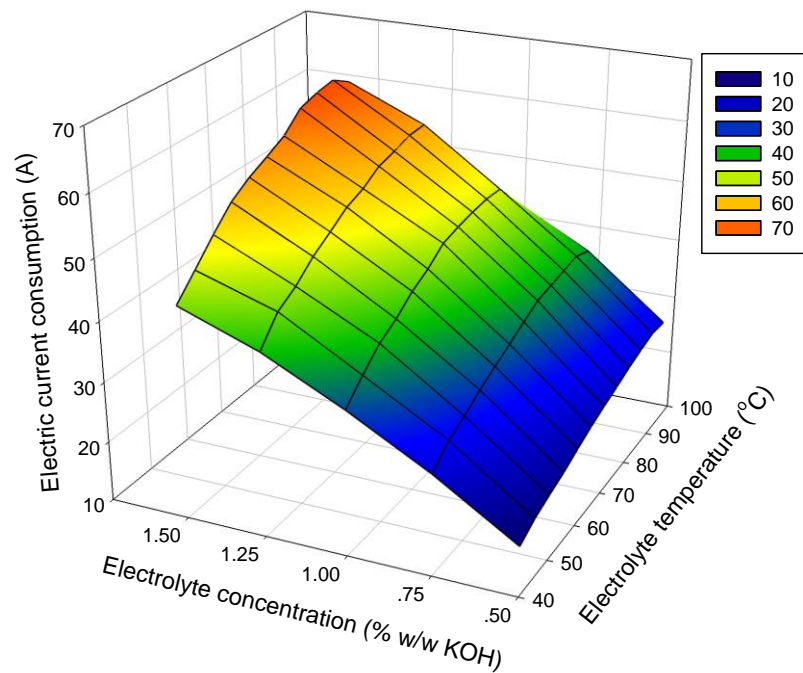


Figure 41 Electric current consumptions (A) and electrolyte temperatures ($^{\circ}\text{C}$) by varying electrolyte concentrations from 0.50 to 1.50% w/w KOH of 9 mm cell gap.

The Figure 39 to Figure 41 are the trend of positive productivity of HHO production. By the trend of electric current consumptions and electrolyte temperatures, the results showed when the electrolyte temperature was increased the current would increase also. This phenomenon began the first time at the cell gap condition of 5 mm and also took place at 7 and 9 mm cell gap with the same fixed parameters. At 5 mm cell gap, the trend of current behave like a parabola the maximum peak of current has occurred at electrolyte temperature approx. 65°C . then slightly decrease to the end point at 95°C . For 7 and 9 mm cell gap the maximum point of current would skipped to the higher temperature at 80°C (except 0.50% w/w KOH) and 85°C , respectively.

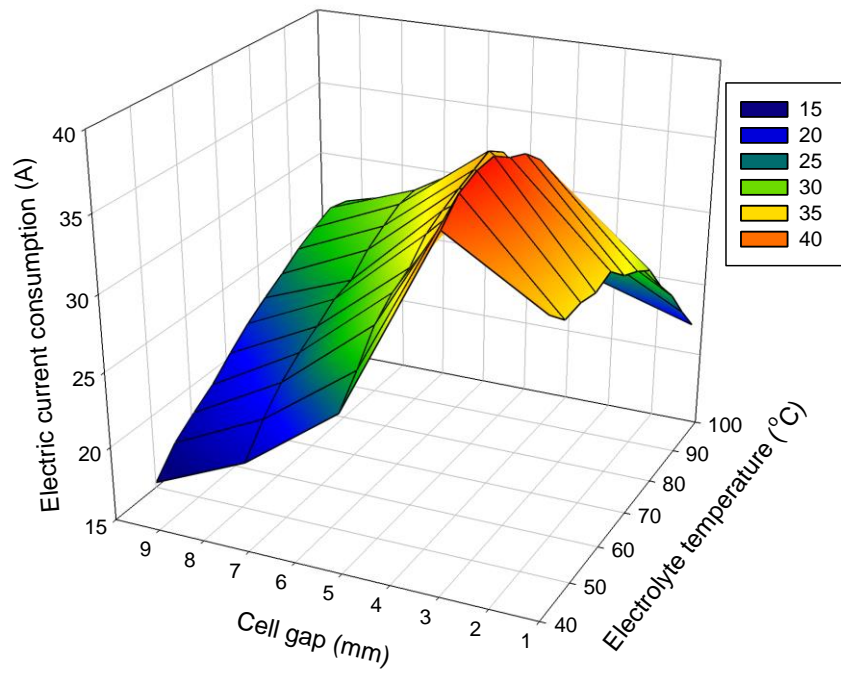


Figure 42 Electric current consumptions (A) and electrolyte temperatures (°C) by varying cell gaps from 0.50 to 1.50% w/w KOH of 0.50% w/w KOH.

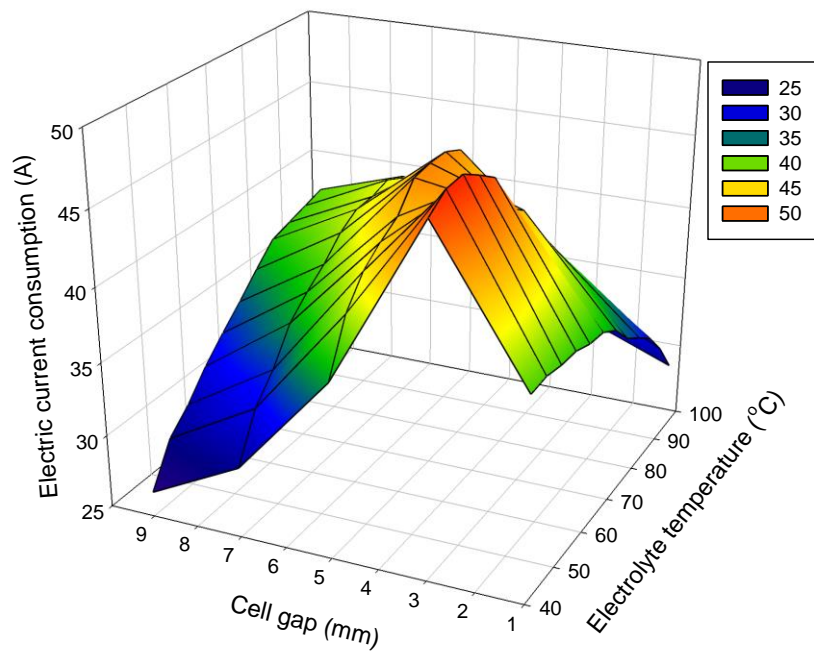


Figure 43 Electric current consumptions (A) and electrolyte temperatures (°C) by varying cell gaps from 0.50 to 1.50% w/w KOH of 0.75% w/w KOH.

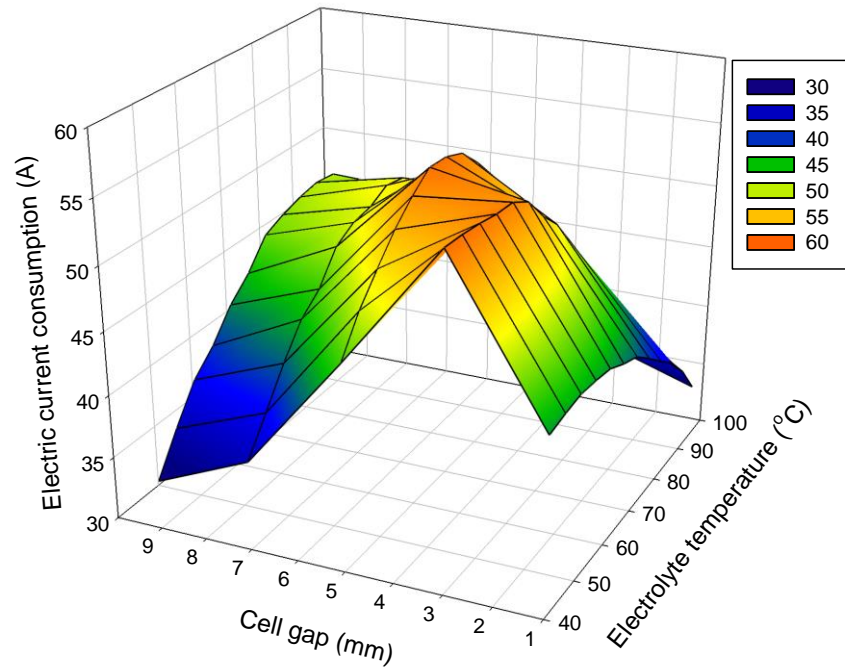


Figure 44 Electric current consumptions (A) and electrolyte temperatures (°C) by varying cell gaps from 0.50 to 1.50% w/w KOH of 1.00% w/w KOH.

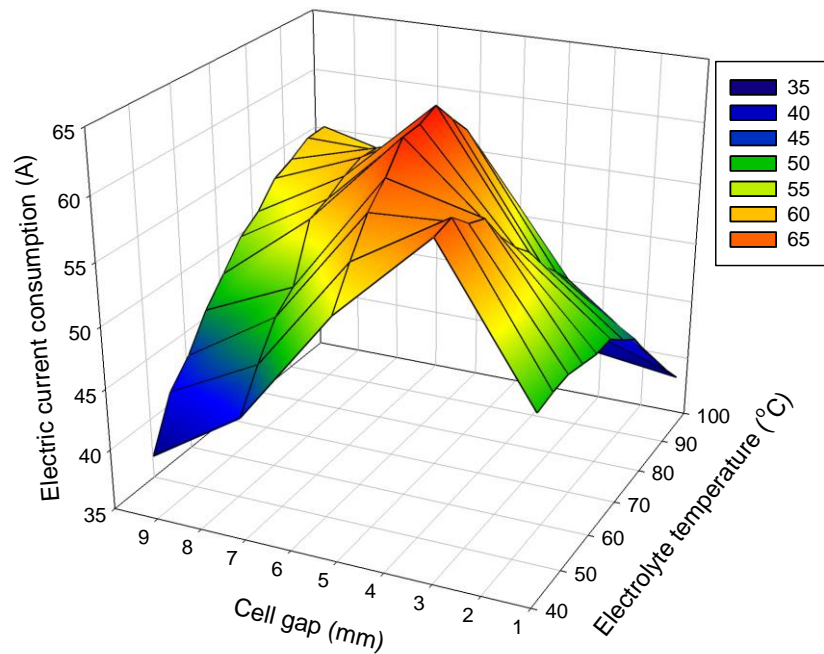


Figure 45 Electric current consumptions (A) and electrolyte temperatures (°C) by varying cell gaps from 0.50 to 1.50% w/w KOH of 1.25% w/w KOH.

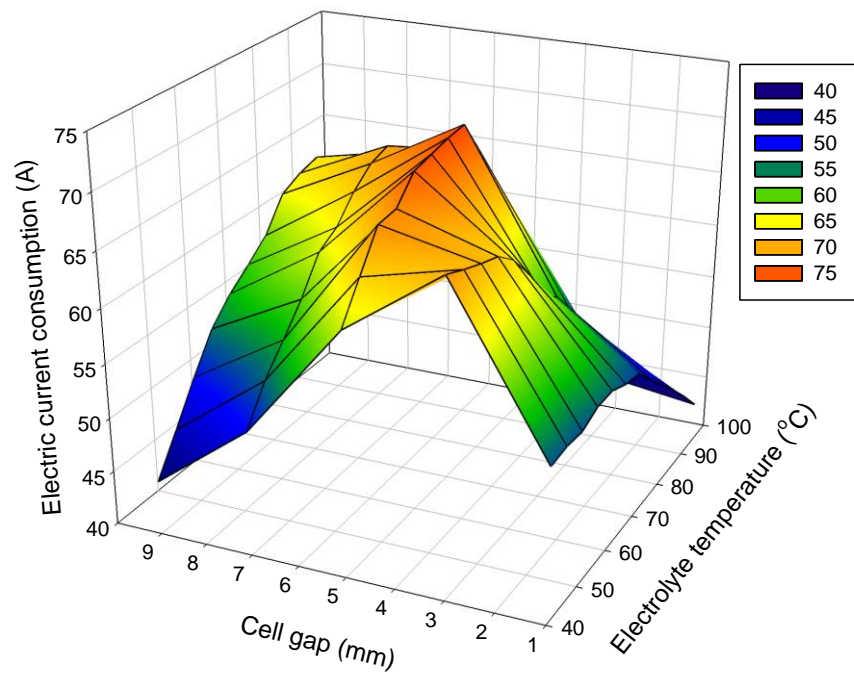


Figure 46 Electric current consumptions (A) and electrolyte temperatures ($^{\circ}\text{C}$) by varying cell gaps from 0.50 to 1.50% w/w KOH of 1.50% w/w KOH.

Figure 42 to Figure 46 are the trends of electric current consumption and electrolyte temperature by varying cell gap set up. These trends obviously performed the two paths of current behavior; the negative path was occurred at the condition of 1 and 3 mm cell gap for all electrolyte concentrations. And the positive paths were of 5, 7 and 9 mm.

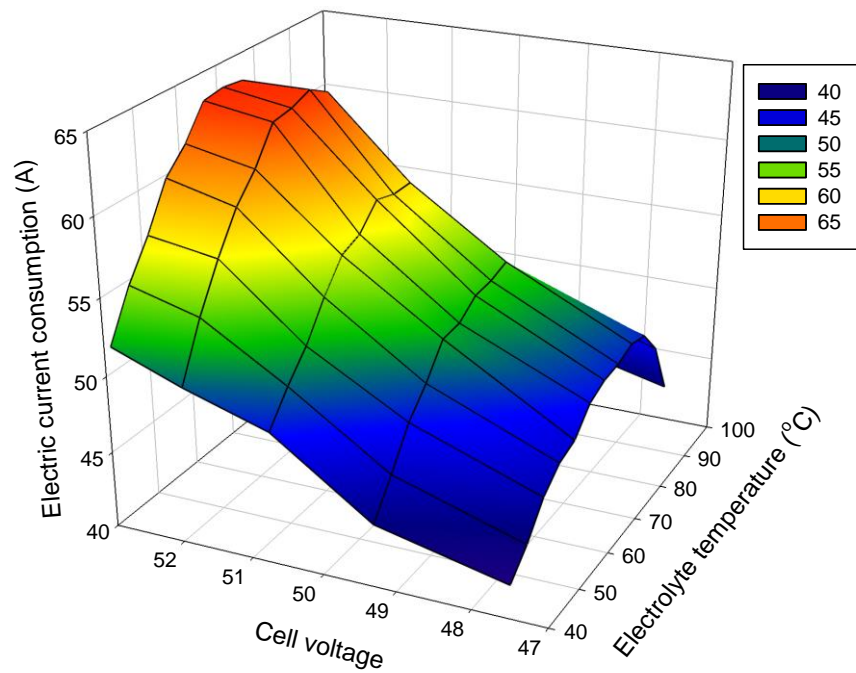


Figure 47 Electric current consumptions (A) and electrolyte temperatures ($^{\circ}\text{C}$) by varying cell voltages from 47.5 to 52.9 volt of 5 mm cell gap and 1.25% w/w KOH.

Figure 47 is the relation between the electric current consumptions and electrolyte temperatures by varying the electric voltage supply. This result indicated the current consumption also change by feed the different voltage supply. In this case, at the same electrolyte temperature, the electrical resistances for all voltage supplies are the same value so that increasing electric voltage would effect to increase the current.

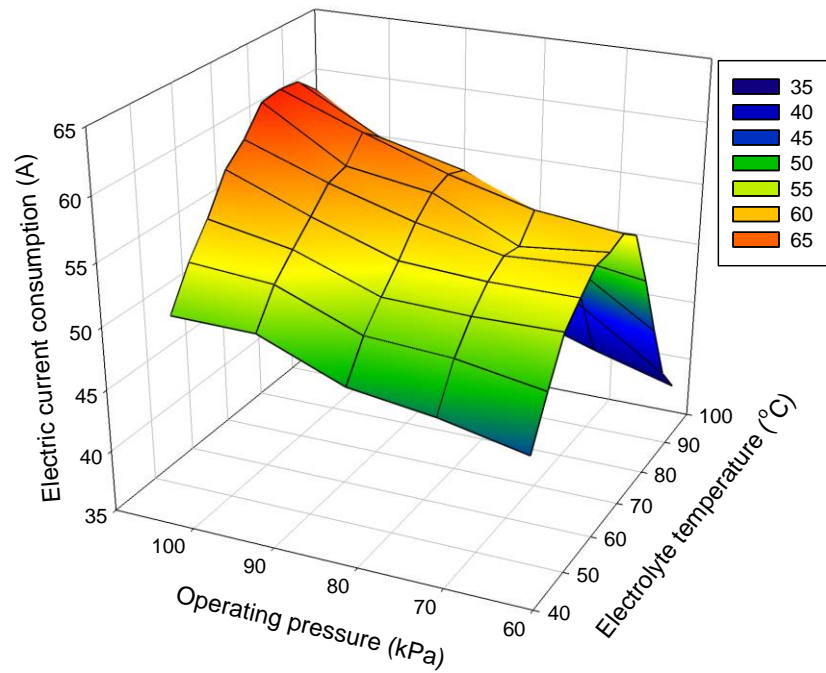


Figure 48 Electric current consumptions (A) and electrolyte temperatures ($^{\circ}\text{C}$) by varying operating pressures from 60.8 to 101.3 kPa abs of 5 mm cell gap and 1.25% w/w KOH.

Figure 48 illustrates the relation between electrolyte temperature and electric current consumptions by varying the operating pressures from 60.8 kPa abs to 101.3 kPa abs. It was found the operating pressure obvious effect to the electric current consumption. Increasing of negative pressure effected to decreasing of electric current. As described before the operating pressures are relate to the B.P. of electrolyte solution and the escape velocity of HHO between cell gaps.

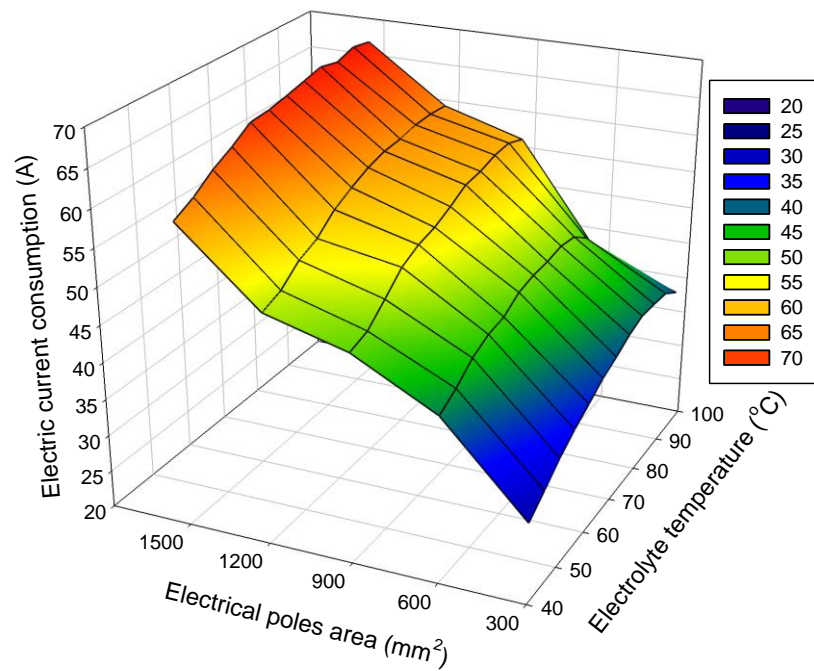


Figure 49 Electric current consumptions (A) and electrolyte temperatures (°C) by varying electrical poles areas from 300 mm² to 1500 mm² of 5 mm cell gap and 1.25% w/w KOH.

Figure 49 is the trend of electric current consumption and electrolyte temperature by varying the anode-cathode area from 300 to 1500 mm². This results indicated that the area of anode and cathode is also one parameter that effect to the electric current consumption.

3.2 Phase II: Optimization of the Operating Pressure of a Closed-loop HHO production system for operation with an Internal Combustion Engine (ICE)

The results of this experiment were indicated in three topics as bellow.

1. The HHO gas product temperature while increasing the operating temperatures.

2. Display of electrical current consumption (A) with atmospheric and vacuum pressures (kPa abs).

3. Relationship between electrical current consumption and operating pressure at 80, 85, 90 and 95°C.

4. The HHO production throughput while running the system at atmosphere and vacuum pressures.

Results of HHO production throughput have obviously presented the two different production paths. The negative paths of: 1-mm and 3-mm cell gaps illustrated in Figure Figure 50(a) and Figure 50(b). It can be seen that for both cell gaps, the maximum HHO production throughputs occurred at the initial electrolyte temperature of 40°C then declined with increasing electrolyte temperature from initial to the end at 95°C. This gap results are in accordance with Göllei (2014) who reported that the closer the anode and cathode plates are, the better the efficiency [20]. For the positive parts of 5-mm, 7-mm and 9-mm cell gaps in Figure 51(a), Figure 51(b), Figure 51(c), the opposite production paths have performed in this condition. The production throughputs for these cell gaps increased with increasing electrolyte temperature from 40°C to 95°C. All results which presented in Figure Figure 50 and Figure 51 confirmed that: the production throughputs varied with the electrolyte temperature significantly - the two different production paths of this experiment are cause by cell gap set up. At the same operating temperature - the higher electrolyte concentration provided higher HHO production yield.

3.3 The relation between HHO production rate (L/h) and electrolyte temperature (°C)

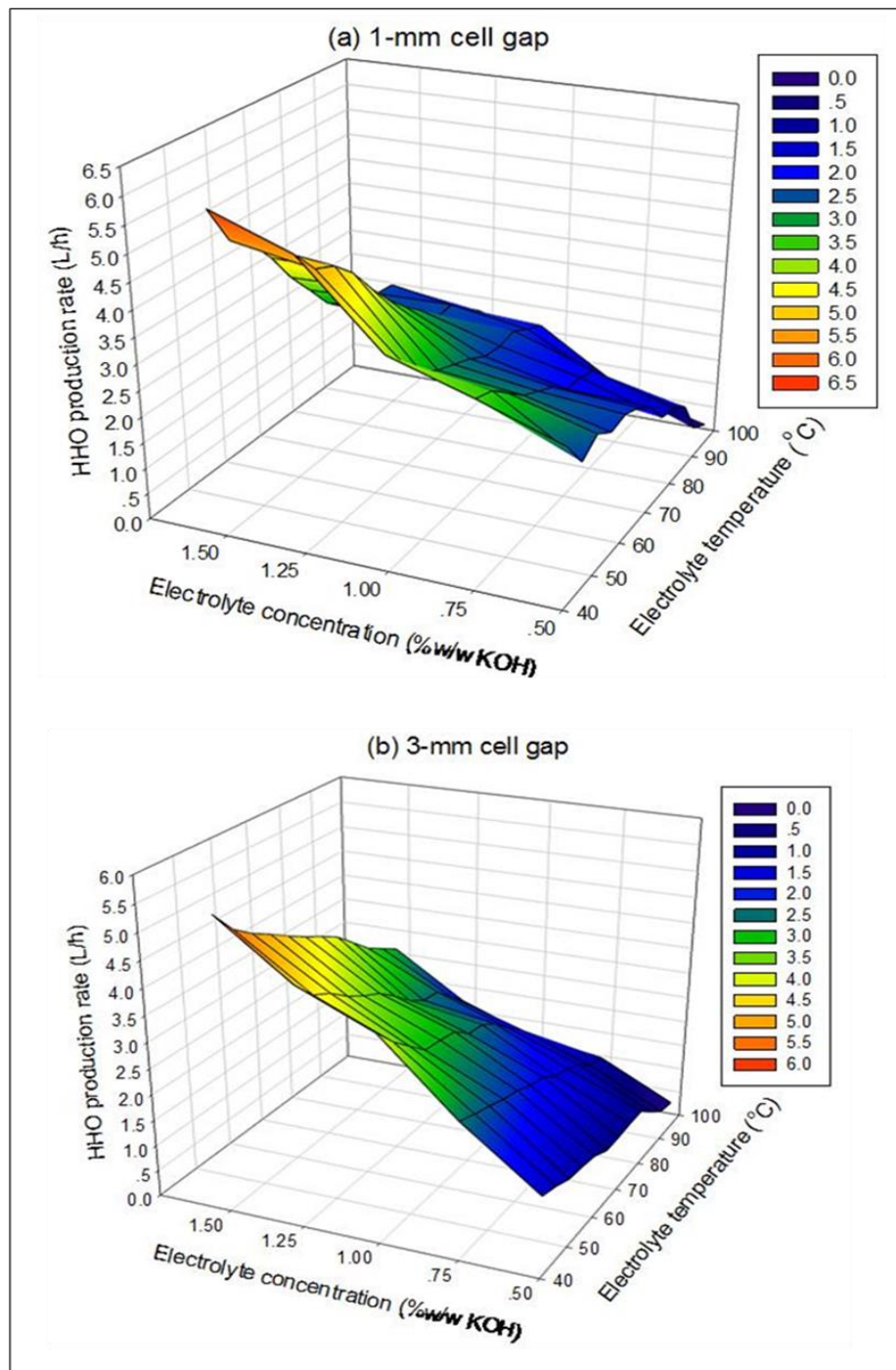


Figure 50 HHO production throughput at cell gap of: (a) 1-mm. (b) 3-mm.

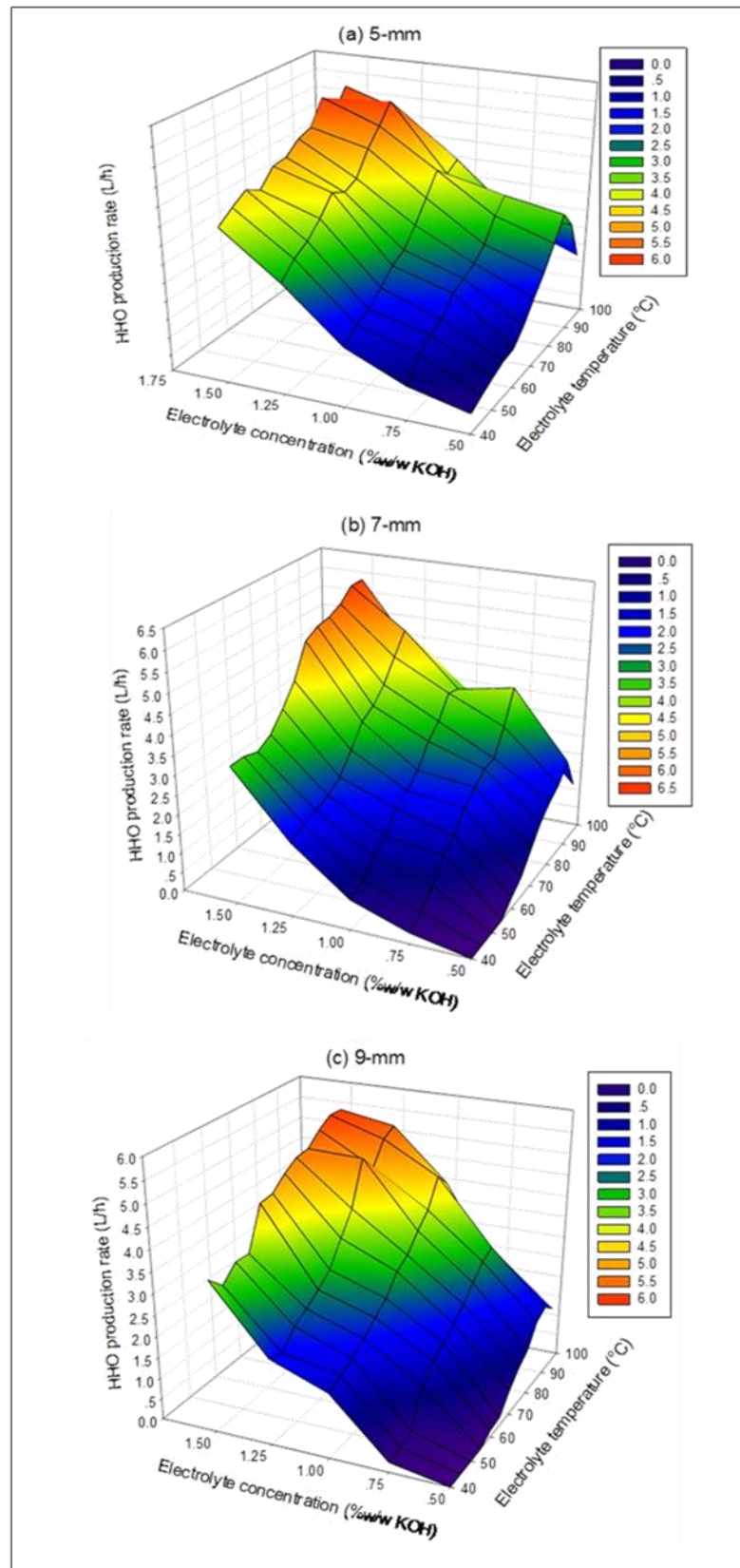


Figure 51 HHO production throughput at cell gap of: (a) 5-mm. (b) 7-mm (c) 9-mm.

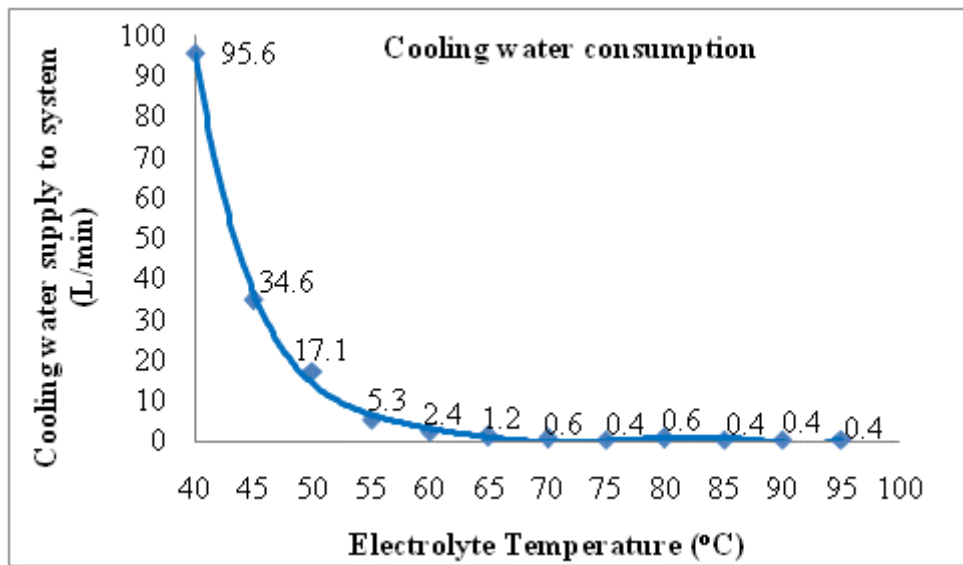


Figure 52 Cooling water (28°C) consumption.

Table 7 Results of HHO production rate (L/h) at 5 mm cell gap with electrolyte temperature from 40°C to 65°C (Figure 51(a)).

Electrolyte	% w/w KOH				
	Temp. (°C)	0.50	0.75	1.00	1.25
40	0.10 (0.07) ^a	0.48 (0.11) ^{b,c}	1.18 (0.11) ^{d,e}	2.56 (0.05) ^l	3.72 (0.11) ^p
45	0.28 (0.08) ^{a,b}	1.02 (0.08) ^d	1.50 (0.12) ^{f,g}	2.94 (0.09) ^m	4.00 (0.16) ^r
50	0.44 (0.11) ^{b,c}	1.26 (0.11) ^e	1.64 (0.09) ^g	3.16 (0.15) ⁿ	4.24 (0.18) ^s
55	0.58 (0.08) ^c	1.38 (0.13) ^{e,f}	1.96 (0.11) ^{h,i}	3.52 (0.13) ^o	4.02 (0.18) ^r
60	0.62 (0.08) ^c	1.84 (0.21) ^h	2.30 (0.12) ^{j,k}	3.98 (0.13) ^{q,r}	4.44 (0.13) ^t
65	0.98 (0.18) ^d	1.98 (0.33) ^{h,i}	2.48 (0.28) ^{k,l}	3.78 (0.18) ^{p,q}	4.48 (0.11) ^t
70	1.48 (0.18) ^{f,g}	2.14 (0.29) ^{i,j}	2.92 (0.16) ^m	3.94 (0.19) ^{q,r}	4.78 (0.13) ^u

Groups with same letter indicate that there is no statistical difference ($p \leq 0.05$) between samples according Duncan's multiply range test; values in parentheses are standard deviations;

Table 8 Results of HHO production rate (L/h) at 5 mm cell gap with electrolyte temperature from 70°C to 95°C. (Figure 51(a)).

Electrolyte Temp. (°C)	% w/w KOH				
	0.50	0.75	1.00	1.25	1.50
70	1.48	2.14	2.92	3.94	4.78
	(0.18) ^{a,b}	(0.29) ^{c,d,e}	(0.16) ^{f,g,h,i}	(0.19) ^m	(0.13) ^{n,o}
75	1.92	2.42	3.44	4.54	4.90
	(0.15) ^{b,c}	(0.26) ^{d,e}	(0.19) ^{j,k,l}	(0.26) ^{n,o}	(0.56) ^{n,o}
80	2.48	2.98	3.98	4.96	5.52
	(0.38) ^{d,e,f}	(0.47) ^{g,h,i,j}	(0.36) ^m	(0.42) ^{n,o}	(0.38) ^q
85	3.04	3.32	3.68	5.44	4.96
	(0.46) ^{h,i,j}	(0.29) ^{i,j,k}	(0.29) ^{k,l,m}	(0.33) ^{p,q}	(0.42) ^{n,o}
90	2.54	2.58	3.88	5.02	5.50
	(0.34) ^{e,f,g}	(0.43) ^{e,f,g,h}	(0.52) ^{l,m}	(0.44) ^{o,p}	(0.41) ^q
95	1.44	2.04	1.92	4.06	4.52
	(0.15) ^a	(0.40) ^{c,d}	(0.16) ^{b,c}	(0.29) ^m	(0.23) ⁿ

Groups with same letter indicate that there is no statistical difference ($p \leq 0.05$) between samples according Duncan's multiply range test; values in parentheses are standard deviations;

Table 9 Results of HHO production rate (L/h) at 7 mm cell gap with electrolyte temperature from 40°C to 65°C (Figure 51(b)).

Electrolyte Temp. (°C)	% w/w KOH				
	0.50	0.75	1.00	1.25	1.50
40	0.00 (0.00) ^a	0.28 (0.04) ^b	0.78 (0.08) ^d	1.90 (0.07) ^h	3.50 (0.07) ^{n,o}
45	0.00 (0.00) ^a	0.52 (0.08) ^c	0.96 (0.11) ^e	2.10 (0.07) ^{ij}	3.50 (0.07) ^{n,o}
50	0.00 (0.00) ^a	0.88 (0.08) ^{d,e}	1.30 (0.07) ^f	2.18 (0.13) ^{jk}	3.38 (0.04) ⁿ
55	0.00 (0.00) ^a	1.38 (0.08) ^f	1.54 (0.05) ^g	2.30 (0.12) ^k	3.58 (0.13) ^o
60	0.30 (0.07) ^b	1.58 (0.08) ^g	2.00 (0.20) ^{hi}	2.52 (0.08) ^l	4.00 (0.20) ^p
65	0.54 (0.05) ^c	2.04 (0.11) ^{h,ij}	2.20 (0.12) ^{jk}	2.98 (0.18) ^m	4.50 (0.20) ^q
60	0.98 (0.24) ^e	2.32 (0.13) ^k	2.48 (0.15) ^l	3.48 (0.15) ^{n,o}	5.30 (0.25) ^f

Groups with same letter indicate that there is no statistical difference ($p \leq 0.05$) between samples according Duncan's multiply range test; values in parentheses are standard deviations;

Table 10 Results of HHO production rate (L/h) at 7 mm cell gap with electrolyte temperature from 70°C to 95°C ((Figure 51(b)).

Electrolyte Temp.	% w/w KOH				
	0.50	0.75	1.00	1.25	1.50
70	0.98	2.32	2.48	3.48	5.30
	(0.24) ^a	(0.13) ^d	(0.15) ^{d,e}	(0.15) ^{h,i}	(0.25) ^{m,n}
75	1.42	2.54	3.00	3.68	5.48
	(0.15) ^b	(0.17) ^{d,e}	(0.16) ^{f,g}	(0.23) ^{i,j}	(0.18) ^{n,o}
80	1.70	2.58	3.30	4.02	5.54
	(0.16) ^{b,c}	(0.13) ^{d,e}	(0.31) ^{g,h}	(0.33) ^{j,k}	(0.21) ^{n,o}
85	1.90	3.18	3.82	4.54	5.70
	(0.32) ^c	(0.23) ^{g,h}	(0.33) ^{i,j}	(0.30) ^l	(0.40) ^{o,p}
90	2.28	3.98	3.72	5.04	6.00
	(0.24) ^d	(0.36) ^{j,k}	(0.33) ^{i,j}	(0.42) ^m	(0.35) ^p
95	1.42	2.82	3.50	4.30	6.00
	(0.33) ^b	(0.23) ^{e,f}	(0.3) ^{h,i}	(0.25) ^{k,l}	(0.31) ^p

Groups with same letter indicate that there is no statistical difference ($p \leq 0.05$) between samples according Duncan's multiply range test; values in parentheses are standard deviations;

Figure 50(a) indicates that the highest throughput occurred at the initial electrolyte temperature of 40°C; however, once the electrolyte temperature increases, the HHO throughput significantly decreases. Overall, the production throughputs for all electrolyte concentrations decrease by more than 60% at 95°C.

Effects of increasing the cell gap from 1 mm to 3 mm were compared. In general, at same electrolyte concentrations, the HHO production showed the same

trend; however, the throughput decreased more slightly for the larger gap. For the 3-mm cell gap, production of HHO decreased nearly 50% when the electrolyte temperature increased from 40°C to 95°C. Nonetheless, Figure 50(b) clearly shows that at the same electrolyte temperature, increasing the electrolyte concentrations contributed to a higher production throughput. This corresponds to discussions by Nikolic et al. (2010) which mentioned that the electrolysis process is much more efficient at raised temperatures [52].

Since small cell gaps required low operating temperature and a large amount of cooling water to maintain the process showed as Figure 52, larger cell gaps of 5, 7, and 9 mm were investigated to study the production throughput capability. Figure 51(a), Figure 50(b) and Figure 50(c) illustrate that for all cell gaps ranging from 5-9 mm HHO production increased with increasing electrolyte temperature. Udagawa, Aguiar and Brandon (2007) cited that the energy potential for the splitting reaction of water molecules is known to be reduced as the temperature rises, while the ionic conductivity and surface reaction of electrolyte at the active sites increase directly with temperature [53]. In general, distinct peaks were reached at approx. 85°C before declining slightly at 90 and 95°C as electrolyte solutions began to boil between the electrical poles.

Moreover, experimental results – particularly in Figure 51(b) and Figure 51(c) - show that for the minimum electrolyte concentration of 0.50% w/w, productions of HHO gas were nearly zero at both 7 and 9-mm cell gaps for electrolyte temperatures ranging from 40-55°C. However, as operation temperature increased, higher rates of HHO gas were produced. Udagawa, Aguiar and Brandon (2007) found the ionic conductivity and surface reaction of electrolyte at the active sites increase directly with temperature [53]. One other conclusion thus is that increasing the cell gap helps reduce the boiling electrolyte solution between the electrical poles and enhancing the overall rate of HHO production.

When considering the practicality of using low reaction temperature of 40°C because of its high HHO production in Figure 50(a) and Figure 50(b) it was found in Figure 52 that the amount of cooling water required, regardless of the gap size, was exponentially higher than that at 65-95°C. While the reaction temperature of

95°C requires only 0.38 L/h of cooling water, more than 95 L/h of cooling water is required at 40°C in order to maintain constant operating temperature.

To apply the HHO production system to vehicles, the installation area and the weight of additional devices should be kept as low as possible. Therefore, an HHO generator with a smaller cell gap of 5 mm is preferred. From Table 8 and Table 11, the appropriate production condition was at electrolyte concentration of 1.25% w/w KOH and operating temperature of 85°C.

Maximum HHO production throughputs for the 7 and 9-mm cell gaps occurred at the electrolyte temperature of approx. 90°C. For an actual operation, there would exist deviation factors caused by human and hardware and hence some tolerance should be applied; one recommendation is $90.0 \pm 1.0^\circ\text{C}$. This final result followed the trend in a higher temperature and fairly agreed with the recommendation by Joshi (2015) that a typical temperature should be between 70 to 100°C [21].

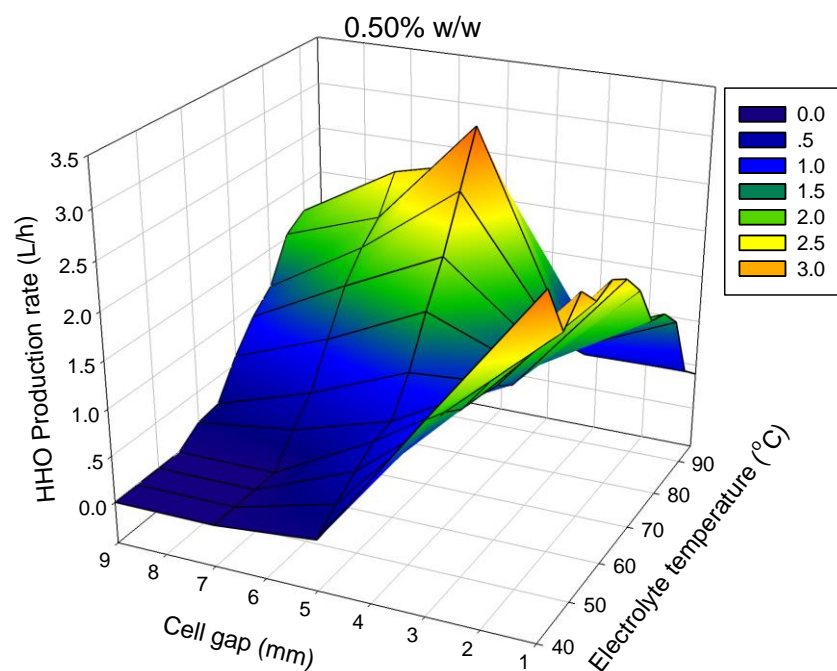


Figure 53 HHO production throughput of KOH electrolyte concentration at 0.50% w/w.

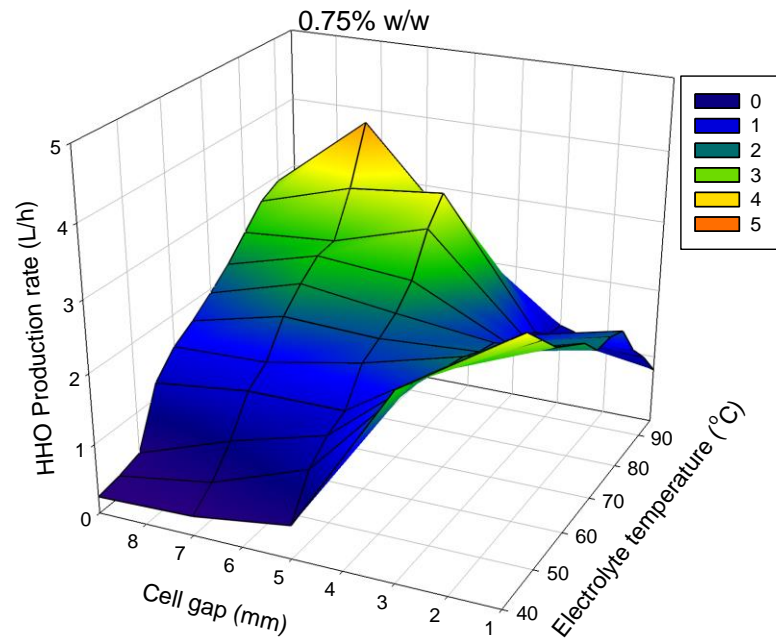


Figure 54 HHO production throughput of KOH electrolyte concentration at 0.75% w/w.

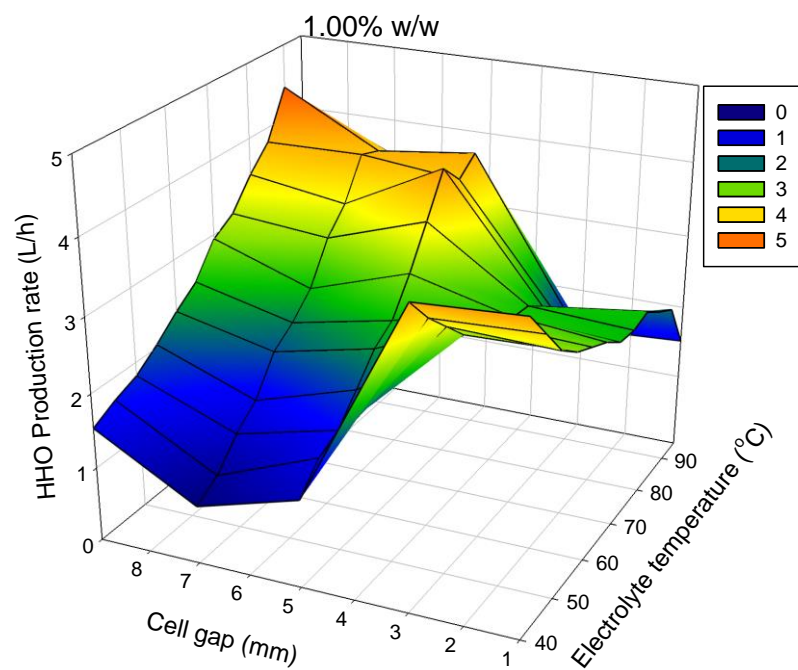


Figure 55 HHO production throughput of KOH electrolyte concentration at 1.00% w/w.

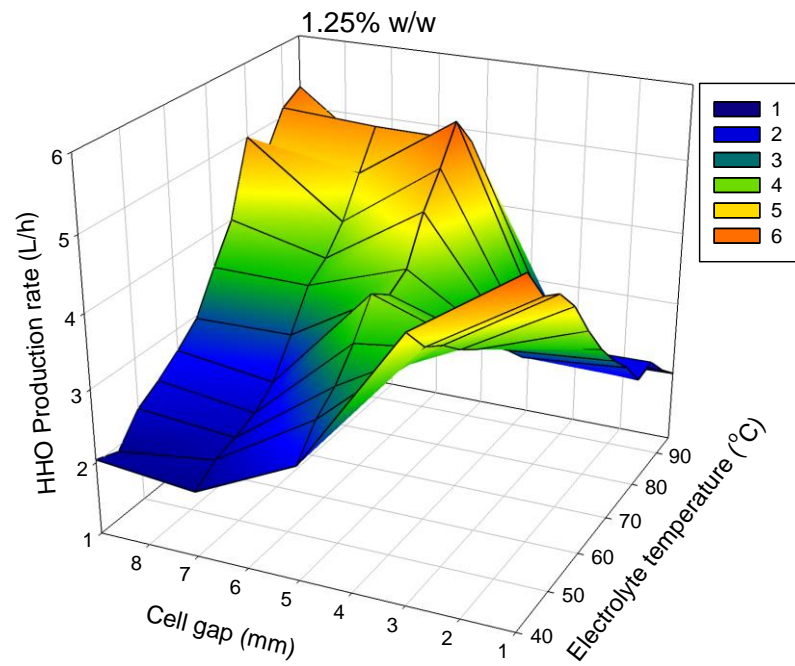


Figure 56 HHO production throughput of KOH electrolyte concentration at 1.25% w/w.

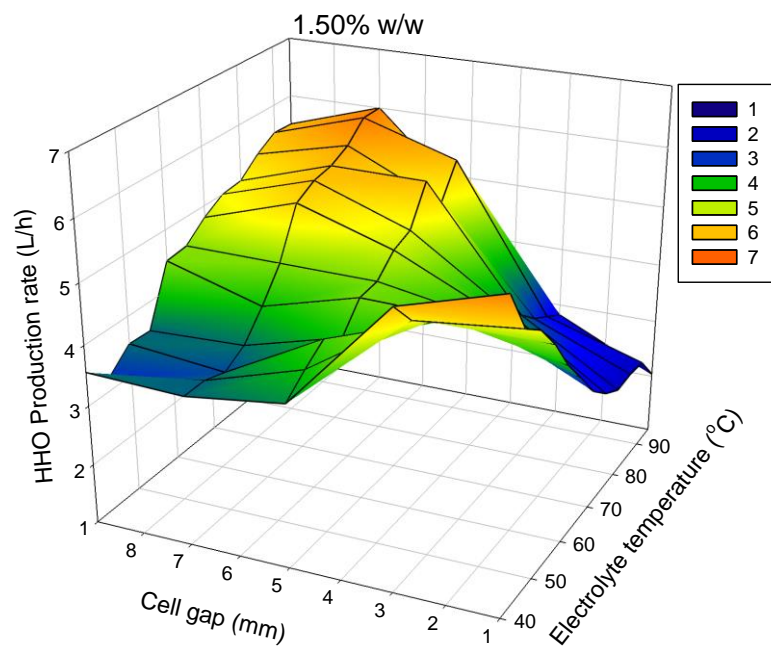


Figure 57 HHO production throughput of KOH electrolyte concentration at 1.50% w/w.

To produce HHO with an optimized production cost target, cell gaps of 1 and 3 mm at the cooler electrolyte temperature of 40°C - at the cost of very high amount of required cooling water - are not recommended. At this condition it was found that even after increasing the electrolyte concentration to its maximum value, there were negative effects - lower HHO throughputs - caused by too small the cell gap which led to the decrease in production toward the end of the run.

Higher electrical current consumption, moreover, led to increasing HHO gas bubbles formed between the gaps, while the higher electrolyte temperature caused the bubble size to increase, leading to obstruction of active reaction sites. Nagai *et al.*, (2003) found that increasing current density increased the bubble rising velocity from 4-25 cm/s and average bubble diameter from 0.01-0.5 mm [54]. Increasing the cell gaps should allow the HHO gas bubbles to float to the outside faster and not be attached to the cell surfaces.

Table 11 Optimized conditions of HHO production throughput.

Electrolyte Concentration (%w/w KOH)	Operation Conditions		
	HHO throughput (L/h)	Cell Gap (mm)	Electrolyte Temperature (°C)
0.50	3.90±0.05	3.00	40.0
0.75	3.90±0.06	7.00	90.0
1.00	4.40±0.07	9.00	90.0
1.25	5.50±0.05	1.00	40.0
1.50	6.00±0.11	7.00	90.0

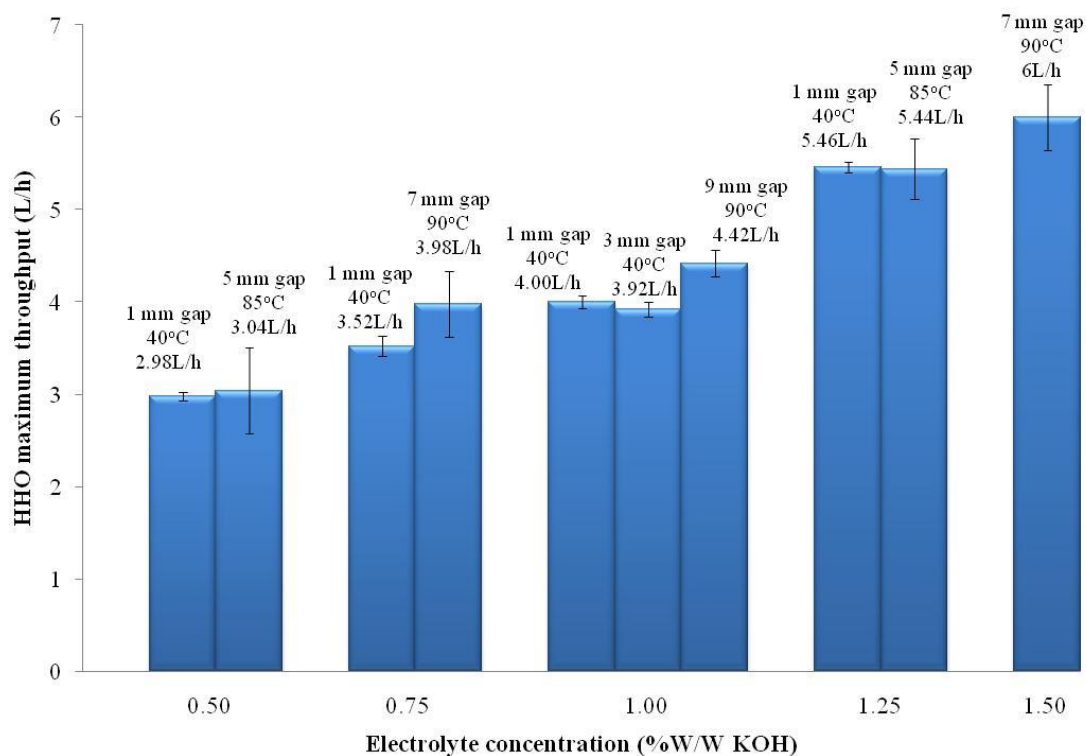


Figure 58 Maximum HHO production throughput (L/h) versus electrolyte concentration, anode-cathode area: 600 mm², AC voltage: 52.9 V, operating temperature: 40 to 95°C.

From Table 11 and Figure 58, the maximum HHO production throughput was conducted at 7-mm cell gap, an electrolyte concentration of 1.50% w/w KOH, and an operating temperature at approx. 90°C. At this condition, comparing to the electrolyte concentration of 0.50% w/w KOH, the amount of cooling water consumption was 99.86% reduced.

CHAPTER 4

Conclusions and Suggestions

4.1 Conclusions

4.1.1 Conclusion (phase I)

HHO production throughputs were found to be dependent on a larger cell gap set up, a higher electrolyte concentration and a higher operating temperature. In the continuous process of the closed-loop HHO production system studied, the appropriate production conditions with lower material consumption were found to be: an anode-cathode cell gap of 7 mm; an electrolyte solution concentration of 1.50% w/w KOH; and an operating temperature of $90.0 \pm 1.0^\circ\text{C}$. Narrower electrolyte cell gaps (1 and 3 mm) led to lower HHO production rates at high electrolyte temperatures due to hindrance from the generated HHO gas bubbles which obstructed the reaction active sites along the surface of the anode-cathode plates. Finally, increasing of electrolyte concentration from 0.50 to 1.50% w/w KOH, and the electrolyte temperature from 40 to 95°C led to an increased HHO product throughput by more than 50 and 60%, respectively.

4.1.2 Conclusion (phase II)

This research analyzed the effect of vacuum pressure and electrolyte temperature on HHO production. The design of the closed-loop system was based on future integration to Internal Combustion Engine (ICE). Using cathode-anode plates, the maximum HHO throughput was found to be at 85°C and 81.0 kPa abs. A correlation between the electrolyte temperature and the product temperature were

obtained and suggested for possible control design. In addition, the electrical current consumption showed an upside down parabolic trend with increasing electrolyte temperature. It also decreased linearly with increasing degree of vacuum pressure at a constant electrolyte temperature. Finally, the overall production throughput increased from atmospheric pressure to vacuum pressure from 101.3 to 81.0 kPa abs; however, at lower vacuum pressure below 72.0 kPa abs, the effect of solution boiling point decreased the production capacity dramatically.

4.2 Suggestions

1) To running the closed-loop circulation of HHO production with high stability with uniform volume flow rate of KOH electrolyte solution, inside liquid-gas separator tank which perform like a buffer container should keep the electrolyte solution level at least 30%, to protect vortex phenomenon take place while running the overall system.

2) Because there are HHO bubbles and KOH solution flow along the production pipe line continuously, the system must not have leaking point at all connection joint and unit operation.

3) Due to widely operating temperature in this experiment (40 to 95°C), the experimenter should closely monitor the volume flow rate of cooling water supply, and try to keep the steady state of electrolyte temperature all the running time.

4) All equipments include pipe line and instrument devices in the experiment must have the thermal resistance at least 100°C.

5) Because HHO contain hydrogen and oxygen component inside its molecule, the experimenter should beware for the sparked point while running the system.

6) In the step of changing the level of electrolyte concentration, the experimenter have to flushing system with clean water until the water conductivity inside back to the same as pure water property.

7) By varying the electrical voltages, the experimenter should isolate the electrical supply source first, then switch to the next voltage and turn on power.

8) In the step of operating pressure adjustment, the vacuum pump and breathing valve should locate at the end of HHO pipe line, by this installation, the inlet atmospheric air will not disturb the set up pressure inside HHO production system.

9) Should not touch the KOH solution directly, due to KOH solution with high pH maybe erode user's skin.

10) At the HHO generator, must be kept the KOH electrolyte solution flood the electrical cell (anode-cathode) all the time.

11) Should install the lab-station at a good air ventilation to protect HHO accumulation which is a cause of explosion.

12) Every running condition, the experimenter should inspect the surface of anode-cathode cell and clean it if found a dirty film took place.

13) Release HHO to ambient or burn it with the air is more appropriate than compress it in the vessel.

14) To apply the closed loop HHO production system with engine, the experimenter have to mention that have to install a flame arrestor at the outlet of HHO before feed into internal combustion engine (ICE) to protect the sparking flame back to system.

15) The electrical grounding have to connect directly to all unit operations and metal pipe lines to protect fire sparking point by electrostatic and electrical source.

REFERENCES

- [1] M. Momirlan and T. N. Veziroglu, "The properties of hydrogen as fuel tomorrow in sustainable energy system for a cleaner planet," *Int. J. Hydrogen Energy*, vol. 30, no. 7, pp. 795–802, 2005.
- [2] Ruggero Maria Santilli, "A new gaseous and combustible form of water," *Int. J. Hydrogen Energy*, vol. 31, pp. 1113–1128, 2006.
- [3] R. M. Santilli, "Foundations of hadronic chemistry with applications to new clean energies and fuels," Boston-Dordrecht-London: Kluwer Academic Publishers, 2001.
- [4] Z. DuÈlger and K.R. Ozcelik, "Fuel economy improvement by on board electrolytic hydrogen production," *Int. J. Hydrogen Energy*, vol. 25, no. 1, pp. 895–897, 2000.
- [5] A. C. Yilmaz, E. Uludamar, and K. Aydin, "Effect of hydroxy (HHO) gas addition on performance and exhaust emissions in compression ignition engines," *Int J Hydrog. Energy*, vol. 35, no. 20, pp. 11366–11372, 2010.
- [6] A. A. Al-Rousan, "Reduction of fuel consumption in gasoline engines by introducing HHO gas into intake manifold," *Int J Hydrog. Energy*, vol. 35, no. 23, pp. 12930–12935, 2010.
- [7] S. A. Musmar and A. A. Al-Rousan, "Effect of HHO gas on combustion emissions in gasoline engines," *Fuel*, vol. 90, no. 10, pp. 3066–3070, 2011.
- [8] R. B. Durairaja, J. Shanker, and M. Sivasankar, "HHO Gas with Bio Diesel as a Dual Fuel with Air preheating Technology," *Procedia Eng.*, vol. 38, pp. 1112–1119, 2012.
- [9] H. H. Masjuki, A. M. Ruhul, N. N. Mustafi, M. A. Kalam, M. I. Arbab, and I. M. R. Fattah, "Study of production optimization and effect of hydroxyl gas on a CI engine performance and emission fueled with biodiesel blends," *Int J Hydrog. Energy*, vol. 41, no. 33, pp. 14519–14528, 2016.
- [10] M. K. Arat, Hüseyin Turan Baltacıoglu, M. Özcanli, and K. Aydin, "Effect of using Hydroxy – CNG fuel mixtures in a non-modified diesel engine by substitution of diesel fuel," *Int J Hydrog. Energy*, vol. 41, no. 19, pp. 8354–8363, 2016.

- [11] M. K. Baltacioglu, H. T. Arat, M. Ozcanli, and K. Aydin, "Experimental comparison of pure hydrogen and HHO (hydroxy) enriched biodiesel (Bio) fuel in a commercial diesel engine," *Int J Hydrog. Energy*, vol. 41, no. 19, pp. 8347–8353, 2016.
- [12] M. M. EL-Kassaby, Y. A. Eldrainy, M. E. Khidr, and K. I. Khidr, "Effect of hydroxyl (HHO) gas addition on gasoline engine performance and emissions," *Alexandria Eng J*, vol. 55, no. 1, pp. 243–251, 2016.
- [13] M. R. Dahake, S. D. Patil, and S. E. Patil, "Effect of Hydroxy Gas Addition on Performance and Emissions of Diesel," *Int Res J Eng Technol*, vol. 3, no. 1, pp. 756–760, 2016.
- [14] P. K. Putha and G. S. Babu, "Performance of I.C. engines using HHO gas," *Int Res J Eng Technol*, vol. 4, no. 16, pp. 2994–2998, 2015.
- [15] V. P. Bharathi, I. P. Rao, V. N. Deepthi, I. Prasanna, and A. L. Jyothi, "Improving The Efficiency Of I.C. Engine Using Secondary Fuel," *Int J Adv Res Eng Manag*, vol. 1, no. 4, pp. 69–78, 2015.
- [16] F. Desai, P. Dave, and H. Tailor, "Performance and emission assessment of hydro-oxy gas in 4-stroke S.I. engine," *Int J Mech. Eng Technol*, vol. 5, no. 9, pp. 455–462, 2014.
- [17] S. V. Chaudhari, A. A. Gupta, S. R. Dafal, A. V. Gawas, and V. K. JavanJal, "Effect of hydrogen blending on performance and emission of a four-stroke single cylinder S.I engine," *Int J Innov Mech Automot Res*, vol. 1, no. 2, pp. 84–89, 2015.
- [18] V. J. A. Vino, V. S. Ramanlal, and Y. Madhusudhan, "Performance Analysis of Petrol - HHO Engine," *Middle-East J Sci Res*, vol. 12, no. 12, pp. 1634–1637, 2012.
- [19] Dweepson, S. C. Subramanian, J. A. Kumar, and S. Sakthivel, "An experimental assessment of performance and exhaust emission characteristics by addition of hydroxy (HHO) gas in twin cylinder C.I. engine," *Int J Innov Res Sci Eng Technol*, vol. 3, no. 2, pp. 60–67, 2014.
- [20] A. GÖLLEI, "Measuring and optimization of HHO dry cell for energy efficiency," *ACTA Teh. CORVINIENSIS-Bulletin Eng.*, vol. 7, no. 4, pp. 19–22, 2014.

- [21] N. Joshi and D. Naik, "Onboard production of hydrogen gas for power generation," *J Res Mech Eng*, vol. 2, no. 6, pp. 1–11, 2015.
- [22] G. De Wilde, "Yull Brown: Bulgarian heavy water physicist," 2012. [Online]. Available: <http://knol.go-here.nl/yull-brown.html>. [Accessed: 15-Jul-2015].
- [23] "Yull Brown: Brown's Gas." [Online]. Available: <http://www.nottaughtinschools.com/Yull-Brown/Free-Energy-Interview.html>. [Accessed: 15-Jul-2015].
- [24] "William A. Rhodes." [Online]. Available: <http://www.hydrogen-gas-savers.com/william-a-rhodes.htm>. [Accessed: 15-Jul-2015].
- [25] "Andrija Puharich: Water Decomposition by AC Electrolysis." [Online]. Available: <http://rexresearch.com/puharich/1puhar.htm>. [Accessed: 15-Jul-2015].
- [26] E. Ruoho, "Steve Windisch: Brown's Gas ('HHO'): Clean, Cheap, and Suppressed Energy," 2008. [Online]. Available: <http://merlib.org/node/5676>. [Accessed: 15-Jul-2015].
- [27] Jeane, "HHO – not combustion & maybe not hydrogen," 2011. [Online]. Available: <http://changingpower.net/hho-not-combustion-maybe-not-hydrogen/>. [Accessed: 15-Jul-2015].
- [28] "Truest Natural Scientist." [Online]. Available: <https://truespring.wordpress.com/truest-natural-scientist/>.
- [29] J. J. Hurtak and D. Hurtak, "The history and future of brown's gas," *NEXUS*, pp. 49–54, 80–81, 2014.
- [30] M. Dansie, "Compressable HHO: An alternative for Hydrogen Storage?," 2014. [Online]. Available: <http://revolution-green.com/compressable-hho-alternative-hydrogen-storage/>. [Accessed: 15-Jul-2015].
- [31] Wikipedia, "John Kanzius," 2016. [Online]. Available: https://en.wikipedia.org/wiki/John_Kanzius. [Accessed: 10-Mar-2016].
- [32] C. Beiser, "PROJEKT AUKW – UPDATE KW 16/2015." [Online]. Available: <http://gaia-energy.org/projekt-aukw-update-kw162015/>. [Accessed: 15-Jul-2015].
- [33] "Browns Gas." [Online]. Available: <http://www.svpvriil.com/svpweb9.html>. [Accessed: 15-Jul-2015].

- [34] J. Wall, "Affirmative Expert Report: An Assessment of the Fuel Economy Claims Made for the Hydro Assist Fuel Cell (HAFC) System," 2010.
- [35] T. Prisecaru, C. Dica, M. Teodorescu, M. Prisecaru, and L. Mihaescu, "Experimental validation of an HHO gas cutting flame CFD model," in 9th International Conference on Quantitative InfraRed Thermography, 2008.
- [36] College of the Desert and SunLine Transit Agency, Hydrogen Fuel Cell Engines and Related Technologies. CA, USA: College of the Desert, Palm Desert, 2001.
- [37] "The Energy and Fuel Data Sheet," 2011.
- [38] HydrogenEnergySystems, "Hydrogen Fuel Cost vs Gasoline." [Online]. Available: <http://heshydrogen.com/hydrogen-fuel-cost-vs-gasoline/>. [Accessed: 15-Jul-2015].
- [39] M. Wang, "Fuel choices for fuel-cell vehicles: well-to-wheels energy and emission impacts," *J. Power Sources*, vol. 112, no. 1, pp. 307–321, 2002.
- [40] hho-generator.de, "Twin HHO Generator Hydrogen System." [Online]. Available: <http://www.hho-generator.de/en/hydrogen-generator-system.htm>. [Accessed: 15-Jul-2015].
- [41] T. De Silva, L. Senevirathne, and T. Warnasooriya, "HHO generator-an approach to increase fuel efficiency in spark ignition engines," *Euro J Adv Eng Technol*, vol. 2, no. 4, pp. 1–7, 2015.
- [42] N. Chraplewska, K. Duda, and M. Meus, "Evaluation of usage brown gas generator for aided admission of diesel engine with fermentative biogas and producer gas," *J. KONES Powertrain Transp.*, vol. 18, no. 3, pp. 53–60, 2011.
- [43] Y. Milind S., S. S. M., A. Jayesh A., and C. Hemant V., "Investigations on generation methods for oxy-hydrogen gas, its blending with conventional fuels and effect on the performance of internal combustion engine," *J. Mech. Eng. Res.*, vol. 3, no. 9, pp. 325–332, 2011.
- [44] S. Khulbe, N. Khatri, and P. S. Ranjit, "Feasibility establishment with on board generated hydrogen supplementation and studies on emission characteristics of gasoline engine," *J. Mech. Civ. Eng.*, vol. 11, no. 6, pp. 52–59, 2014.
- [45] V. J. Ananth Vino and Ap, "HHO assisted LPG Engine," *Int. J. Comput. Trends Technol.*, vol. 44–60, no. 3, p. 6, 2012.

- [46] C. Naresh, Y. Sureshbabu, and S. Bhargavi Devi, "Performance and Exhaust Gas Analysis Of A Single Cylinder Diesel Engine Using HHO Gas (Brown's Gas)," *Int. J. Eng. Res.*, vol. 3, no. 1, pp. 40–47, 2014.
- [47] R. A. Lodhi, A. Nawaz, and R. R. Ahmed, "An empirical study for achieving economies of scale by utilization of (HHO) hydrogen hydroxy gas as additional fuel," *J. Energy Technol. Policy*, vol. 5, no. 4, pp. 1–10, 2015.
- [48] T. Rajasekaran, K. Duraiswamy, M. Bharathiraja, and S. Poovaragavan, "Characteristics of engine at various speed conditions by mixing of HHO with gasoline and LPG," *J. Eng. Appl. Sci.*, vol. 10, no. 1, pp. 46–51, 2015.
- [49] P. Andersson, "Comparison of two exhaust manifold estimation methods," in *The third computer science and engineering system conference*, 2001.
- [50] P. Andersson, *Intake air dynamics on a turbocharged SI-engine with waste gate*, Ph.D. Thesis. Electrical Engineering, Linkoping University, Sweden, 2002.
- [51] E. Zoulias, E. Varkaraki, N. Lymberopoulos, C. N. Christodoulou, and G. N. Karagiorgis, "Review on water electrolysis," *TCJST*, vol. 4, no. 2, pp. 41–71, 2004.
- [52] V. M. Nikolic, G. S. Tasic, A. D. Maksic, D. P. Saponjic, S. M. Miulovic, and M. P. Marceta Kaninski, "Raising efficiency of hydrogen generation from alkaline water electrolysis – Energy saving," *Int. J. Hydrogen Energy*, vol. 35, no. 22, pp. 12369–12373, 2010.
- [53] J. Udagawa, P. Aguiar, and N. P. Brandon, "Hydrogen production through steam electrolysis: Model-based steady state performance of a cathode-supported intermediate temperature solid oxide electrolysis cell," *J. Power Sources*, vol. 166, no. 1, pp. 127–136, 2007.
- [54] N. Nagai, M. Takeuchi, and M. Nakao, "Influences of bubbles between electrodes onto efficiency of alkaline water electrolysis," in *Proceedings of PSFVIP-4*, 2003.

APPENDICES

Appendix A

Experiment data

Table 12 Relation between electrolyte temperature (°C) and HHO product temperature (°C) of electrolyte concentration from 0.50 to 1.50% w/w KOH, 1 mm cell gap, 20 x 30 mm², 52.9 volt and 1 atm.

Elec. Temp. (°C)	HHO product temperature (°C)				
	0.50%w/w KOH	0.75% w/w KOH	1.00% w/w KOH	1.25% w/w KOH	1.50% w/w KOH
40	31.3	32.6	32.4	31.9	32.3
45	35.4	35.8	35.6	35.1	33.8
50	39.5	40.1	39.5	38.3	36.9
55	43.8	44.6	43.0	42.5	40.8
60	48.7	48.7	48.1	47.5	45.8
65	54.1	53.4	53.2	52.1	51.3
70	60.2	58.8	59.2	57.9	58.4
75	66.6	66.4	65.3	65.0	65.7
80	73.5	72.0	71.8	71.7	72.0
85	79.3	78.5	77.2	77.5	78.4
90	84.5	84.7	83.3	84.2	83.8
95	90.7	90.9	89.6	89.8	89.3

Table 13 Relation between electrolyte temperature ($^{\circ}\text{C}$) and HHO product temperature ($^{\circ}\text{C}$) of electrolyte concentration from 0.50 to 1.50% w/w KOH, 3 mm cell gap, 20 x 30 mm², 52.9 volt and 1 atm.

Elec. Temp. ($^{\circ}\text{C}$)	HHO product temperature ($^{\circ}\text{C}$)				
	0.50% w/w KOH	0.75% w/w KOH	1.00% w/w KOH	1.25% w/w KOH	1.50% w/w KOH
40	30.9	30.9	31.2	32.8	32.3
45	34.2	34.2	33.6	34.7	34.5
50	38.8	38.8	37.1	37.5	37.0
55	43.9	43.9	42.2	42.1	40.7
60	48.1	48.1	46.5	46.3	45.5
65	53.0	53.0	50.5	51.4	50.7
70	58.4	58.4	56.0	56.6	58.2
75	64.2	64.2	63.0	64.8	65.7
80	71.7	71.7	70.8	72.7	72.1
85	79.4	79.4	77.5	77.9	77.9
90	85.3	85.3	84.1	85.0	84.1
95	91.2	91.2	91.0	89.9	89.7

Table 14 Relation between electrolyte temperature ($^{\circ}\text{C}$) and HHO product temperature ($^{\circ}\text{C}$) of electrolyte concentration from 0.50 to 1.50% w/w KOH, 5 mm cell gap, 20 x 30 mm², 52.9 volt and 1 atm.

Elec. Temp. ($^{\circ}\text{C}$)	HHO product temperature ($^{\circ}\text{C}$)				
	0.50% w/w KOH	0.75% w/w KOH	1.00% w/w KOH	1.25% w/w KOH	1.50% w/w KOH
40	32.3	31.8	33.7	32.2	32.5
45	35.9	35.0	36.8	34.8	33.9
50	40.4	38.2	39.4	38.6	37.0
55	44.7	42.9	42.7	41.8	40.6
60	49.3	47.5	47.5	46.0	44.6
65	54.1	51.8	51.8	50.4	49.6
70	59.2	57.0	56.1	55.0	53.9
75	65.1	62.7	62.5	60.0	59.7
80	70.1	68.9	69.6	66.3	66.3
85	76.4	76.9	77.4	72.0	77.5
90	83.2	84.2	84.4	80.9	82.8
95	90.7	90.3	90.0	88.3	89.3

Table 15 Relation between electrolyte temperature (°C) and HHO product temperature (°C) of electrolyte concentration from 0.50 to 1.50% w/w KOH, 7 mm cell gap 20 x 30 mm² 52.9 volt and 1 atm.

Elec. Temp. (°C)	HHO product temperature (°C)				
	0.50% w/w KOH	0.75% w/w KOH	1.00% w/w KOH	1.25% w/w KOH	1.50% w/w KOH
40	31.9	33.9	33.6	33.4	31.2
45	35.4	36.3	35.6	35.9	33.4
50	39.3	39.7	39.0	38.5	36.0
55	43.3	43.1	42.4	41.7	41.7
60	48.0	47.4	46.4	46.3	45.1
65	52.5	51.6	51.0	50.3	50.2
70	57.6	56.2	55.9	54.7	54.0
75	63.1	61.6	61.1	60.3	60.8
80	68.1	66.6	66.7	66.2	66.2
85	74.6	73.1	73.4	73.0	73.5
90	81.0	79.7	80.7	82.6	79.3
95	88.7	87.8	89.2	89.7	87.2

Table 16 Relation between electrolyte temperature ($^{\circ}\text{C}$) and HHO product temperature ($^{\circ}\text{C}$) of electrolyte concentration from 0.50 to 1.50% w/w KOH, 9 mm cell gap, 20 x 30 mm², 52.9 volt and 1 atm.

Elec. Temp. ($^{\circ}\text{C}$)	HHO product temperature ($^{\circ}\text{C}$)				
	0.50% w/w KOH	0.75% w/w KOH	1.00% w/w KOH	1.25% w/w KOH	1.50% w/w KOH
40	33.3	34.7	33.1	31.9	32.2
45	37.2	37.5	35.9	34.7	33.6
50	41.0	40.6	39.6	38.2	36.2
55	45.2	44.1	42.8	42.7	40.3
60	50.0	48.2	46.8	46.7	44.3
65	54.5	53.0	51.5	51.3	49.3
70	59.3	57.8	56.3	56.1	53.2
75	64.7	63.1	61.7	61.3	58.2
80	70.3	68.8	67.0	66.3	64.7
85	76.0	75.5	75.8	74.4	71.6
90	82.6	82.6	81.8	81.7	78.8
95	89.8	89.9	89.4	88.0	86.8

Table 17 Relation between electrolyte temperature ($^{\circ}\text{C}$) and HHO product temperature ($^{\circ}\text{C}$) of cell gap set up from 1 to 9 mm, 0.50% w/w KOH, 20 x 30 mm², 52.9 volt and 1 atm.

Elec. Temp. ($^{\circ}\text{C}$)	HHO product temperature ($^{\circ}\text{C}$)				
	1 mm cell gap	3 mm cell gap	5 mm cell gap	7 mm cell gap	9 mm cell gap
40	31.3	30.9	32.3	31.9	33.3
45	35.4	34.2	35.9	35.4	37.2
50	39.5	38.8	40.4	39.3	41.0
55	43.8	43.9	44.7	43.3	45.2
60	48.7	48.1	49.3	48.0	50.0
65	54.1	53.0	54.1	52.5	54.5
70	60.2	58.4	59.2	57.6	59.3
75	66.6	64.2	65.1	63.1	64.7
80	73.5	71.7	70.1	68.1	70.3
85	79.3	79.4	76.4	74.6	76.0
90	84.5	85.3	83.2	81.0	82.6
95	90.7	91.2	90.7	88.7	89.8

Table 18 Relation between electrolyte temperature ($^{\circ}\text{C}$) and HHO product temperature ($^{\circ}\text{C}$) of cell gap set up from 1 to 9 mm, 0.75% w/w KOH, 20 x 30 mm², 52.9 volt and 1 atm.

Elec. Temp. ($^{\circ}\text{C}$)	HHO product temperature ($^{\circ}\text{C}$)				
	1 mm cell gap	3 mm cell gap	5 mm cell gap	7 mm cell gap	9 mm cell gap
40	32.6	33.4	31.8	33.9	34.7
45	35.8	36.9	35.0	36.3	37.5
50	40.1	40.0	38.2	39.7	40.6
55	44.6	44.0	42.9	43.1	44.1
60	48.7	48.4	47.5	47.4	48.2
65	53.4	53.0	51.8	51.6	53.0
70	58.8	59.0	57.0	56.2	57.8
75	66.4	65.0	62.7	61.6	63.1
80	72.0	71.2	68.9	66.6	68.8
85	78.5	78.0	76.9	73.1	75.5
90	84.7	84.3	84.2	79.7	82.6
95	90.9	90.1	90.3	87.8	89.9

Table 19 Relation between electrolyte temperature ($^{\circ}\text{C}$) and HHO product temperature ($^{\circ}\text{C}$) of cell gap set up from 1 to 9 mm, 1.00% w/w KOH, 20 x 30 mm², 52.9 volt and 1 atm.

Elec. Temp. ($^{\circ}\text{C}$)	HHO product temperature ($^{\circ}\text{C}$)				
	1 mm cell gap	3 mm cell gap	5 mm cell gap	7 mm cell gap	9 mm cell gap
40	32.4	31.9	33.7	33.6	33.1
45	35.6	33.5	36.8	35.6	35.9
50	39.5	36.6	39.4	39.0	39.6
55	43.0	41.3	42.7	42.4	42.8
60	48.1	46	47.5	46.4	46.8
65	53.2	50.5	51.8	51.0	51.5
70	59.2	55.2	56.1	55.9	56.3
75	65.3	60.1	62.5	61.1	61.7
80	71.8	66.5	69.6	66.7	67.0
85	77.2	75.5	77.4	73.4	75.8
90	83.3	82.2	84.4	80.7	81.8
95	89.6	89.1	90.0	89.2	89.4

Table 20 Relation between electrolyte temperature ($^{\circ}\text{C}$) and HHO product temperature ($^{\circ}\text{C}$) of cell gap set up from 1 to 9 mm, 1.25% w/w KOH, 20 x 30 mm², 52.9 volt and 1 atm.

Elec. Temp. ($^{\circ}\text{C}$)	HHO product temperature ($^{\circ}\text{C}$)				
	1 mm cell gap	3 mm cell gap	5 mm cell gap	7 mm cell gap	9 mm cell gap
40	31.9	32.8	32.2	33.4	31.9
45	35.1	34.7	34.8	35.9	34.7
50	38.3	37.5	38.6	38.5	38.2
55	42.5	42.1	41.8	41.7	42.7
60	47.5	46.3	46.0	46.3	46.7
65	52.1	51.4	50.4	50.3	51.3
70	57.9	56.6	55.0	54.7	56.1
75	65.0	64.8	60.0	60.3	61.3
80	71.7	72.7	66.3	66.2	66.3
85	77.5	77.9	72.0	73.0	74.4
90	84.2	85.0	80.9	82.6	81.7
95	89.8	89.9	88.3	89.7	88.0

Table 21 Relation between electrolyte temperature ($^{\circ}\text{C}$) and HHO product temperature ($^{\circ}\text{C}$) of cell gap set up from 1 to 9 mm, of 1.50% w/w KOH, 20 x 30 mm², 52.9 volt and 1 atm.

Elec. Temp. ($^{\circ}\text{C}$)	HHO product temperature ($^{\circ}\text{C}$)				
	1 mm cell gap	3 mm cell gap	5 mm cell gap	7 mm cell gap	9 mm cell gap
40	32.3	32.3	32.5	31.2	32.2
45	33.8	34.5	33.9	33.4	33.6
50	36.9	37.0	37.0	36.0	36.2
55	40.8	40.7	40.6	41.7	40.3
60	45.8	45.5	44.6	45.1	44.3
65	51.3	50.7	49.6	50.2	49.3
70	58.4	58.2	53.9	54.0	53.2
75	65.7	65.7	59.7	60.8	58.2
80	72.0	72.1	66.3	66.2	64.7
85	78.4	77.9	77.5	73.5	71.6
90	83.8	84.1	82.8	79.3	78.8
95	89.3	89.7	89.3	87.2	86.8

Table 22 Relation between electrolyte temperature ($^{\circ}\text{C}$) and HHO product temperature ($^{\circ}\text{C}$) of electrical voltage from 47.5 to 52.9 volt of 1.25% w/w KOH, 20 x 30 mm², 5 mm cell gap, 47.5 to 52.9 volt and 1 atm.

Elec Temp. ($^{\circ}\text{C}$)	HHO product temperature ($^{\circ}\text{C}$)				
	47.5 Volt	49.3 Volt	50.7 Volt	51.9 Volt	52.9 Volt
40	30.7	31.0	31.2	31.2	31.9
45	33.9	33.9	34.4	33.8	33.2
50	37.6	38.0	37.6	36.9	36.6
55	40.7	41.6	41.5	41.3	41.0
60	43.7	45.1	44.7	45.9	45.3
65	47.7	49.4	48.5	50.1	48.7
70	52.4	52.6	53.9	55.0	53.6
75	57.7	58.8	59.4	62.4	61.0
80	66.2	66.4	65.8	69.4	68.5
85	74.6	74.7	75.5	75.6	75.3
90	82.5	81.6	81.6	83.5	82.1
95	88.9	87.8	88.2	89.9	89.2

Table 23 Relation between electrolyte temperature ($^{\circ}\text{C}$) and HHO product temperature ($^{\circ}\text{C}$) of operating pressure from 60.8 to 101.3 kPa of 1.25% w/w KOH, 20 x 30 mm², 5 mm cell gap, 52.9 volt and 1 atm.

Elec Temp. ($^{\circ}\text{C}$)	HHO product temperature ($^{\circ}\text{C}$)				
	101.3 kPa abs	91.2 kPa abs	81.0 kPa abs	70.9 kPa abs	60.8 kPa abs
40	31.9	31.7	31.4	30.6	31.8
45	33.2	32.8	32.5	31.4	33.7
50	36.6	36.2	34.2	33.7	36.4
55	41.0	40.7	37.2	37.6	40.1
60	45.3	44.4	40.3	42.2	45.5
65	48.7	48.8	44.0	46.7	50.4
70	53.6	53.6	48.0	51.4	55.5
75	61.0	58.3	53.9	57.0	64.1
80	68.5	64.1	60.4	64.4	70.9
85	75.3	70.2	66.8	72.7	80.7
90	82.1	78.4	76.5	82.4	89.0
95	89.2	84.8	88.1	93.5	94.8

Table 24 Relation between electrolyte temperature ($^{\circ}\text{C}$) and HHO product temperature ($^{\circ}\text{C}$) of anode-cathode area from 300 to 1500 mm^2 of 1.25% w/w KOH, 20 x 30 mm^2 , 5 mm cell gap, 52.9 volt and 1 atm.

Elec Temp. ($^{\circ}\text{C}$)	HHO product temperature ($^{\circ}\text{C}$)				
	300 mm^2	600 mm^2	900 mm^2	1200 mm^2	1500 mm^2
40	31.8	30.7	31.4	31.9	32.3
45	34.8	33.9	32.8	35.5	34.2
50	39.1	37.6	38.7	40.1	37.2
55	42.1	40.7	43.1	45.0	41.4
60	47.0	43.7	46.9	48.9	45.0
65	51.5	47.7	51.8	54.4	50.0
70	51.3	52.4	56.1	58.6	54.8
75	61.2	57.7	61.6	64.3	61.0
80	67.7	66.2	66.6	70.6	67.2
85	73.6	74.6	72.5	76.5	74.2
90	79.7	82.5	77.1	83.0	81.0
95	86.4	88.9	84.1	88.4	87.5

Table 25 Relation between electrolyte temperature ($^{\circ}\text{C}$) and electrical current consumption (A) of electrolyte concentration from 0.50 to 1.50% w/w KOH, of 1 mm cell gap, 20 x 30 mm², 52.9 volt and 1 atm.

Elec. Temp. ($^{\circ}\text{C}$)	Electrical Current (Amp.)				
	0.50% w/w KOH	0.75% w/w KOH	1.00% w/w KOH	1.25% w/w KOH	1.50% w/w KOH
40	33.8	38.6	44.0	50.1	54.1
45	32.6	38.7	44.3	50.4	54.3
50	32.7	38.4	44.5	50.5	54.1
55	32.4	38.3	44.3	50.1	54.8
60	32.8	37.8	44.0	49.7	54.8
65	31.7	37.6	43.2	49.7	54.0
70	31.1	36.8	42.6	48.5	53.6
75	30.3	35.3	41.3	47.4	51.6
80	28.4	34.4	39.9	45.2	49.7
85	26.9	33.4	38.6	43.3	47.8
90	24.9	31.7	36.7	41.3	45.8
95	23.1	29.5	34.2	39.5	43.6

Table 26 Relation between electrolyte temperature ($^{\circ}\text{C}$) and electrical current consumption (A) of electrolyte concentration from 0.50 to 1.50% w/w KOH, of 3 mm cell gap, 20 x 30 mm², 52.9 volt and 1 atm.

Elec. Temp. ($^{\circ}\text{C}$)	Electrical Current (Amp.)				
	0.50% w/w KOH	0.75% w/w KOH	1.00% w/w KOH	1.25% w/w KOH	1.50% w/w KOH
40	37.5	47.9	55.7	61.2	68.2
45	38.8	48.8	55.6	61.6	67.4
50	39.3	48.9	55.4	60.2	66.7
55	39.4	48.1	55.1	59.6	66.1
60	38.6	47.2	54.8	57.3	64.6
65	38.1	44.5	54.1	55.5	62.2
70	37.0	43.6	52.1	54.1	59.1
75	35.3	41.3	50.5	52.0	57.7
80	33.1	39.8	48.2	50.5	55.2
85	30.4	37.8	44.2	48.8	52.6
90	28.1	34.9	40.4	43.7	49.5
95	25.0	31.9	36.6	40.5	44.8

Table 27 Relation between electrolyte temperature ($^{\circ}\text{C}$) and electrical current consumption (A) of electrolyte concentration from 0.50 to 1.50% w/w KOH, of 5 mm cell gap, $20 \times 30 \text{ mm}^2$, 52.9 volt and 1 atm.

Elec. Temp. ($^{\circ}\text{C}$)	Electrical Current (Amp.)				
	0.50% w/w KOH	0.75% w/w KOH	1.00% w/w KOH	1.25% w/w KOH	1.50% w/w KOH
40	25.5	36.8	46.2	54.3	62.1
45	27.2	40.2	48.9	57.2	65.3
50	29.1	42.0	50.9	59.8	68.5
55	30.2	43.0	52.8	61.4	68.7
60	30.9	43.8	54.3	63.5	70.8
65	32.2	45.5	55.5	63.6	71.2
70	32.9	45.7	55.4	64.2	71.6
75	33.5	45.7	54.8	62.4	71.8
80	34.0	45.1	53.2	60.7	68.5
85	34.5	43.1	50.1	58.2	61.7
90	33.7	39.7	45.9	53.1	57.3
95	29.3	35.9	41.9	47.0	52.2

Table 28 Relation between electrolyte temperature ($^{\circ}\text{C}$) and electrical current consumption (A) of electrolyte concentration from 0.50 to 1.50% w/w KOH, of 7 mm cell gap, $20 \times 30 \text{ mm}^2$, 52.9 volt and 1 atm.

Elec. Temp. ($^{\circ}\text{C}$)	Electrical Current (Amp.)				
	0.50% w/w KOH	0.75% w/w KOH	1.00% w/w KOH	1.25% w/w KOH	1.50% w/w KOH
40	21.0	29.8	37.1	45.0	51.5
45	22.8	32.8	39.7	48.0	54.7
50	24.2	34.4	42.4	50.6	57.0
55	25.2	36.6	44.7	51.9	59.4
60	26.0	37.8	46.0	56.2	62.4
65	26.9	38.8	48.3	56.8	63.5
70	27.3	40.1	49.2	57.7	65.6
75	28.5	40.9	49.5	58.3	67.1
80	29.3	41.0	50.3	58.2	67.7
85	30.0	41.4	50.0	56.9	66.2
90	30.2	40.9	48.0	55.4	63.9
95	29.3	37.3	45.5	50.8	56.4

Table 29 Relation between electrolyte temperature ($^{\circ}\text{C}$) and electrical current consumption (A) of electrolyte concentration from 0.50 to 1.50% w/w KOH, of 9 mm cell gap, 20 x 30 mm², 52.9 volt and 1 atm.

Elec. Temp. ($^{\circ}\text{C}$)	Electrical Current (Amp.)				
	0.50% w/w KOH	0.75% w/w KOH	1.00% w/w KOH	1.25% w/w KOH	1.50% w/w KOH
40	18.3	26.7	33.9	40.3	45.0
45	19.9	29.4	36.9	44.3	48.4
50	20.9	30.7	39.6	46.1	51.9
55	21.8	32.4	41.2	48.7	55.1
60	23.0	33.8	43.4	50.6	57.1
65	24.1	35.1	44.9	52.6	58.6
70	25.0	36.5	47.0	53.7	60.2
75	25.8	37.8	47.7	55.5	63.0
80	26.7	38.2	48.2	56.2	63.9
85	27.4	38.6	48.5	57.1	64.4
90	28.0	39.0	48.3	57.2	62.6
95	27.7	37.9	44.7	53.3	55.9

Table 30 Relation between electrolyte temperature ($^{\circ}\text{C}$) and electrical current consumption (A) of cell gap set up from 1 to 9 mm, of 0.50% w/w KOH, 20 x 30 mm^2 , 52.9 volt and 1 atm.

Elec. Temp. ($^{\circ}\text{C}$)	Electrical Current (Amp.)				
	1 mm cell gap	3 mm cell gap	5 mm cell gap	7 mm cell gap	9 mm cell gap
40	33.8	37.5	25.5	21.0	18.3
45	32.6	38.8	27.2	22.8	19.9
50	32.7	39.3	29.1	24.2	20.9
55	32.4	39.4	30.2	25.2	21.8
60	32.8	38.6	30.9	26.0	23.0
65	31.7	38.1	32.2	26.9	24.1
70	31.1	37.0	32.9	27.3	25.0
75	30.3	35.3	33.5	28.5	25.8
80	28.4	33.1	34.0	29.3	26.7
85	26.9	30.4	34.5	30.0	27.4
90	24.9	28.1	33.7	30.2	28.0
95	23.1	25.0	29.3	29.3	27.7

Table 31 Relation between electrolyte temperature ($^{\circ}\text{C}$) and electrical current consumption (A) of cell gap set up from 1 to 9 mm, of 0.75% w/w KOH, 20 x 30 mm^2 , 52.9 volt and 1 atm.

Elec. Temp. ($^{\circ}\text{C}$)	Electrical Current (Amp.)				
	1 mm cell gap	3 mm cell gap	5 mm cell gap	7 mm cell gap	9 mm cell gap
40	38.6	47.9	36.8	29.8	26.7
45	38.7	48.8	40.2	32.8	29.4
50	38.4	48.9	42.0	34.4	30.7
55	38.3	48.1	43.0	36.6	32.4
60	37.8	47.2	43.8	37.8	33.8
65	37.6	44.5	45.5	38.8	35.1
70	36.8	43.6	45.7	40.1	36.5
75	35.3	41.3	45.7	40.9	37.8
80	34.4	39.8	45.1	41.0	38.2
85	33.4	37.8	43.1	41.4	38.6
90	31.7	34.9	39.7	40.9	39.0
95	29.5	31.9	35.9	37.3	37.9

Table 32 Relation between electrolyte temperature ($^{\circ}\text{C}$) and electrical current consumption (A) of cell gap set up from 1 to 9 mm, of 1.00% w/w KOH, 20 x 30 mm^2 , 52.9 volt and 1 atm.

Elec. Temp. ($^{\circ}\text{C}$)	Electrical Current (Amp.)				
	1 mm cell gap	3 mm cell gap	5 mm cell gap	7 mm cell gap	9 mm cell gap
40	44.0	55.7	46.2	37.1	33.9
45	44.3	55.6	48.9	39.7	36.9
50	44.5	55.4	50.9	42.4	39.6
55	44.3	55.1	52.8	44.7	41.2
60	44.0	55.0	54.3	46.0	43.4
65	43.2	54.1	55.5	48.3	44.9
70	42.6	52.1	55.4	49.2	47.0
75	41.3	50.5	54.8	49.5	47.7
80	39.9	48.2	53.2	50.3	48.2
85	38.6	44.2	50.1	50.0	48.5
90	36.7	40.4	45.9	48.0	48.3
95	34.2	36.6	41.9	45.5	44.7

Table 33 Relation between electrolyte temperature ($^{\circ}\text{C}$) and electrical current consumption (A) of cell gap set up from 1 to 9 mm, of 1.25% w/w KOH, 20 x 30 mm^2 , 52.9 volt and 1 atm.

Elec. Temp. ($^{\circ}\text{C}$)	Electrical Current (Amp.)				
	1 mm cell gap	3 mm cell gap	5 mm cell gap	7 mm cell gap	9 mm cell gap
40	50.1	61.2	54.3	45.0	40.3
45	50.4	61.6	57.2	48.0	44.3
50	50.5	60.2	59.8	50.6	46.1
55	50.1	59.6	61.4	51.9	48.7
60	49.7	57.3	63.5	56.2	50.6
65	49.7	55.5	63.6	56.8	52.6
70	48.5	54.1	64.2	57.7	53.7
75	47.4	52.0	62.4	58.3	55.5
80	45.2	50.5	60.7	58.2	56.2
85	43.3	48.8	58.2	56.9	57.1
90	41.3	43.7	53.1	55.4	57.2
95	39.5	40.5	47.0	50.8	53.3

Table 34 Relation between electrolyte temperature ($^{\circ}\text{C}$) and electrical current consumption (A) of cell gap set up from 1 to 9 mm, of 1.50% w/w KOH, 20 x 30 mm^2 , 52.9 volt and 1 atm.

Elec. Temp. ($^{\circ}\text{C}$)	Electrical Current (Amp.)				
	1 mm cell gap	3 mm cell gap	5 mm cell gap	7 mm cell gap	9 mm cell gap
40	54.1	68.2	62.1	51.5	45.0
45	54.3	67.4	65.3	54.7	48.4
50	54.1	66.7	68.5	57.0	51.9
55	54.8	66.1	68.7	59.4	55.1
60	54.8	64.6	70.8	62.4	57.1
65	54.0	62.2	71.2	63.5	58.6
70	53.6	59.1	71.6	65.6	60.2
75	51.6	57.7	71.8	67.1	63.0
80	49.7	55.2	68.5	67.7	63.9
85	47.8	52.6	61.7	66.2	64.4
90	45.8	49.5	57.3	63.9	62.6
95	43.6	44.8	52.2	56.4	55.9

Table 35 Relation between electrolyte temperature ($^{\circ}\text{C}$) and electrical current consumption (A) of electrical voltage from 47.5 to 52.9 volt of 1.25% w/w KOH, 20 x 30 mm², 5 mm cell gap, 47.5 to 52.9 volt and 1 atm.

Elec. Temp. ($^{\circ}\text{C}$)	Electrical Current (Amp.)				
	47.5 Volt	49.3 Volt	50.7 Volt	51.9 Volt	52.9 Volt
40	42.2	44.1	48.6	50.3	52.0
45	43.6	46.2	50.5	53.8	55.0
50	45.5	48.5	52.1	56.6	57.3
55	46.6	50.0	54.3	59.0	60.1
60	47.0	51.9	56.1	60.6	61.5
65	48.4	52.0	56.6	62.8	63.5
70	48.9	52.9	58.0	63.0	63.7
75	49.0	53.0	57.6	63.5	63.5
80	49.4	53.4	57.6	62.7	62.1
85	49.0	51.4	55.7	60.1	60.0
90	47.2	49.9	52.1	56.1	55.1
95	43.5	45.5	47.0	50.1	50.0

Table 36 Relation between electrolyte temperature ($^{\circ}\text{C}$) and electrical current consumption (A) of operating pressure from 60.8 to 101.3 kPa of 1.25% w/w KOH, 20 x 30 mm², 5 mm cell gap, 52.9 volt and 1 atm.

Elec. Temp. ($^{\circ}\text{C}$)	Electrical Current (Amp.)				
	101.3 kPa abs	91.2 kPa abs	81.0 kPa abs	70.9 kPa abs	60.8 kPa abs
40	52.0	51.9	49.2	48.3	46.9
45	55.0	54.5	51.9	51.5	50.4
50	57.3	56.1	53.7	53.5	53.6
55	60.1	57.6	55.4	55.0	55.0
60	61.5	59.2	57.3	55.9	56.3
65	63.5	59.6	58.6	55.6	56.3
70	63.7	61.3	59.1	57.4	56.7
75	63.5	60.1	58.5	55.5	55.6
80	62.1	58.0	55.8	52.0	51.0
85	60.0	56.3	53.1	50.0	45.8
90	55.1	53.3	48.9	45.4	41.0
95	50.0	47.6	42.8	40.6	38.7

Table 37 Relation between electrolyte temperature ($^{\circ}\text{C}$) and electrical current consumption (A) of anode-cathode area from 300 to 1500 mm^2 of 1.25% w/w KOH, 20*30 mm^2 , 5 mm cell gap, 52.9 volt and 1 atm.

Elec. Temp. ($^{\circ}\text{C}$)	Electrical Current (Amp.)				
	300 mm^2	600 mm^2	900 mm^2	1200 mm^2	1500 mm^2
40	30.9	42.2	47.9	50.8	60.2
45	32.8	43.6	48.7	51.8	61.6
50	34.8	45.5	50.9	53.9	63.5
55	36.4	46.6	53.2	55.0	64.9
60	37.7	47.0	54.4	57.1	66.6
65	39.1	48.4	55.0	58.4	66.8
70	40.0	48.9	56.1	59.5	67.3
75	41.1	49.0	57.4	60.2	67.9
80	41.8	49.4	57.7	60.4	68.5
85	41.6	49.0	58.4	60.9	67.9
90	41.3	47.2	58.6	61.0	68.7
95	39.7	43.5	57.7	60.8	68.2

Table 38 Relation between electrolyte temperature ($^{\circ}\text{C}$) and HHO production rate (L/h) of anode-cathode area 600 mm^2 , 0.50% w/w KOH, 1 mm cell gap, 52.9 volt and 1 atm.

Elec. Temp. ($^{\circ}\text{C}$)	HHO production rate (L/h)				
	Run#1	Run#2	Run#3	Run#4	Run#5
40	3.0	2.9	3.0	3.0	3.0
45	2.4	2.4	2.5	2.5	2.4
50	2.7	2.7	2.7	2.6	2.6
55	2.3	2.5	2.4	2.4	2.5
60	2.5	2.6	2.5	2.4	2.4
65	2.4	2.5	2.3	2.3	2.2
70	2.2	2.2	2.0	2.2	1.8
75	1.7	1.4	1.6	1.6	1.8
80	1.4	1.3	1.5	1.7	1.8
85	1.0	1.5	1.3	1.3	1.4
90	0.4	0.5	0.6	0.8	0.7
95	0.2	0.5	0.4	0.5	0.4

Table 39 Relation between electrolyte temperature ($^{\circ}\text{C}$) and HHO production rate (L/h) of anode-cathode area 600 mm^2 , 0.75% w/w KOH, 1 mm cell gap, 52.9 volt and 1 atm.

Elec. Temp. ($^{\circ}\text{C}$)	HHO production rate (L/h)				
	Run#1	Run#2	Run#3	Run#4	Run#5
40	3.4	3.7	3.5	3.5	3.5
45	3.3	3.4	3.4	3.4	3.5
50	3.0	3.0	3.1	3.2	3.2
55	2.7	2.7	2.8	2.9	2.9
60	2.8	2.6	2.6	2.5	2.6
65	2.5	2.3	2.4	2.4	2.6
70	2.0	1.9	2.2	2.3	2.3
75	1.8	2.3	2.1	2.3	2.1
80	1.6	2.3	1.9	1.9	2.3
85	1.1	1.4	1.5	1.8	1.8
90	1.0	0.9	1.2	1.4	1.5
95	0.8	0.8	0.8	0.7	0.9

Table 40 Relation between electrolyte temperature ($^{\circ}\text{C}$) and HHO production rate (L/h) of anode-cathode area 600 mm^2 , 1.00% w/w KOH, 1 mm cell gap, 52.9 volt and 1 atm.

Elec. Temp. ($^{\circ}\text{C}$)	HHO production rate (L/h)				
	Run#1	Run#2	Run#3	Run#4	Run#5
40	4.0	3.9	4.0	4.1	4.0
45	3.6	3.6	3.6	3.7	3.5
50	3.0	3.1	3.2	3.4	3.3
55	2.9	2.8	3.0	3.1	3.1
60	2.7	2.8	2.8	2.9	3.0
65	2.9	2.5	2.7	2.6	2.8
70	2.1	2.8	2.5	2.5	2.6
75	2.2	2.1	2.5	2.8	2.7
80	2.3	2.3	2.5	2.7	2.8
85	1.9	2.0	2.3	2.7	2.7
90	1.9	1.9	2.1	2.4	2.5
95	1.6	1.3	1.5	1.7	1.5

Table 41 Relation between electrolyte temperature ($^{\circ}\text{C}$) and HHO production rate (L/h) of anode-cathode area 600 mm^2 , 1.25% w/w KOH, 1 mm cell gap, 52.9 volt and 1 atm.

Elec. Temp. ($^{\circ}\text{C}$)	HHO production rate (L/h)				
	Run#1	Run#2	Run#3	Run#4	Run#5
40	5.4	5.4	5.5	5.5	5.5
45	4.9	4.9	5.0	5.1	5.1
50	4.7	5.0	4.8	4.8	4.9
55	4.4	4.5	4.5	4.5	4.6
60	3.9	4.0	4.0	4.1	4.0
65	3.6	3.5	3.5	3.7	3.5
70	3.1	3.1	3.2	3.3	3.3
75	2.5	3.0	2.9	3.0	3.1
80	2.2	3.0	2.7	2.1	2.6
85	3.0	2.9	2.5	2.2	2.2
90	2.2	1.8	2.2	2.5	2.5
95	1.8	1.6	2.0	2.3	2.2

Table 42 Relation between electrolyte temperature ($^{\circ}\text{C}$) and HHO production rate (L/h) of anode-cathode area 600 mm^2 , 1.50% w/w KOH, 1 mm cell gap, 52.9 volt and 1 atm.

Elec. Temp. ($^{\circ}\text{C}$)	HHO production rate (L/h)				
	Run#1	Run#2	Run#3	Run#4	Run#5
40	5.9	5.9	6.0	6.1	6.1
45	5.3	5.2	5.3	5.3	5.2
50	4.9	5.2	5.0	5.0	4.9
55	4.6	4.6	4.5	4.5	4.5
60	3.8	3.9	4.0	4.1	4.0
65	3.7	3.5	3.5	3.6	3.2
70	2.8	2.6	3.0	3.3	3.4
75	2.7	2.3	2.7	2.9	3.0
80	2.2	2.2	2.5	2.8	2.9
85	2.3	3.0	2.6	2.6	2.2
90	2.1	3.1	2.5	2.7	2.1
95	2.4	2.0	2.2	1.9	1.7

Table 43 Relation between electrolyte temperature ($^{\circ}\text{C}$) and HHO production rate (L/h) of anode-cathode area 600 mm^2 , 0.50% w/w KOH, 3 mm cell gap, 52.9 volt and 1 atm.

Elec. Temp. ($^{\circ}\text{C}$)	HHO production rate (L/h)				
	Run#1	Run#2	Run#3	Run#4	Run#5
40	1.7	1.6	1.5	1.6	1.4
45	1.6	1.5	1.4	1.4	1.4
50	1.3	1.4	1.3	1.4	1.2
55	1.2	1.2	1.3	1.3	1.4
60	1.1	1.2	1.2	1.2	1.4
65	1.0	1.0	1.1	1.0	1.2
70	0.8	0.9	1.2	1.2	1.2
75	0.7	1.3	1.1	1.4	0.9
80	0.7	1.2	1.0	1.3	1.2
85	0.5	1.1	0.8	0.9	0.8
90	0.4	1.0	0.6	0.4	0.5
95	0.3	0.4	0.5	0.7	0.7

Table 44 Relation between electrolyte temperature ($^{\circ}\text{C}$) and HHO production rate (L/h) of anode-cathode area 600 mm^2 , 0.75% w/w KOH, 3 mm cell gap, 52.9 volt and 1 atm.

Elec. Temp. ($^{\circ}\text{C}$)	HHO production rate (L/h)				
	Run#1	Run#2	Run#3	Run#4	Run#5
40	2.6	2.6	2.6	2.7	2.6
45	2.5	2.4	2.5	2.6	2.5
50	2.3	2.3	2.4	2.4	2.6
55	2.1	2.2	2.3	2.3	2.5
60	2.0	2.1	2.2	2.3	2.4
65	2.0	1.9	2.1	2.2	2.1
70	1.8	1.7	2.0	2.2	2.2
75	1.8	1.6	1.8	1.6	2.0
80	1.7	1.2	1.7	1.6	2.2
85	1.1	1.8	1.5	1.9	1.3
90	1.0	1.6	1.3	1.3	1.2
95	1.1	0.9	1.2	1.4	1.5

Table 45 Relation between electrolyte temperature ($^{\circ}\text{C}$) and HHO production rate (L/h) of anode-cathode area 600 mm^2 , 1.00% w/w KOH, 3 mm cell gap, 52.9 volt and 1 atm.

Elec. Temp. ($^{\circ}\text{C}$)	HHO production rate (L/h)				
	Run#1	Run#2	Run#3	Run#4	Run#5
40	3.8	3.9	3.9	4.0	4.0
45	3.5	3.6	3.5	3.6	3.5
50	3.2	3.4	3.2	3.2	3.2
55	2.8	3.0	3.0	2.9	3.0
60	2.9	2.9	2.9	2.7	3.1
65	2.6	2.9	2.8	3.0	2.9
70	2.3	2.4	2.6	2.8	2.8
75	2.2	2.8	2.5	2.5	2.7
80	2.0	1.9	2.3	2.8	2.7
85	1.7	1.9	2.0	2.2	2.4
90	1.6	1.7	1.8	1.8	2.1
95	1.2	1.6	1.4	1.6	1.4

Table 46 Relation between electrolyte temperature ($^{\circ}\text{C}$) and HHO production rate (L/h) of anode-cathode area 600 mm^2 , 1.25% w/w KOH, 3 mm cell gap, 52.9 volt and 1 atm.

Elec. Temp. ($^{\circ}\text{C}$)	HHO production rate (L/h)				
	Run#1	Run#2	Run#3	Run#4	Run#5
40	4.5	4.6	4.5	4.6	4.4
45	4.1	4.2	4.2	4.1	4.1
50	3.9	4.0	4.0	3.9	4.0
55	3.8	3.8	3.7	3.6	3.6
60	3.3	3.4	3.5	3.6	3.7
65	3.2	3.4	3.3	3.5	3.3
70	3.0	2.9	3.1	3.3	3.1
75	2.8	2.4	2.8	2.7	3.2
80	2.2	2.9	2.6	2.9	2.3
85	2.2	2.8	2.5	2.8	2.4
90	1.9	2.1	2.3	2.4	2.5
95	1.8	2.0	2.0	2.0	1.9

Table 47 Relation between electrolyte temperature ($^{\circ}\text{C}$) and HHO production rate (L/h) of anode-cathode area 600 mm^2 , 1.50% w/w KOH, 3 mm cell gap, 52.9 volt and 1 atm.

Elec. Temp. ($^{\circ}\text{C}$)	HHO production rate (L/h)				
	Run#1	Run#2	Run#3	Run#4	Run#5
40	5.5	5.6	5.5	5.5	5.5
45	5.0	5.1	5.1	5.0	5.2
50	4.9	5.0	4.8	4.8	4.6
55	4.7	4.5	4.6	4.6	4.7
60	4.3	4.5	4.4	4.3	4.5
65	3.9	4.0	4.2	4.5	4.4
70	3.6	3.9	4.0	4.4	4.2
75	3.6	3.5	3.8	4.1	4.1
80	3.1	3.7	3.5	3.8	3.5
85	3.0	3.5	3.2	3.2	3.2
90	2.7	3.3	3.0	3.3	2.8
95	2.6	3.0	2.8	2.6	3.1

Table 48 Relation between electrolyte temperature ($^{\circ}\text{C}$) and HHO production rate (L/h) of anode-cathode area 600 mm^2 , 0.50% w/w KOH, 5 mm cell gap, 52.9 volt and 1 atm.

Elec. Temp. ($^{\circ}\text{C}$)	HHO production rate (L/h)				
	Run#1	Run#2	Run#3	Run#4	Run#5
40	0.2	0.1	0.1	0.0	0.1
45	0.4	0.2	0.3	0.2	0.3
50	0.4	0.6	0.4	0.3	0.5
55	0.7	0.5	0.5	0.6	0.6
60	0.5	0.7	0.6	0.7	0.6
65	1.2	0.7	1.0	1.0	1.0
70	1.3	1.3	1.5	1.7	1.6
75	2.1	2.0	1.9	1.7	1.9
80	2.2	2.8	2.5	2.0	2.9
85	2.5	3.4	3.0	3.6	2.7
90	2.2	2.7	2.6	3.0	2.2
95	1.5	1.6	1.5	1.4	1.2

Table 49 Relation between electrolyte temperature ($^{\circ}\text{C}$) and HHO production rate (L/h) of anode-cathode area 600 mm^2 , 0.75% w/w KOH, 5 mm cell gap, 52.9 volt and 1 atm.

Elec. Temp. ($^{\circ}\text{C}$)	HHO production rate (L/h)				
	Run#1	Run#2	Run#3	Run#4	Run#5
40	0.5	0.3	0.5	0.5	0.6
45	1.1	0.9	1.0	1.1	1.0
50	1.3	1.4	1.3	1.2	1.1
55	1.3	1.2	1.5	1.4	1.5
60	1.6	2.0	1.8	2.1	1.7
65	1.7	2.0	2.0	2.5	1.7
70	1.9	1.8	2.3	2.2	2.5
75	2.2	2.1	2.5	2.6	2.7
80	3.4	3.5	2.9	2.4	2.7
85	3.1	3.3	3.5	3.0	3.7
90	2.2	2.1	2.6	3.0	3.0
95	1.7	1.6	2.0	2.4	2.5

Table 50 Relation between electrolyte temperature ($^{\circ}\text{C}$) and HHO production rate (L/h) of anode-cathode area 600 mm^2 , 1.00% w/w KOH, 5 mm cell gap, 52.9 volt and 1 atm.

Elec. Temp. ($^{\circ}\text{C}$)	HHO production rate (L/h)				
	Run#1	Run#2	Run#3	Run#4	Run#5
40	1.0	1.2	1.2	1.3	1.2
45	1.5	1.4	1.5	1.4	1.7
50	1.5	1.7	1.7	1.6	1.7
55	2.0	2.1	2.0	1.8	1.9
60	2.3	2.1	2.3	2.4	2.4
65	2.7	2.2	2.5	2.2	2.8
70	3.1	3.0	3.0	2.7	2.8
75	3.3	3.5	3.5	3.7	3.2
80	4.1	4.5	4.0	3.7	3.6
85	3.9	3.3	3.5	4.0	3.7
90	3.2	3.7	3.7	4.3	4.5
95	1.7	2.1	2.0	1.8	2.0

Table 51 Relation between electrolyte temperature ($^{\circ}\text{C}$) and HHO production rate (L/h) of anode-cathode area 600 mm^2 , 1.25% w/w KOH, 5 mm cell gap, 52.9 volt and 1 atm.

Elec. Temp. ($^{\circ}\text{C}$)	HHO production rate (L/h)				
	Run#1	Run#2	Run#3	Run#4	Run#5
40	2.5	2.5	2.6	2.6	2.6
45	2.9	3.0	3.0	3.0	2.8
50	3.0	3.0	3.2	3.3	3.3
55	3.4	3.4	3.5	3.7	3.6
60	4.1	4.1	4.0	3.8	3.9
65	3.6	3.6	3.8	3.9	4.0
70	4.0	3.7	4.0	3.8	4.2
75	4.2	4.8	4.5	4.4	4.8
80	4.6	5.2	5.0	5.5	4.5
85	5.0	5.3	5.5	5.5	5.9
90	5.3	5.6	5.0	4.6	4.6
95	3.9	4.3	4.0	3.7	4.4

Table 52 Relation between electrolyte temperature ($^{\circ}\text{C}$) and HHO production rate (L/h) of anode-cathode area 600 mm^2 , 1.50% w/w KOH, 5 mm cell gap, 52.9 volt and 1 atm.

Elec. Temp. ($^{\circ}\text{C}$)	HHO production rate (L/h)				
	Run#1	Run#2	Run#3	Run#4	Run#5
40	3.6	3.8	3.8	3.6	3.8
45	4.2	3.8	4.0	3.9	4.1
50	4.0	4.1	4.3	4.4	4.4
55	4.2	4.2	4.0	3.8	3.9
60	4.3	4.5	4.5	4.6	4.3
65	4.6	4.3	4.5	4.5	4.5
70	4.6	4.9	4.8	4.7	4.9
75	5.3	5.5	5.0	4.1	4.6
80	5.2	5.1	5.5	5.8	6.0
85	5.5	4.6	5.0	5.2	4.5
90	5.0	5.2	5.5	5.9	5.9
95	4.7	4.3	4.5	4.3	4.8

Table 53 Relation between electrolyte temperature ($^{\circ}\text{C}$) and HHO production rate (L/h) of anode-cathode area 600 mm^2 , 0.50% w/w KOH, 7 mm cell gap, 52.9 volt and 1 atm.

Elec. Temp. ($^{\circ}\text{C}$)	HHO production rate (L/h)				
	Run#1	Run#2	Run#3	Run#4	Run#5
40	0.0	0.0	0.0	0.0	0.0
45	0.0	0.0	0.0	0.0	0.0
50	0.0	0.0	0.0	0.0	0.0
55	0.0	0.0	0.0	0.0	0.0
60	0.3	0.2	0.3	0.3	0.4
65	0.5	0.6	0.5	0.5	0.6
70	0.7	0.8	1.0	1.1	1.3
75	1.2	1.5	1.4	1.4	1.6
80	1.5	1.9	1.7	1.6	1.8
85	1.7	1.5	1.9	2.1	2.3
90	2.0	2.1	2.3	2.4	2.6
95	1.1	1.1	1.4	1.8	1.7

Table 54 Relation between electrolyte temperature ($^{\circ}\text{C}$) and HHO production rate (L/h) of anode-cathode area 600 mm^2 , 0.75% w/w KOH, 7 mm cell gap, 52.9 volt and 1 atm.

Elec. Temp. ($^{\circ}\text{C}$)	HHO production rate (L/h)				
	Run#1	Run#2	Run#3	Run#4	Run#5
40	0.3	0.2	0.3	0.3	0.3
45	0.4	0.6	0.5	0.5	0.6
50	0.9	0.8	0.9	0.8	1.0
55	1.3	1.3	1.4	1.4	1.5
60	1.5	1.6	1.6	1.5	1.7
65	1.9	2.0	2.0	2.1	2.2
70	2.2	2.4	2.3	2.5	2.2
75	2.7	2.5	2.5	2.7	2.3
80	2.4	2.5	2.6	2.7	2.7
85	2.9	3.0	3.2	3.4	3.4
90	3.7	3.6	3.9	4.3	4.4
95	2.6	2.6	2.8	3.0	3.1

Table 55 Relation between electrolyte temperature ($^{\circ}\text{C}$) and HHO production rate (L/h) of anode-cathode area 600 mm^2 , 1.00% w/w KOH, 7 mm cell gap, 52.9 volt and 1 atm.

Elec. Temp. ($^{\circ}\text{C}$)	HHO production rate (L/h)				
	Run#1	Run#2	Run#3	Run#4	Run#5
40	0.7	0.7	0.8	0.9	0.8
45	0.8	0.9	1.0	1.1	1.0
50	1.2	1.3	1.3	1.4	1.3
55	1.5	1.6	1.5	1.6	1.5
60	1.8	1.8	2.0	2.2	2.2
65	2.2	2.0	2.2	2.3	2.3
70	2.4	2.3	2.5	2.5	2.7
75	2.8	2.9	3.0	3.1	3.2
80	3.0	3.0	3.3	3.5	3.7
85	3.5	3.5	3.8	4.1	4.2
90	3.4	3.4	3.7	4.0	4.1
95	3.2	3.2	3.5	3.8	3.8

Table 56 Relation between electrolyte temperature ($^{\circ}\text{C}$) and HHO production rate (L/h) of anode-cathode area 600 mm^2 , 1.25% w/w KOH, 7 mm cell gap, 52.9 volt and 1 atm.

Elec. Temp. ($^{\circ}\text{C}$)	HHO production rate (L/h)				
	Run#1	Run#2	Run#3	Run#4	Run#5
40	1.8	1.9	1.9	2.0	1.9
45	2.0	2.1	2.1	2.2	2.1
50	2.0	2.1	2.2	2.3	2.3
55	2.1	2.3	2.3	2.4	2.4
60	2.4	2.5	2.5	2.6	2.6
65	2.8	2.8	3.0	3.1	3.2
70	3.3	3.4	3.5	3.5	3.7
75	3.4	3.5	3.7	3.9	3.9
80	3.7	3.7	4.0	4.3	4.4
85	4.2	4.3	4.5	4.8	4.9
90	4.7	4.6	5.0	5.3	5.6
95	4.0	4.1	4.3	4.5	4.6

Table 57 Relation between electrolyte temperature ($^{\circ}\text{C}$) and HHO production rate (L/h) of anode-cathode area 600 mm^2 , 1.50% w/w KOH, 7 mm cell gap, 52.9 volt and 1 atm.

Elec. Temp. ($^{\circ}\text{C}$)	HHO production rate (L/h)				
	Run#1	Run#2	Run#3	Run#4	Run#5
40	3.4	3.5	3.5	3.6	3.5
45	3.4	3.5	3.5	3.6	3.5
50	3.3	3.4	3.4	3.4	3.4
55	3.4	3.5	3.6	3.7	3.7
60	3.8	4.2	4.0	4.2	3.8
65	4.3	4.3	4.5	4.7	4.7
70	5.0	5.1	5.3	5.6	5.5
75	5.3	5.3	5.5	5.6	5.7
80	5.3	5.8	5.5	5.4	5.7
85	5.3	5.3	5.7	6.1	6.1
90	5.6	5.7	6.0	6.3	6.4
95	5.7	5.7	6.0	6.2	6.4

Table 58 Relation between electrolyte temperature ($^{\circ}\text{C}$) and HHO production rate (L/h) of anode-cathode area 600 mm^2 , 0.50% w/w KOH, 9 mm cell gap, 52.9 volt and 1 atm.

Elec. Temp. ($^{\circ}\text{C}$)	HHO production rate (L/h)				
	Run#1	Run#2	Run#3	Run#4	Run#5
40	0.0	0.0	0	0.0	0.0
45	0.0	0.0	0	0.0	0.0
50	0.0	0.0	0	0.0	0.0
55	0.0	0.0	0	0.0	0.0
60	0.2	0.1	0.1	0.2	0.2
65	0.2	0.3	0.2	0.2	0.1
70	0.5	0.5	0.6	0.7	0.6
75	0.6	0.9	0.8	1.0	1.1
80	1.2	1.0	1.1	0.9	1.2
85	1.4	1.5	1.5	1.7	1.6
90	1.6	1.7	1.7	1.5	1.9
95	1.6	1.2	1.4	1.2	1.7

Table 59 Relation between electrolyte temperature ($^{\circ}\text{C}$) and HHO production rate (L/h) of anode-cathode area 600 mm^2 , 0.75% w/w KOH, 9 mm cell gap, 52.9 volt and 1 atm.

Elec. Temp. ($^{\circ}\text{C}$)	HHO production rate (L/h)				
	Run#1	Run#2	Run#3	Run#4	Run#5
40	0.2	0.2	0.2	0.3	0.3
45	0.4	0.3	0.3	0.3	0.2
50	0.4	0.4	0.4	0.3	0.5
55	1.1	1.4	1.2	1.3	1.1
60	1.4	1.5	1.5	1.7	1.6
65	1.5	1.9	1.7	1.7	1.8
70	1.8	1.7	1.9	2.1	2.2
75	2.2	2.0	2.2	2.0	2.5
80	2.1	2.8	2.5	2.3	2.7
85	2.6	3.2	2.8	2.3	3.0
90	2.7	3.2	2.9	3.3	2.5
95	1.7	2.3	2.0	2.3	1.7

Table 60 Relation between electrolyte temperature ($^{\circ}\text{C}$) and HHO production rate (L/h) of anode-cathode area 600 mm^2 , 1.00% w/w KOH, 9 mm cell gap, 52.9 volt and 1 atm.

Elec. Temp. ($^{\circ}\text{C}$)	HHO production rate (L/h)				
	Run#1	Run#2	Run#3	Run#4	Run#5
40	1.5	1.5	1.5	1.6	1.6
45	1.7	1.6	1.7	1.7	1.8
50	1.6	1.9	1.8	2.0	1.8
55	2.0	2.0	2.0	2.1	2.1
60	2.3	2.2	2.3	2.4	2.3
65	2.4	2.6	2.5	2.6	2.5
70	3.1	2.8	3.0	2.8	3.0
75	3.2	3.0	3.1	3.4	2.9
80	3.6	3.8	3.5	3.1	3.5
85	3.3	3.9	3.8	3.8	4.2
90	4.5	4.2	4.4	4.4	4.6
95	3.8	4.2	4.0	4.1	4.3

Table 61 Relation between electrolyte temperature ($^{\circ}\text{C}$) and HHO production rate (L/h) of anode-cathode area 600 mm^2 , 1.25% w/w KOH, 9 mm cell gap, 52.9 volt and 1 atm.

Elec. Temp. ($^{\circ}\text{C}$)	HHO production rate (L/h)				
	Run#1	Run#2	Run#3	Run#4	Run#5
40	2.2	1.9	2.0	2.0	2.1
45	1.9	1.8	1.9	2.0	2.0
50	2.2	2.2	2.3	2.4	2.4
55	2.5	2.4	2.5	2.4	2.6
60	2.7	2.7	2.7	2.6	2.8
65	3.0	3.0	3.0	2.8	3.0
70	3.1	3.4	3.5	3.7	3.8
75	3.7	3.8	4.0	4.3	4.2
80	4.5	5.1	5.0	4.9	5.5
85	4.2	4.6	4.6	4.7	5.0
90	4.8	5.1	4.9	5.3	5.5
95	5.0	5.4	5.3	5.4	5.3

Table 62 Relation between electrolyte temperature ($^{\circ}\text{C}$) and HHO production rate (L/h) of anode-cathode area 600 mm^2 , 1.50% w/w KOH, 9 mm cell gap, 52.9 volt and 1 atm.

Elec. Temp. ($^{\circ}\text{C}$)	HHO production rate (L/h)				
	Run#1	Run#2	Run#3	Run#4	Run#5
40	3.5	3.6	3.5	3.7	3.5
45	3.3	3.3	3.2	3.2	3.1
50	3.5	3.6	3.5	3.5	3.6
55	3.4	3.5	3.5	3.6	3.6
60	4.4	4.4	4.5	4.6	4.5
65	4.5	4.4	4.5	4.7	4.5
70	4.8	4.6	4.8	5.1	4.7
75	5.0	4.8	5.0	5.2	5.0
80	5.1	5.0	5.0	5.1	5.0
85	5.4	5.3	5.3	5.2	5.4
90	5.6	5.5	5.5	5.7	5.3
95	5.2	5.5	5.5	5.8	5.5

Appendix B Equipments

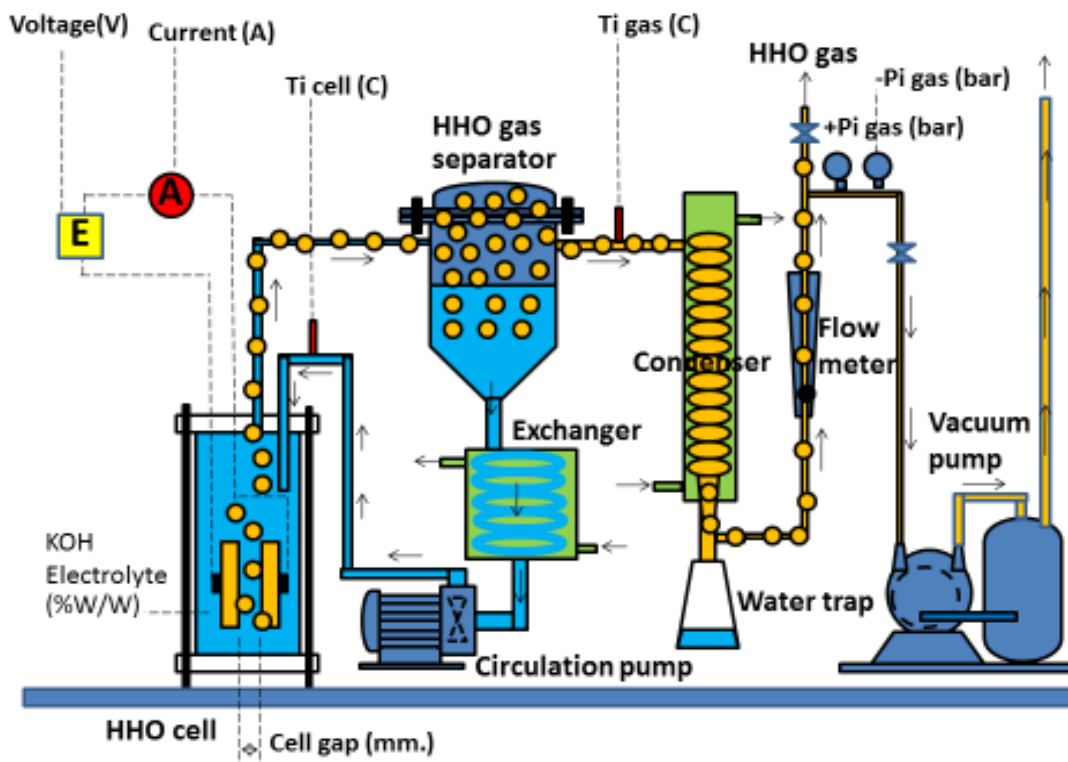


Figure 59 Simple diagram of HHO production system (color).



Figure 60 Weigh distilled water on weight scale.

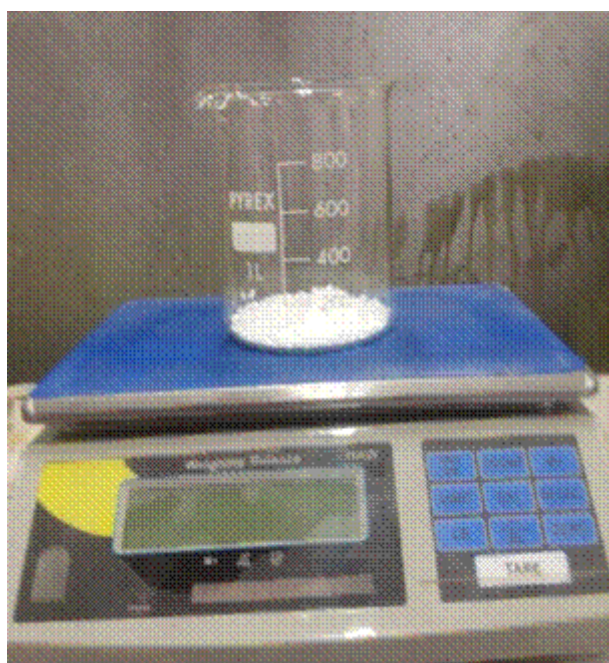


Figure 61 Weigh electrolyte KOH(s) on scale weight.

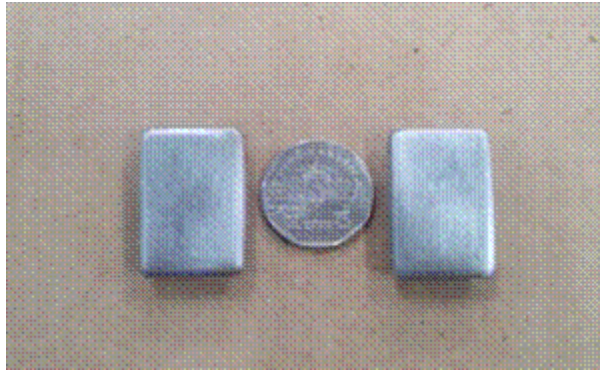


Figure 62 Anode-cathode poles: stainless steel plate.



Figure 63 Set up cell gap with digital Vernier Caliper.



Figure 64 Liquid-gas separator with temperature sensor.



Figure 65 Shell and SS. ring coil exchanger.



Figure 66 Centrifugal circulation pump and cooling fan.



Figure 67 Temperature control panel.



Figure 68 Glass type HHO generator.



Figure 69 HHO gas condenser.



Figure 70 Breathing valve with positive & negative pressure indicator.



Figure 71 Water bath for checking HHO bubble.

VITAE

Name Mr. Nuttaporn Choodum

Student ID 5510130020

Educational Attainment

Degree	Name of Institution	Year of Graduation
Bachelor of Engineering (Chemical Engineering)	Prince of Songkla University (Hatyai Campus)	2003

Scholarship Awards during Enrolment

- The Graduate School Research Fund from the Prince of Songkla University
- The Lecturer Development Scholarship from the Prince of Songkla University